UNIVERSITÀ DEGLI STUDI DI SASSARI

Dipartimento di Scienze Biomediche

PhD course in Life Sciences and Biotechnologies

PhD course coordinator: Prof. Leonardo A. Sechi

IDENTIFICATION, CELLULAR TROPISM AND *IN VITRO* TRANSFORMING PROPERTIES OF OVINE PAPILLOMAVIRUSES

Tutor:
Prof. Alberto Alberti

PhD student:
Gessica Tore

Università degli Studi di Sassari

Corso di Dottorato di ricerca in

Life Sciences and Biotechnologies

La presente tesi è stata prodotta durante la frequenza del corso di dottorato in Life Sciences and Biotechnologies dell'Università degli Studi di Sassari, a.a. 2013/2014- XXIX ciclo, con il sostegno di una borsa di studio cofinanziata con le risorse del P.O.R. SARDEGNA F.S.E. 2007-2013 - Obiettivo competitività regionale e occupazione, Asse IV Capitale umano, Linea di Attività l.3.1 "Finanziamento di corsi di dottorato finalizzati alla formazione di capitale umano altamente specializzato, in particolare per i settori dell'ICT, delle nanotecnologie e delle biotecnologie, dell'energia e dello sviluppo sostenibile, dell'agroalimentare e dei materiali tradizionali".

La tesi è stata prodotta, altresì, grazie al contributo della Fondazione di Sardegna.

TABLE OF CONTENTS

ABSTRACT

To date, about 150 animal papillomaviruses (PV) have been identified in benign and malignant lesions of the skin and mucosa in 75 vertebrate host species. In sheep, three ovine PV types have been described so far, namely OaPV1, OaPV2, and OaPV3. All of them infect skin epithelium, but while OaPV1, OaPV2 belong to the *Delta-genus* and cause benign fibropapillomas, OaPV3 is part of the distant *Dyokappa-genus* and has been detected in squamous cell carcinomas (SCC). This research aims to identify and genetically characterize novel ovine papillomaviruses types, and to investigate their role in skin carcinogenesis. The identification of OaPV4, a novel ovine PV type within *Deltapapillomaviruses 3* in a fibropapilloma of a ram is reported. *In vitro* transforming abilities of OaPV3 and OaPV4 E6 and E7 PV oncogenes are evaluated in a comparative study to investigate a potential role of *Delta* and *Dyokappa* viruses in non-melanoma skin cancer development. Both OaPV3 and OaPV4 E6 and E7 transduction alter cell growth profile of primary human and sheep keratinocytes, but while OaPV4-E6E7 determine a strong lifespan increase OaPV3-E6E7 are able to promote immortalization. Furthermore, pRB protein levels are altered upon E6 and E7 expression, and pulldown assays reveal stronger ability of OaPV3-E7 to efficiently associate with pRB leading to its destabilization. Results support the existence of peculiar *in vitro* transformation properties for ovine papillomaviruses reinforcing the thesis of a direct link between cutaneous papillomaviruses, cellular transformation, and NMSC progression.

1. INTRODUCTION

1.1 Papillomavirus: a general overview

Papillomaviruses (PVs) are small, non-enveloped, double-stranded DNA, icosahedral viruses. They commonly infect the stratified squamous epithelium of the skin and mucosa in a wide variety of vertebrates where they can induce cellular proliferation or persist asymptomatically. Papillomaviruses are highly species-specific and diverse and most of the hundreds types are identified in human, which is the only intensively studied host. Nevertheless, the direct link between papillomavirus infection and neoplasia, and the relationship between virus and environmental co-carcinogens was first established for animal papillomaviruses, particularly cottontail rabbit (Shope) papillomavirus (CRPV), bovine papillomaviruses (BPVs), and canine oral papillomavirus (COPV) (Campo, 2002). CRPV was indeed the first oncogenic virus to be identified in mammals: in 1933, this virus was found to be associated with the appearance of wart like tumours in the cottontail rabbit (*S. floridanus*) (Shope and Hurst, 1933).

The link between human papillomavirus and human cancer was established in 1970s. Harald zur Hausen and his team established a relationship between papillomavirus infections and cervical cancer (zur Hausen, 2009, 2002). As a result of these findings, the International Agency for Research on Cancer (IARC) classified 12 high-risk human papillomaviruses (HR-HPV) as carcinogenic for humans: types 16, 18, 31, 33, 35, 39, 45, 51, 52, 56, 58, 59 (Bouvard et al., 2009). On the other hand, many PV types cause only asymptomatic infections in immunocompetent individuals and can be detected in healthy skin and mucosa (Bottalico et al., 2011; Nindl et al., 2007).

1.2 Classification of Papillomaviruses

Papillomaviruses were initially classified together with the polyomaviruses in one family, the *Papovaviridae.* When it was established that the two viruses have different genome sizes and organization, and no major nucleotide or amino acid sequence similarities, the 7th Report of the International Commitee on the Taxonomy of Viruses (ICTV) decided to split the *Papovaviridae* into two families: *Polyomaviridae* and *Papillomaviridae* (De Villiers et al., 2004; Fauquet and Mayo, 2001). The establishment of a papillomavirus taxonomy based on biological properties was limited by the absence of an adequate tissue culture system to propagate these viruses. A nucleotide sequence-based classification has been developed over the last 40 years, given that there is a strong evidence that papillomavirus genomes are very static and mutation or recombination are very rare events (De Villiers et al., 2004).

The L1 open reading frame (ORF) is the most conserved gene among the *Papillomaviridae* family, so it has been used for the identification and classification of new PV types. A new PV is designated as such if the complete genome has been isolated, cloned and fully sequenced. The abbreviation HPV is used for PVs identified in humans, followed by a number that indicates, consecutively, the viral type. Instead, animal PV nomenclature is based on the scientific name of the host by using the host genus and species designation, for example OaPV1 for *Ovis aries* PV type 1 (Bernard et al., 2010).

Nucleotide sequence comparison of the L1 ORF allows to classify a new PV isolate according to the following criteria (De Villiers et al., 2004).

1. The higher-order taxon is called ″genus″. Different genera, designated by Greek letters, share less than 60% nucleotide sequence identity in the L1 ORF. Since genera are more than the alphabet letters, it's been allowed to use the greek nomenclature a second time employing the prefix "dyo" (e.g. DyoLambda PV) (Bernard et al., 2010).
2. Lower-order taxon is called ″species″. Such species within a genus share between 60% and 70% nucleotide identity.
3. The traditional PV types within a species share between 71% and 89% nucleotide identity within the complete L1 ORF. A new type is identified when the L1 ORF differs by more than 10% from the closest known PV type.
4. Differences between 2% and 10% in the L1 homology define a ″subtype″ and less than 2% a ″variant″.

Figure 1 *Papillomavirus phylogenetic tree based on alignment of E1, E2, L1 and L2 of 241 papillomaviruses* (Van Doorslaer, 2013).

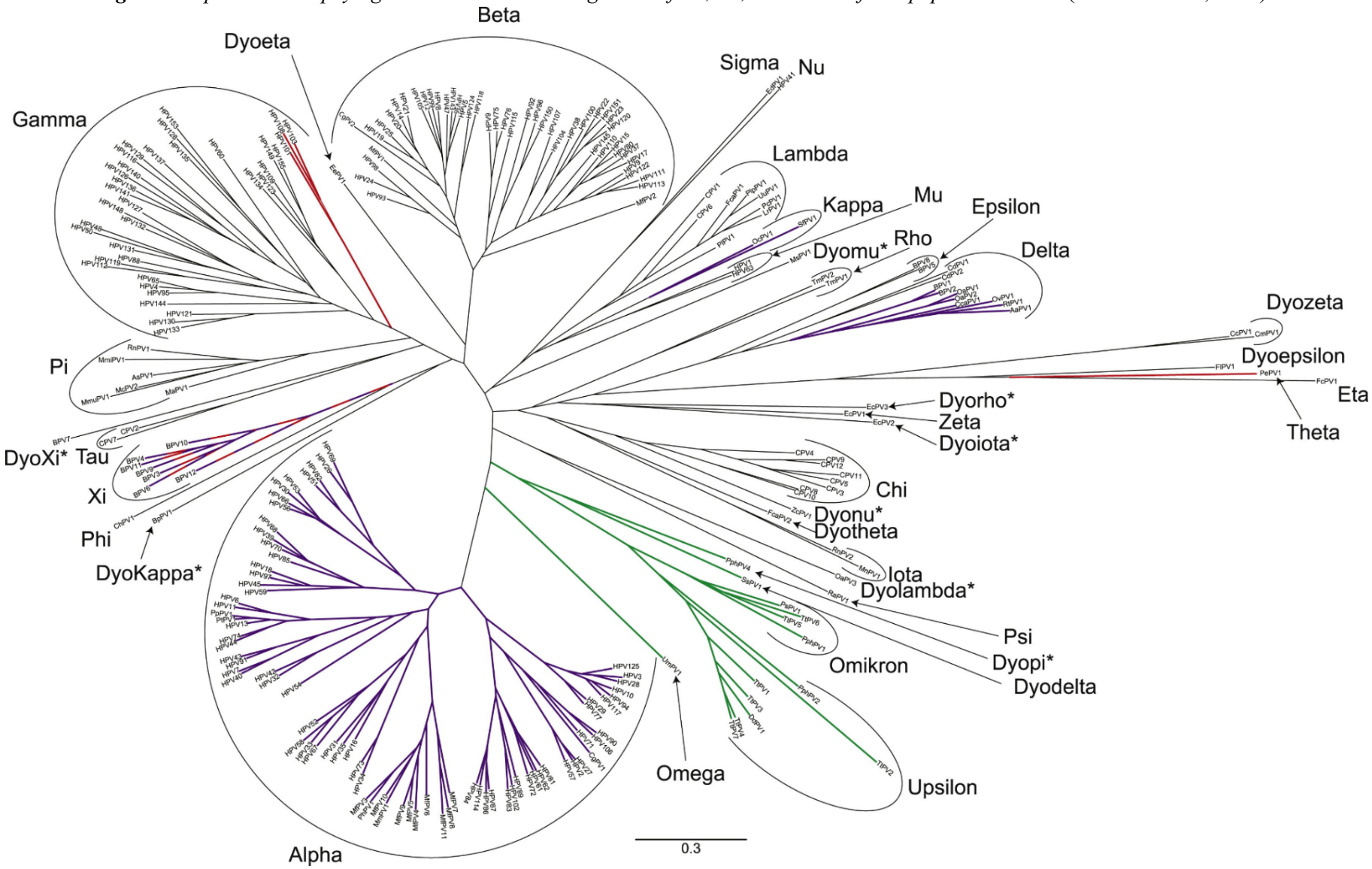

1.3 Viral genome organization and viral proteins

All PV types display a common conserved genomic organization, which was initially established by DNA sequencing of the bovine papillomavirus type 1 (BPV1), the first PV to be fully sequenced together with HPV1 (Chen et al., 1982; de Villiers, 2013). Papillomaviruses have a small circular double-stranded DNA genome approximately 7-8 kb in size, which can be divided into three regions separated by two polyadenylation (pA) sites (early pA and late pA sites):

- **non-coding region** (LCR, URR, NCR): containing most of the regulatory elements involved in viral DNA replication and transcription.
- **early region**: containing genes encoding for E1, E2, E6, E7, E5, E4 proteins.
- **late region:** containing late structural genes L1 and L2.

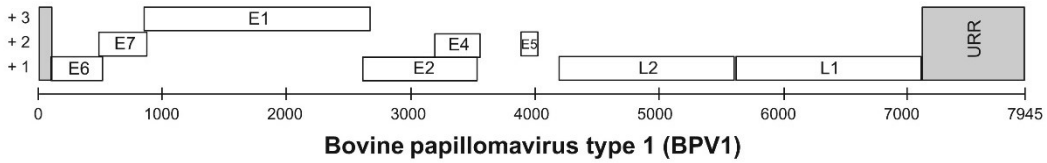

Figure 2 *BPV1 genome organization* (Rector and Van Ranst, 2013). *Initially, BPV-1 was used as prototype to study the molecular biology of papillomaviruses.*

The ORFs lie in one strand of the viral DNA and are transcribed as polycistronic messages that are alternatively spliced to yield individual gene products (Anacker and Moody, 2016; Graham and Faizo, 2016).

LCR (long control region)

The LCR represents the 10% of the genome and is located between the L1 and the first ORF of the early region. It contains the viral origin of replication (ori) as well as multiple transcription factor binding sites, which are important in the regulation of RNA polymerase II-initiated transcription from both early and late viral promoters (Zheng and Baker, 2006). The ori is typically comprised of two to three E2-binding sites (E2BS) flanking a palindromic E1-binding region (E1BS) and an AT-rich sequence, all of which are required for optimal ori functioning (Bergvall et al., 2013).

Early region

The early region occupies over 50% of the virus genome from its 5′ half and encodes six common genes (E1, E2, E4, E5, E6 and E7) expressed since the early stages of infection.

The well-conserved E1 protein is the only enzyme encoded by PVs genome. The enzymatically active form is a double-hexameric helicase capable of unwinding the ori and the DNA ahead of the replication fork, in an ATP-dependent manner (Bergvall et al., 2013). Together with E2, it forms an E1-E2 ori complex essential for the replication of viral DNA.

The full-length E2 is a dimeric multifunctional protein involved in many viral and cellular processes, above all viral DNA replication and transcription. Within the E1-E2 protein complex, the E2 recognizes E2BS with high affinity and thus acts to load E1 onto the ori to initiate transcription. Other shorter E2 forms are encoded by spliced mRNAs. The protein named E2^E8 originates from an alternative reading frame in the E1 region of the genome (designated E8) and the C-terminus of E2. Invariably, the shorter forms of E2 act as repressors of viral transcription and replication and are important to limit the expression of viral E6 and E7 oncoproteins in carcinogenic PVs (Dreer et al., 2016; McBride, 2013).

The E4 protein origins from alternative splicing of an mRNA that includes the E1 initiation codon and adjacent sequences. Despite being located in the early region, it is expressed during the late stage of infection. The E4 has different functions in viral life cycle such as disruption of cellular keratin network that facilitates virus release (Doorbar, 2013).

The E6, together with the E7, is one of the major papillomaviral oncoproteins. Despite its small size, many direct and indirect protein interactions have been reported, even if, in most cases, its biological significance is not yet understood. In particular, it is not clear which of these viral/cellular protein complexes are only involved in the viral life cycle and which also contribute to the malignant transformation of the infected cells (Ghittoni et al., 2010).

The E6 commonly contains two zinc-binding regions [CXXC-X(28-30)-CXXC], which are located at the amino and the carboxy-terminus of the protein and named E6N and E6C (Figure 3). The structure of entire E6 proteins, and both E6N and E6C, has been determined (Zanier et al., 2012). Despite the divergent primary E6 sequences, E6N and E6C have a conserved overall crystal structure among PV types. All E6 proteins examined so far bind cellular proteins by docking on similar acidic alpha-helical conserved motif (LXXLL), even if the final targets (E6AP, MAML, and paxillin) are seemingly unrelated (Vande Pol et al., 2015). Typically, alpha-E6 proteins interact with LXXLL of E6AP to indirectly bind and degrade p53; on the

other hand, BPV1 E6 and HPV-E6 of the beta genus bind the LXXLL of MAML proteins to repress Notch signaling (Brimer et al., 2012; Meyers et al., 2017, 2013; Tan et al., 2012).

The E7 is an acidic phosphoprotein that resembles structurally and functionally to the adenovirus E1A and the Simian Vacuolating virus (SV40) large tumour antigen (Chellappan et al., 1992; Figge et al., 1988; Phelps et al., 1992). Due to these similarities, the E7 can be divided into three conserved regions (CR1-3). The CR2 of many PVs (but not Delta-fibropapillomaviruses) contains the Leu-X-Cys-X-Glu (LXCXE) motif, which is necessary and sufficient to bind the retinoblastoma tumour suppressor protein (pRB) and its related pocket proteins p107 and p130 (Ghittoni et al., 2010; Munger et al., 1989). Furthermore, the E7 carboxy terminus contains a zinc-binding domain composed of two CXXC motifs (Figure 3). Given that also E6 proteins consist of two tandem copies of CXXC motif with sequence similarity to the E7 carboxy terminus, it has been suggested that E6 and E7 might have evolved from a common ancestor (Cole and Danos, 1987; Van Doorslaer, 2013; Van Doorslaer et al., 2009).

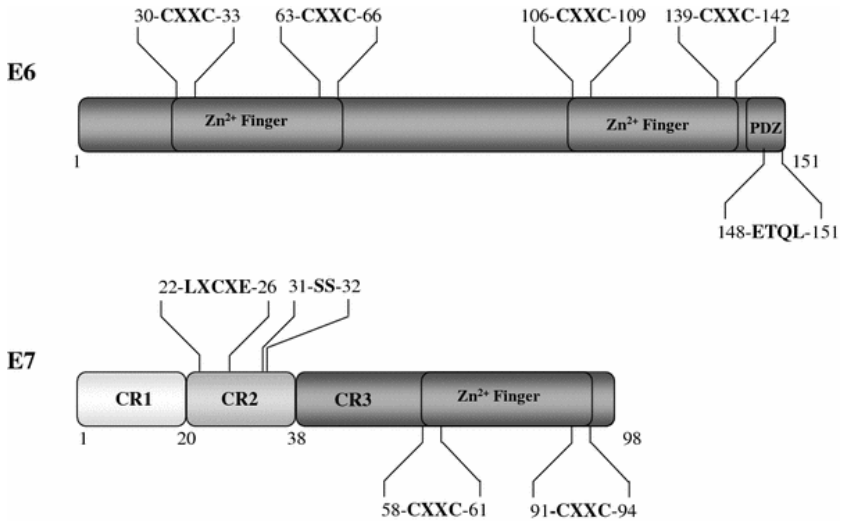

Figure 3 *E6 and E7 structure of high-risk HPV types: both contain CXXC motifs* (Ghittoni et al., 2010).

The E5 oncoprotein is not encoded by all PVs, but when present it can increase the E6 and E7 function contributing to tumour progression. HPV16 E5 and BPV E5 are the most studied E5 proteins; although they show different primary sequences, they both transform cells and display overlapping targets and activities. The E5 is a short membrane hydrophobic

associated peptide, expressed from a spliced mRNA that initiates upstream of the E2 gene (DiMaio and Petti, 2013). It is largely located in the membranes of the endoplasmic reticulum (ER) and Golgi apparatus (GA) of the host cells (Pennie et al., 1993; Schlegel et al., 1986). In particular, BPV1-E5 binds and activates the PDGFß-receptor stimulating cell proliferation (Borzacchiello et al., 2006) and decreases cell-surface expression of major histocompatibility complex class I (MHCI) antigens (Ashrafi et al., 2006, 2002).

Late region

The late region covers almost 40% of the virus genome and follows the early region. It contains the L1 and L2 ORFs, which encode for a major (L1) and a minor (L2) capsid protein (Zheng and Baker, 2006).

The L1 major capsid protein is highly conserved among all PVs and can spontaneously self-assemble into 72-pentamer virus-like particles (VLPs) (Buck et al., 2013).

The L2 minor capsid protein represents the 20% of capsid proteins and lacks the ability to form VLPs. L2 plays major role in both papillomavirus assembly and infectious process and facilitates encapsidation of the viral genome (Wang and Roden, 2013).

L1 and L2 interacts to form the viral icosahedral capsid arranged as 72 capsomers (Buck et al., 2008; Cerqueira and Schiller, 2016)

1.4 Life cycle

Since PVs lack replicative enzymes (except for the E1), their life cycle is strictly associated to host cell factors, and it is tightly linked to host cell keratinocyte differentiation in order to release virions and establish a productive infection. The initial phase of PV life cycle requires the infection of stem cells in the basal layer of epithelia, through a break or a microwounding of the skin or mucosa that allows infective particles to reach the basal lamina (Egawa, 2003). Since the hair follicles are reach in stem cells, they could represent an important site of entry especially for cutaneous papillomaviruses (Doorbar, 2005; Schmitt et al., 1996). Receptors and mechanism through which viruses can entry into host cells are not completely known yet, although most studies have proposed a pivotal role of heparan sulphate proteoglycan interaction (Giroglou et al., 2001; Johnson et al., 2009). Following internalization and uncoating, the viral DNA genome is transported into the nucleus and it is maintained as a low copy number episome (10-200 copies) in the basal cells of the epithelium (Doorbar et al., 2012). The replication protein E1 and E2 are essential during the initial phase of amplification: the E2 recruits the helicase E1 and loads it onto the viral origin of replication located in the LCR. Furthermore, the E2 has a role in the regulation of viral transcription (Bergvall et al., 2013; McBride, 2013).

At this point the longevity of the stem cells is a key factor for the establishment of a persistent and productive lesion (Egawa, 2003), especially for low-risk HPV types (LR-HPV) that are not capable to induce a strong basal cell proliferation (Doorbar et al., 2012). In the case of HR-HPVs that cause cell proliferation and neoplasia, the role of E6 and E7 during this phase is clear and essential (Doorbar et al., 2012). Alternatively, a latent phase can take place with low-viral gene expression and viral copy number (Maglennon and Doorbar, 2012). The outcome of the infection (productive phase, latent phase, lesion regression, clearance) is mostly related to the type of PV and, especially, to the host immune response. Immunodeficiency conditions, such as organ transplant or immunodeficiency virus infections (humans and felines), can lead to lesion development or activation of latent infections (Maglennon et al., 2014).

The genome maintenance or the latent phase can be followed by a proliferative-phase, characterized by the expression of E6 and E7 oncogenes that stimulate cell cycle progression and delay normal keratinocyte differentiation. The delay of differentiation stimulates the amplification of viral genome from hundreds to thousands of copies per cell of the suprabasal epithelial layer, also producing the thickening of the skin (wart) typical of many papillomavirus infections.

To complete the PV life cycle, the structural proteins L1 and L2 are also expressed in the upper layer of the epithelium where the viral genomes are encapsidated. At this point well-differentiated keratinocites exit from cell cycle, and the infective virions are released with the contribution of the abundant E4 protein that disrupts keratine structure (Doorbar, 2013; Doorbar et al., 2012).

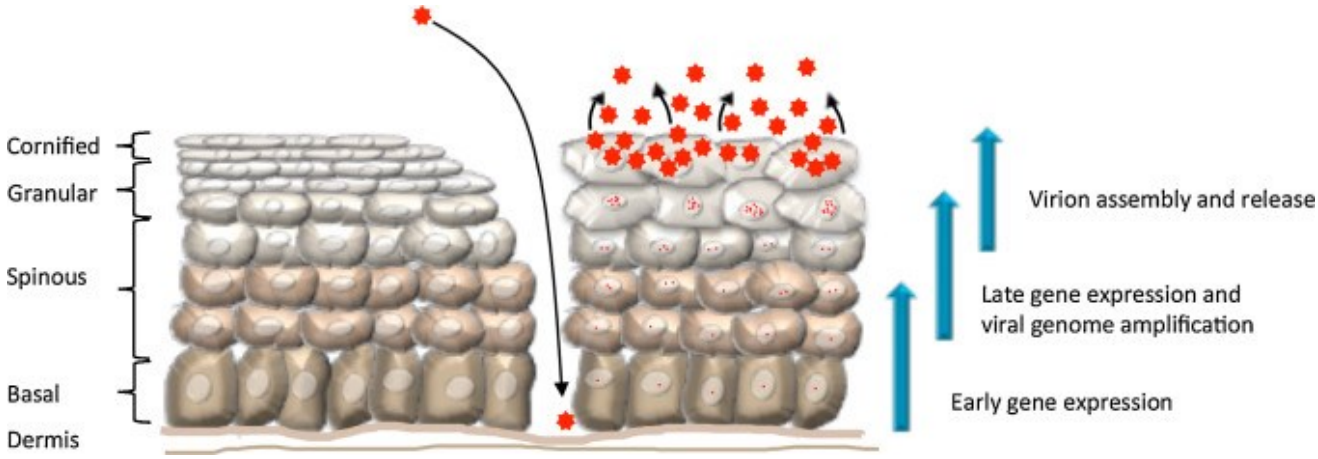

Figure 4 *PV life cycle representation* (Anacker and Moody, 2016)*: viral protein E1, E2, E6,E7 are expressed erly during infection that occurs in the stem cells of the basal epithelial layer. Late genes (L1 and L2) are expressed later in the suprabasal cells and assembled into virions in the well differentiated keratinocytes of the upper layer.*

The productive life cycle that leads to virus synthesis cannot be completed in PV-associated cancers. Compared to the high prevalence of PVs, the number of benign lesions that progress to cancer is very low. For mucosal HR-HPV types, the progression from productive lesions to high-grade neoplasia is the result of a deregulated long-term overexpression of E6 and E7 viral transforming proteins, which facilitates the accumulation of host-DNA damages (Doorbar, 2005). Furthermore, the integration of viral DNA into the host chromosome is another key factor for cancer progression. Around 70% of cervical cancers caused by HPV16 cointain integrated HPV16 genome, while HPV18 genome is almolst exclusively integrated (Doorbar et al., 2012). The integration occurs randomly and the break point in the viral genome lies within the E1 or E2 genes (Yu et al., 2005), whose regulative function is lost facilitating the persistent high-level expression of E6 and E7 genes.

1.5 Papillomavirus transforming properties and skin carcinogenesis

Since the discovery of the papillomavirus aetiology of human cervical carcinoma, most of the studies regarding PV transforming activity have been focused on mucosal HPVs belonging to the alpha genus due to their medical importance. Indeed, the same amount of investigation

about cutaneous types is not available yet. Most of PVs do not have a role in tumour progression and are found in healthy skin and mucosa (Antonsson and McMillan, 2006). The current thinking is that these viruses are well adapted to their host and are controlled by the host immune system, with only limited production of virions (Doorbar, 2016).

Non-melanoma skin cancers (NMSC) comprise basal cell carcinoma (BCC), Bowen's disease, cutaneous squamous cell carcinoma (SCC), and its early stage actinic keratosis (AK). They primarily develop in sun-exposed areas of the body, revealing that UV radiation is a main risk factor for tumour progression. The implication of HPVs in skin cancer was first reported in patients with epidermodysplasia verruciformis (EV). EV condition increases the risk of developing SCC on sun-exposed areas of the body 30–40 years after infection. Isolation of HPVs (especially HPV5 and 8) from 90% of EV associated-SCC, suggested that HPVs might act as a co-carcinogen with UVR (Accardi and Gheit, 2014). For this reason HPV5 and HPV8 have been classified by the IARC as ''possibly carcinogenic'' (group 2B) to patients with EV (Bouvard et al., 2009). However, the role of PVs in the development of SCCs among normal population is not clear. In fact, cutaneous beta HPV prevalence is definitely higher in precancerous lesions of actinic keratosis than in SCCs (Howley and Pfister, 2015). The hypothesis is that, oppositely to alpha genus HPV- associated cancers, cutaneous PVs may have a role only during early stages of cancer formation but are not necessary for tumour maintenance and they may act with a "hit-and-run" mechanism (Howley and Pfister, 2015; Tommasino, 2016). This can be generally assumed also for cutaneous animal papillomaviruses probably involved in NMSC genesis, even if only few types have been studied for their transforming properties as model systems for PV-associated human diseases (Doorbar, 2016). Recently Altamura et al. demonstrated the expression of FcaPV2 genes in oral and skin SCCs and the transforming ability of E6 and E7 oncoproteins in corrupting p53 and pRb pathways, suggesting a possible causative role of this virus in the development of feline SCC (Altamura et al., 2016).

E6 and E7 are considered the major papillomavirus oncoproteins and they have developed several mechanisms to target the regulation of DNA repair machinery and apoptosis (Tommasino, 2016) leading to cellular immortalization and transformation.

Transforming properties of E6

The best-known function of alpha HPV E6 proteins is the capacity to promote p53 proteasome degradation by interacting with the conserved LXXL motif of the ubiquitin ligase E3 enzyme (E6AP). p53 guarantees the integrity of the cellular genome by regulating the cell

cycle, DNA repair machinery, and apoptosis. Its inactivation is a frequent event in cancer, and it is a key event in virus-induced transformation, as demonstrated by strategies evolved by oncogenic viruses to inactivate it (Accardi and Gheit, 2014). E6 proteins of cutaneous types are more enigmatic regarding their cellular transformation activities. Some of them do not interfere with p53 signalling or use different mechanisms. For instance, E6 and E7 genes of HPV 38 increase Δnp73 expression that inhibits the capacity of p53 to induce transcription of factors involved in growth suppression and apoptosis (Accardi et al., 2006). As for alpha types, some beta HPVs can also inhibit the expression of p53 regulated genes by directly interacting with the p300, an acetyltransferase involved in p53 gene acetylation and activation (Muench et al., 2010). Similarly to alpha types, the E6 of several beta HPVs and of BPV1 binds the LXXL motif of the Mastermind-like 1 (MAML1), a core component of the canonical Notch signalling pathway (Brimer et al., 2012; Tan et al., 2012). In keratinocytes, the Notch signalling pathway has a key role in cell-cycle arrest and differentiation (Rangarajan et al., 2001) and its inactivation by E6 might support viral life cycle. Moreover, beta HPVs efficiently inhibit UV-induced apoptosis by stimulating the degradation of the proapoptotic protein bak, a member of the bcl-2 family that is activated in the epidermis after UV irradiation (Jackson et al., 2000; Underbrink et al., 2008). All these functions cause persistent UV-induced DNA damages and suggest that cutaneous PV types may act as co-factors during skin cancer development.

Transforming properties of E7

The most studied property of mucosal HR-HPV E7 oncoproteins is the ability to associate with the tumour suppressor retinoblastoma protein (pRB) and the related pocket proteins p107 and p130, via the LXCXE motif located in the CR2 region. The three proteins are involved in cell cycle control by modulating G1/S entry and progression. In quiescent cells, pRb binds and inhibits transcriptional factors of the E2F family. Phosphorylation of pRB, mediated by cyclin-dipendent kinase (CDK) activity, leads to the disruption of pRB/E2F complexes, with consequent activation of E2F transcription factors. HR-HPV E7s mimic this phosphorylation by binding pRB and promoting pRB proteasomal degradation. The activation of E2F factors results in the transcription of genes encoding proteins such as cyclin E and cyclin A, whose accumulation activates CDKs and guarantee cell cycle progression (Tommasino, 2014). pRB degradation and the resulting activation of E2F-mediated transcription are pivotal mechanisms by which these viruses achieve and maintain DNA synthesis competence in differentiated epithelial cells (McLaughlin-Drubin and Münger, 2009). Nevertheless, pRb binding efficiency does not necessarily correlate with the ability to degrade the tumour suppressor and to induce cellular transformation as it has been demonstrated especially for cutaneous PV types (Caldeira et al., 2003; Ciccolini et al., 1994). Very few studies demonstrate that also the E7 of cutaneous HPVs containing the LXCE motif can bind the pRB, even if with different affinities (Altamura et al., 2016; Caldeira et al., 2003; Cornet et al., 2012). For instance, HPV38 E7 efficiently binds pRB but, instead promoting its degradation, leads to pRB hyper-phosphorylation and stabilization in human primary keratinocyte models. As for the E6, E7 biological properties of cutaneous PVs have not been well identified yet. Therefore, this research project intends to investigate the role of E6 and E7 of cutaneous animal PVs in cell immortalization and transformation.

1.6 Animal papillomaviruses

More than 220 different HPVs have been identified and classified so far. A comparable PV genotype variety has not yet been detected within other animal species, especially because of the absence of a conventional cell culture system for *in vitro* viral propagation. Although they are less studied, animal papillomaviruses (notably BPV, CRPV and ROPV) have always been used as models to investigate the virus biology, its relationship with the host, the host immune response to the virus and to develop papillomavirus vaccines (Campo, 2002; Doorbar, 2016).

In the last decade, thanks to the introduction of the multiple primed rolling circle amplification (RCA) for PV detection (Johne et al., 2009; Rector et al., 2004; Stevens et al., 2010), many new PV types were discovered and fully characterized. Since PVs have not been found in amphibians so far, it is probable that the host range of these viruses is restricted to amniotes (Rector and Van Ranst, 2013). Papillomaviruses are highly species-specific and co-evolve with their natural hosts. However, few types are able to cross-infect species (Scagliarini et al., 2013). The bovine PV types 1 and 2 are able to infect horses and cause the equine sarcoid, the most diagnosed skin tumour among equidae (Chambers et al., 2003; Lancaster et al., 1979). Recently a papillomaviral aetiology has been proposed also for feline sarcoids, due to the detection of the BPV14 in these lesions but not in any non-sarcoid feline sample (Munday et al., 2015).

All non-human PVs identified so far are listed in Table 1. To date, 71 PV species (belonging to 46 PV genera) have been rescued from 75 vertebrate host species, including 5 birds, 3 reptiles and, recently, 1 fish (López-Bueno et al., 2016). The majority of them are recovered from benign lesions of the skin and mucosa but some types are implicated in carcinogenesis, in many cases as cofactors together with UV-exposition or chemicals [e.g. quercetin in bracken fern in the case of bovine gastrointestinal SCCs caused by BPV4 (Pennie and Saveria Campo, 1992)].

Table 1 *Animal papillomaviruses listed on Papillomavirus Episteme (https://pave.niaid.nih.gov).*

Virus	PaVE Name	Species Name	Host Common Name	Host Scientific Name	Isolated from	Genbank ID
AaPV1*	Alces alces Papillomavirus 1	Deltapapillomavirus 1	European elk	Alces Alces	Cutaneous fibroma	M15953
AgPV1	Alouatta guariba papillomavirus 1	Dyoomikronpapillomavirus	Brown howler	Alouatta guariba	Healthy oral mucosa	KP861980
AsPV1	Apodemus sylvaticus Papillomavirus 1	Pipapillomavirus 2	Long tailed field mouse	Apodemus sylvaticus	Normal skin ear	HQ625440
BPV1*	Bos taurus Papillomavirus 1	Deltapapillomavirus 4	Domestic Cow	Bos Taurus	Cutaneous fibropapilloma	X02346
BPV2*	Bos taurus Papillomavirus 2	Deltapapillomavirus 4	Domestic cow	Bos taurus	Cutaneous fibropapilloma	M20219
BPV3*	Bos taurus Papillomavirus 3	Xipapillomavirus 1	Domestic cow	Bos taurus	Cutaneous papilloma	AF486184
BPV4*	Bos taurus Papillomavirus 4	Xipapillomavirus 1	Domestic cow	Bos taurus	Oral/esophageal papilloma	X05817
BPV5*	Bos taurus Papillomavirus 5	Epsilonpapillomavirus 1	Domestic cow	Bos taurus	Udder fibropapilloma	AF457465
BPV6*	Bos taurus Papillomavirus 6	Xipapillomavirus 1	Domestic cow	Bos taurus	Udder papilloma	AJ620208
BPV7*	Bos taurus Papillomavirus 7	Dyoxipapillomavirus 1	Domestic cow	Bos taurus	Teat papilloma and healthy skin	DQ217793
BPV8*	Bos taurus Papillomavirus 8	Epsilonpapillomavirus 1	Domestic cow	Bos taurus	Cutaneous papilloma	DQ098913
BPV9*	Bos taurus Papillomavirus 9	Xipapillomavirus 1	Domestic cow	Bos taurus	Teat papilloma	AB331650
BPV10*	Bos taurus Papillomavirus 10	Xipapillomavirus 1	Domestic cow	Bos taurus	Teat papilloma	AB331651
BPV11*	Bos taurus Papillomavirus 11	Xipapillomavirus 1	Domestic cow	Bos taurus	Cutaneous papilloma	AB543507

BPV12*	Bos taurus Papillomavirus 12	Xipapillomavirus 2	Domestic cow	Bos taurus	Tongue epithelial papilloma	JF834523
BPV13	Bos taurus Papillomavirus 13	Deltapapillomavirus 4	Domestic cow	Bos taurus	Ear cutaneous papilloma	JQ798171
BPV14	Bovine papillomavirus 14	Deltapapillomavirus 4	Domestic cow	Bos taurus	Cutaneous fibropapilloma/Feline sarcoid	KP276343
BPV15	Bovine papillomavirus 15	Xipapillomavirus 1	Domestic cow	Bos taurus		KM983393
BPV16	Bovine papillomavirus 16	Dyokappapapillomavirus	Domestic cow	Bos taurus	Epidermal papillomatosis	KU519391
BPV17	Bovine papillomavirus 17	Xipapillomavirus	Domestic cow	Bos taurus	Epidermal papillomatosis	KU519392
BPV18	Bovine papillomavirus 18	Dyokappapapillomavirus	Domestic cow	Bos taurus	Epidermal papillomatosis	KU519393
BPV19	Bovine papillomavirus 19	Unclassified	Domestic cow	Bos taurus	Epidermal papillomatosis	KU519394
BPV20	Bovine papillomavirus 20	Xipapillomavirus	Domestic cow	Bos taurus	Epidermal papillomatosis	KU519395
BPV21	Bovine papillomavirus 21	Unclassified	Domestic cow	Bos taurus	Epidermal papillomatosis	KU519396
BgPV1	Bos grunniens papillomavirus 1	Deltapapillomavirus 4	Yak	Bos grunniens	Cutaneous fibropapilloma	JX174437
BpPV1	Bettongia penicillata papillomavirus 1	Dyolambdapapillomavirus 1	Brush-tailed Bettong	Bettongia penicillata	Cutaneous papilloma	GU220391
CPV1*	Canis familiaris oral Papillomavirus 1	Lambdapapillomavirus 2	Domestic dog	Canis familiaris	Oral/cutaneous papilloma	D55633
CPV2*	Canis familiaris Papillomavirus 2	Taupapillomavirus 1	Domestic dog	Canis familiaris	Cutaneous papilloma	AY722648
CPV3*	Canis familiaris Papillomavirus 3	Chipapillomavirus 1	Domestic dog	Canis familiaris	Malignant EV lesion	DQ295066
CPV4*	Canis familiaris Papillomavirus 4	Chipapillomavirus 2	Domestic dog	Canis familiaris	Pigmented lesion	EF584537
CPV5*	Canis familiaris Papillomavirus 5	Chipapillomavirus 1	Domestic dog	Canis familiaris	Pigmented plaque	FJ492743

CPV6*	Canis familiaris Papillomavirus 6	Lambdapapillomavirus 3	Domestic dog	Canis familiaris	Inverted papilloma	FJ492744
CPV7*	Canis familiaris Papillomavirus 7	Taupapillomavirus 1	Domestic dog	Canis familiaris	In situ squamous cell carcinoma	FJ492742
CPV8	Canis familiaris papillomavirus 8	Chipapillomavirus 3	Domestic dog	Canis familiaris	Pigmented plaque	HQ262536
CPV9	Canis familiaris papillomavirus 9	Chipapillomavirus 1	Domestic dog	Canis familiaris	Pigmented plaque	JF800656
CPV10	Canis familiaris papillomavirus 10	Chipapillomavirus 3	Domestic dog	Canis familiaris	Pigmented plaque	JF800657
CPV11	Canis familiaris papillomavirus 11	Chipapillomavirus 1	Domestic dog	Canis familiaris	Pigmented plaque	JF800658
CPV12	Canis familiaris papillomavirus 12	Chipapillomavirus 1	Domestic dog	Canis familiaris		JQ754321
CPV13	Canis familiaris papillomavirus 13	Taupapillomavirus 2	Domestic dog	Canis familiaris	Oral papilloma	JX141478
CPV14	Canis familiaris papillomavirus 14	Chipapillomavirus 3	Domestic dog	Canis familiaris	Pigmented plaque	JQ701802
CPV15	Canis familiaris papillomavirus 15	Chipapillomavirus 3	Domestic dog	Canis familiaris		JX899359
CPV16	Canis familiaris papillomavirus 16	Chipapillomavirus 2	Domestic dog	Canis familiaris		KP099966
CPV17	Canis familiaris papillomavirus 17	Taupapillomavirus	Domestic dog	Canis familiaris	Oral squamous cell carcinoma	KT272399
CPV18	Canis familiaris papillomavirus 18	Chipapillomavirus	Domestic dog	Canis familiaris	Pigmented plaques	KT326919
CPV19	Canis familiaris papillomavirus 19	Taupapillomavirus	Domestic dog	Canis familiaris		KX599536

CPV20	Canis familiaris papillomavirus 20	Chipapillomavirus	Domestic dog	Canis familiaris		KT901797
CcPV1*	Caretta caretta Papillomavirus 1	Dyozetapapillomavirus 1	Loggerhead turtle	Caretta caretta	Cutaneous papilloma	EU493092
CcaPV1*	Capreolus capreolus Papillomavirus 1	Deltapapillomavirus 5	Western roe deer	Capreolus capreolus	Cutaneous fibropapilloma	EF680235
CcanPV1	Castor canadensis papillomavirus 1	Dyosigmapapillomavirus 1	North American beaver	Castor canadensis	Cutaneous papilloma	KC020689
CcrPV1	Crocuta crocuta papillomavirus 1	Lambdapapillomavirus 5	Spotted hyena	Crocuta crocuta	Oral papilloma	HQ585856
CdPV1	Camelus dromedarius papillomavirus 1	Deltapapillomavirus 6	Arabian camel	Camelus dromedarius	Cutaneous fibropapilloma	HQ912790
CdPV2	Camelus dromedarius papillomavirus 2	Deltapapillomavirus 6	Arabian camel	Camelus dromedarius	Cutaneous fibropapilloma	HQ912791
CePV*	Cervus elaphus papillomavirus		Red deer	Cervus elaphus	Cutaneous fibropapilloma	JQ744282
CePV1*	Cervus elaphus papillomavirus 1	Epsilonpapillomavirus	Red deer	Cervus elaphus	Pigmented papilloma	KU350625
CePV2	Cervus elaphus papillomavirus 2	Xipapillomavirus	Red deer	Cervus elaphus		KT932712
CgPV1*	Colobus guereza Papillomavirus 1	Alphapapillomavirus 14	Colobus monkey	Colobus guereza		GU014532
CgPV2	Colobus guereza Papillomavirus 2	Betapapillomavirus 1	Colobus monkey	Colobus guereza	Cutaneous papilloma	GU014533
ChPV1*	Capra hircus Papillomavirus 1	Phipapillomavirus 1	Domestic goat	Capra hircus		DQ091200
CmPV1*	Chelonia mydas Papillomavirus 1	Dyozetapapillomavirus 1	Green seaturtle	Chelonia mydas	Cutaneous fibropapilloma	EU493091

DdPV1	Delphinus delphis papillomavirus	Upsilonpapillomavirus 1	Common short beaked dolphin	Delphinus delphis	Penile wart	GU117620
EaPV1*	Equus asinus papillomavirus	Dyochipapillomavirus 1	Donkey	Equus Asinus	Healthy skin	KF741371
EcPV1*	Equus caballus Papillomavirus 1	Zetapapillomavirus 1	Domestic horse	Equus ferus caballus	Cutaneous papilloma	AF498323
EcPV2*	Equus caballus Papillomavirus 2	Dyoiotapapillomavirus 1	Domestic horse	Equus ferus caballus	Equine genital neoplasia	EU503122
EcPV3*	Equus caballus papillomavirus 3	Dyorhopapillomavirus 1	Domestic horse	Equus ferus caballus	Aural plaque	GU384895
EcPV4*	Equus caballus papillomavirus 4	Dyoiotapapillomavirus 2	Domestic horse	Equus ferus caballus	Vulval and inguinal plaque	JQ031032
EcPV5*	Equus caballus papillomavirus 5	Dyoiotapapillomavirus 2	Domestic horse	Equus ferus caballus	Aural plaque	JQ031033
EcPV6*	Equus caballus papillomavirus 6	Dyorhopapillomavirus 1	Domestic horse	Equus ferus caballus	Aural plaque	JQ965698
EcPV7*	Equus caballus papillomavirus 7	Dyorhopapillomavirus 1	Domestic horse	Equus ferus caballus	Penile mass	JX035935
EcPV8	Equus caballus papillomavirus 8	Unclassified	Domestic horse	Equus ferus caballus		KU963288
EdPV1*	Erethizon dorsatum Papillomavirus 1	Sigmapapillomavirus 1	North American porcupine	Erethizon dorsatum	Cutaneous papilloma	AY684126
EePV1*	Erinaceus europaeus Papillomavirus 1	Dyoetapapillomavirus 1	European hedgehog	Erinaceus europaeus	Facial hair follicles	FJ379293
EhPV1	Eidolon helvum papillomavirus 1	Dyoupsilonpapillomavirus 1	straw-colored fruit bat	Eidolon helvum		JX123128
ElPV1	Enhydra lutris papillomavirus 1	Lambdapapillomavirus 4	Sea Otter	Enhydra lutris	Oral lesion	KJ410351

EsPV1	Eptesicus serotinus papillomavirus 1	Dyopsipapillomavirus 1	Serotine bat	Eptesicus serotinus	Oropharyngeal/anogenital swab	KC858263
EsPV2	Eptesicus serotinus papillomavirus 2	Dyoomegapapillomavirus 1	Serotine bat	Eptesicus serotinus	Oropharyngeal/anogenital swab	KC858264
EsPV3	Eptesicus serotinus papillomavirus 3	Dyopsipapillomavirus 1	Serotine bat	Eptesicus serotinus	Anogenital mucosa	KC858265
FcPV1*	Fringilla coelebs Papillomavirus	Etapapillomavirus 1	Common Chaffinch	Fringilla coelebs	Squamous papilloma	AY057109
FcaPV1*	Felis catus domesticus Papillomavirus 1	Lambdapapillomavirus 1	Domestic cat	Felis domesticus	Cutaneous papilloma	AF480454
FcaPV2*	Felis catus domesticus Papillomavirus 2	Dyothetapapillomavirus 1	Domestic cat	Felis domesticus	Pigmented plaque/ Bowenoid in situ carcinoma	EU796884
FcaPV3	Felis catus papillomavirus 3	Taupapillomavirus 3	Domestic cat	Felis domesticus	Bowenoid in situ carcinoma	JX972168
FcaPV4	Felis catus papillomavirus 4	Taupapillomavirus 3	Domestic cat	Felis domesticus	Oral mucosa	KF147892
FgPV1	Fulmarus glacialis papillomavirus 1	Treiszetapapillomavirus	Northern fulmar	Fulmarus Glacialis		KJ452243
FlPV1*	Francolinus leucoscepus Papillomavirus 1	Dyoepsilonpapillomavirus 1	Yellow necked Francolin	Francolinus leucoscepus	Healthy skin	EU188799
GcPV1	Giraffa camelopardalis Papillomavirus 1	Deltapapillomavirus	Giraffe	Giraffa camelopardalis	Fibropapillomas	KX954132
LrPV1*	Lynx rufus Papillomavirus 1	Lambdapapillomavirus 1	Bobcat	Lynx rufus	Oral papilloma	AY904722
MaPV1*	Mesocricetus auratus Papillomavirus 1	Pipapillomavirus 1	Syrian golden hamster	Mesocricetus auratus	Oral papilloma	E15111
McPV2*	Mastomys coucha Papillomavirus 2	Pipapillomavirus 2	Multimammate mouse	Mastomys coucha	Skin carcinoma	DQ664501

MfPV1	Macaca fascicularis Papillomavirus 1	Betapapillomavirus 1	Cynomolgus macaque	Macaca fascicularis	Cutaneous papilloma	EF028290
MfPV2	Macaca fascicularis Papillomavirus 2	Betapapillomavirus 6	Cynomolgus macaque	Macaca fascicularis	Cutaneous papilloma	GU014531
MfPV3	Macaca fascicularis Papillomavirus 3	Alphapapillomavirus 12	Cynomolgus macaque	Macaca fascicularis	Cervical intraepithelial neoplasia	EF558839
MfPV4	Macaca fascicularis Papillomavirus 4	Alphapapillomavirus 12	Cynomolgus macaque	Macaca fascicularis	Cervical intraepithelial neoplasia	EF558841
MfPV5	Macaca fascicularis Papillomavirus 5	Alphapapillomavirus 12	Cynomolgus macaque	Macaca fascicularis	Cervical intraepithelial neoplasia	EF558843
MfPV6	Macaca fascicularis Papillomavirus 6	Alphapapillomavirus 12	Cynomolgus macaque	Macaca fascicularis		EF558840
MfPV7	Macaca fascicularis Papillomavirus 7	Alphapapillomavirus 12	Cynomolgus macaque	Macaca fascicularis		EF558838
MfPV8	Macaca fascicularis Papillomavirus 8	Alphapapillomavirus 12	Cynomolgus macaque	Macaca fascicularis	Cervical intraepithelial neoplasia	EF558842
MfPV9	Macaca fascicularis Papillomavirus 9	Alphapapillomavirus 12	Cynomolgus macaque	Macaca fascicularis		EU490516
MfPV10	Macaca fascicularis Papillomavirus 10	Alphapapillomavirus 12	Cynomolgus macaque	Macaca fascicularis		EU490515
MfPV11	Macaca fascicularis Papillomavirus 11	Alphapapillomavirus 12	Cynomolgus macaque	Macaca fascicularis		GQ227670
MfuPV1	Macaca fuscata papillomavirus 1	Alphapapillomavirus	Japanese Macaque	Macaca fuscata		KT944080
MmPV1*	Macaca mulata Papillomavirus 1	Alphapapillomavirus 12	Rhesus macaque	Macacca mulata	Mucosal genital carcinoma	M60184
MmiPV1	Micromys minutus Papillomavirus 1	Pipapillomavirus 2	Old World harvest mouse	Micromys minutus	Cutaneous papilloma	DQ269468

MmuPV1	Mus musculus papillomavirus type 1	Pipapillomavirus 2	House mouse	Mus musculus	Cutaneous papilloma	GU808564
MnPV1*	Mastomys natalensis Papillomavirus 1	Iotapapillomavirus 1	Multimammate mouse	Mastomys natalensis	Cutaneous papilloma	U01834
MpPV1	Mustela putorius papillomavirus 1	Taupapillomavirus	European polecat	Mustela putorius	Faeces	KF006988
MrPV1	Myotis ricketti papillomavirus 1	Unclassified	Ricketts big-footed bat	Myotis ricketti	Pharyngeal swab or anal swab	JQ814847
MsPV1	Morelia spilota papillomavirus 1	Dyomupapillomavirus 1	Carpet python	Morelia spilota	Pigmented papilloma-like lesions	HQ262535
MscPV1	Miniopterus schreibersii papillomavirus 1	Unclassified	Common bent-wing bat	Miniopterus schreibersii	Pharyngeal swab or anal swab	JQ814848
MscPV2	Miniopterus schreibersii papillomavirus 2	Dyotaupapillomavirus 1	Common bent-wing bat	Miniopterus schreibersii	Rectal swab	JQ692938
OaPV1*	**Ovis aries Papillomavirus 1**	**Deltapapillomavirus 3**	**Domestic sheep**	**Ovis aries**	**Cutaneous fibropapilloma**	**U83594**
OaPV2*	**Ovis aries Papillomavirus 2**	**Deltapapillomavirus 3**	**Domestic sheep**	**Ovis aries**	**Cutaneous fibropapilloma**	**U83595**
OaPV3*	**Ovis aries Papillomavirus 3**	**Dyokappapapillomavirus 1**	**Domestic sheep**	**Ovis aries**	**Squamous carcinoma**	**FJ796965**
OcPV1*	Oryctolagus cuniculus Papillomavirus 2	Kappapapillomavirus 1	New Zealand white rabbit	Oryctolagus cuniculus	Oral papilloma	AF227240
OvPV1*	Odocoileus virginianus Papillomavirus 1	Deltapapillomavirus 2	American White-tailed deer	Odocoileus virginianus	Cutaneous fibroma	M11910
PaPV1	Pygoscelis adeliae papillomavirus	Treisepsilonpapillomavirus 1	Adelie penguin	Pygoscelis adeliae	Faeces	KJ173785
PcPV1*	Puma concolor Papillomavirus 1	Lambdapapillomavirus 1	Puma	Puma concolor	Oral papilloma	AY904723

PePV1*	Psittacus erithacus Papillomavirus 1	Thetapapillomavirus 1	Gray parrot	Psittacus erithacus	Cutaneous papilloma	AF502599
PhPV1	Papio hamadryas papillomavirus 1	Alphapapillomavirus 12	Hamadryas baboon	Papio hamadryas	Cervical samples (CIN1)	JF304764
PlPV1*	Procyon lotor Papillomavirus 1	Lambdapapillomavirus 4	Raccoon	Procyon lotor	Cutaneous papilloma	AY763115
PlpPV1*	Panthera leo persica Papillomavirus 1	Lambdapapillomavirus 1	Asiatic lion	Panthera leo persica	Oral papilloma	AY904724
PmPV1	Peromyscus papillomavirus 1	Iotapapillomavirus	Peromyscus	Peromyscus	Faeces	JF755418
PpPV1*	Pan paniscus Papillomavirus 1	Alphapapillomavirus 10	Pygmy chimpanzee	Pan paniscus	Oral epithelial hyperplasia	X62844
PphPV1	Phocoena phocoena papillomavirus	Omikronpapillomavirus 1	Harbor porpoise	Phocoena phocoena	Penile papilloma	GU117621
PphPV2	Phocoena phocoena papillomavirus	Upsilonpapillomavirus 3	Harbor porpoise	Phocoena phocoena	Penile papilloma	GU117622
PphPV4	Phocoena phocoena papillomavirus	Dyopipapillomavirus 1	Harbor porpoise	Phocoena phocoena	Penile papilloma	GU117623
PpuPV1	Pudu puda papillomavirus type 1	Unclassified	Pudu	Pudu puda		KT932713
PsPV1*	Phocoena spinipinnis Papillomavirus	Omikronpapillomavirus 1	Burmeisters porpoise	Phocoena spinipinnis	Genital papilloma	AJ238373
PsuPV1	Phodopus sungorus papillomavirus type 1	Pipapillomavirus 1	Siberian Hamster	Phodopus sungorus	Anogenital lesion	HG939559
RaPV1*	Rousettus aegyptiacus Papillomavirus 1	Psipapillomavirus 1	Egyptian rousette fruitbat	Rousettus aegyptiacus	Squamous carcinoma	DQ366842
RalPV1	Rusa alfredi Papillomavirus 1	Deltapapillomavirus	Visayan spotted deer	Rusa alfredi	Cutaneous fibropapilloma	KT626573

RfPV1	Rhinolophus ferrumequinum papillomavirus type 1	Treisdeltapapillomavirus 1	Greater horseshoe bat	Rhinolophus ferrumequinum	Mucosal swab	KC858266
RnPV1*	Rattus norvegicus Papillomavirus 1	Pipapillomavirus 2	Norwegian rat	Rattus norvegicus	Normal oral mucosa	GQ180114
RnPV2	Rattus norvegicus Papillomavirus 2	Iotapapillomavirus 1	Norwegian rat	Rattus norvegicus	Rectal smear	HQ625441
RnPV3	Rattus norvegicus Papillomavirus 3	Iotapapillomavirus 1	Norwegian rat	Rattus norvegicus	Faeces	KT945134
RrPV1*	Rupicapra rupicapra papillomavirus 1	Dyokappapapillomavirus 2	Chamois	Rupicapra rupicapra	Cutaneous exophytic cauliflower-like neoplasia	KC876045
RtPV1*	Rangifer tarandus Papillomavirus 1	Deltapapillomavirus 1	Reindeer	Rangifer tarandus	Cutaneous fibropapilloma	AF443292
RtPV2	Rangifer tarandus papillomavirus 2	Xipapillomavirus 3	Reindeer	Rangifer tarandus	Swab of keratoconjunctivitis affected eye	KC810012
RtiPV1	Rusa timorensis papillomavirus 1	Unclassified	Javan rusa	Rusa timorensis		KP757765
SaPV1	Sparus aurata Papillomavirus type 1	Unclassified	Gilt-head bream	Sparus aurata	Lymphocystis disease	KX643372
SfPV1*	Sylvilagus floridanus Papillomavirus 1	Kappapapillomavirus 2	Cottontail rabbit	Sylvilagus floridanus	Cutaneous papilloma	K02708
SsPV1*	Sus scrofa Papillomavirus 1	Dyodeltapapillomavirus 1	Domestic pig	Sus scrofa	Healthy skin swab	EF395818
SscPV1	Saimiri sciureus papillomavirus 1	Dyoomikronpapillomavirus 1	Common squirrel monkey	Saimiri sciureus		JF304765
SscPV2	Saimiri sciureus papillomavirus 2	Dyoomikronpapillomavirus 1	Common squirrel monkey	Saimiri sciureus		JF304766

SscPV3	Saimiri sciureus papillomavirus 3	Dyoomikronpapillomavirus 1	Common squirrel monkey	Saimiri sciureus		JF304767
TePV1*	Talpa europaea papillomavirus 1	Dyophipapillomavirus 1	European mole	Talpa europaea	Healthy epithelial tissue	KC460987
TmPV1*	Trichechus manatus latirostris Papillomavirus 1	Rhopapillomavirus 1	Caribbean manatee	Trichechus manatus latirostris	Cutaneous papilloma	AY609301
TmPV2	Trichechus manatus latirostris Papillomavirus 2	Rhopapillomavirus 1	Caribbean manatee	Trichechus manatus latirostris		JN709473
TmPV3	Trichechus manatus latirostris Papillomavirus 3	Rhopapillomavirus 2	Caribbean manatee	Trichechus manatus latirostris	Mucosa	KP205502
TmPV4	Trichechus manatus latirostris Papillomavirus 4	Rhopapillomavirus 2	Caribbean manatee	Trichechus manatus latirostris	Mucosa	KP205503
TtPV1*	Tursiops truncatus Papillomavirus 1	Upsilonpapillomavirus 1	Bottlenosed dolphin	Tursiops truncatus	Penile wart	EU240894
TtPV2*	Tursiops truncatus Papillomavirus 2	Upsilonpapillomavirus 2	Bottlenosed dolphin	Tursiops truncatus	Genital lesion	AY956402
TtPV3*	Tursiops truncatus Papillomavirus 3	Upsilonpapillomavirus 1	Bottlenosed dolphin	Tursiops truncatus	Penile wart	EU240895
TtPV4	Tursiops truncatus papillomavirus 4	Upsilonpapillomavirus 1	Bottlenosed dolphin	Tursiops truncatus	Genital lesion	JN709469
TtPV5	Tursiops truncatus papillomavirus 5	Omikronpapillomavirus 1	Bottlenosed dolphin	Tursiops truncatus	Genital lesion	JN709470
TtPV6	Tursiops truncatus papillomavirus 6	Omikronpapillomavirus 1	Bottlenosed dolphin	Tursiops truncatus	Genital lesion	JN709471
TtPV7	Tursiops truncatus papillomavirus 7	Upsilonpapillomavirus 1	Bottlenosed dolphin	Tursiops truncatus	Normal genital mucosa	JN709472

UmPV1*	Ursus maritimus Papillomavirus 1	Omegapapillomavirus 1	Polar bear	Ursus maritimus	Tongue papilloma	EF536349
UuPV1*	Uncia uncia Papillomavirus 1	Lambdapapillomavirus 1	Snow leopard	Uncia uncia	Papilloma lower lip	DQ180494
VvPV1	Vulpes vulpes papillomavirus 1	Treisetapapillomavirus	Red fox	Vulpes vulpes	Hair follicles from healthy skin	KF857586
ZcPV1	Zalophus californianus papillomavirus 1	Dyonupapillomavirus 1	Sealion	Zalophus californianus	Cutaneous papilloma	HQ293213

* PV types marked with an asterisk were used for OaPV4 phylogenetic analysis together with the following HPV types: 41, 1, 63, 6, 2, 18, 45, 97, 54, 16, 48, 50, 4, 60, 101, 103, 21, 25, 5, 8, 93, 179, 38, 49, 75, 96, and 92.

Figure 5 *Phylogenetic tree based on L1 nucleotide sequence alignment of 260 PV types listed in the Papillomavirus Episteme (https://pave.niaid.nih.gov)* (Rector and Van Ranst, 2013).

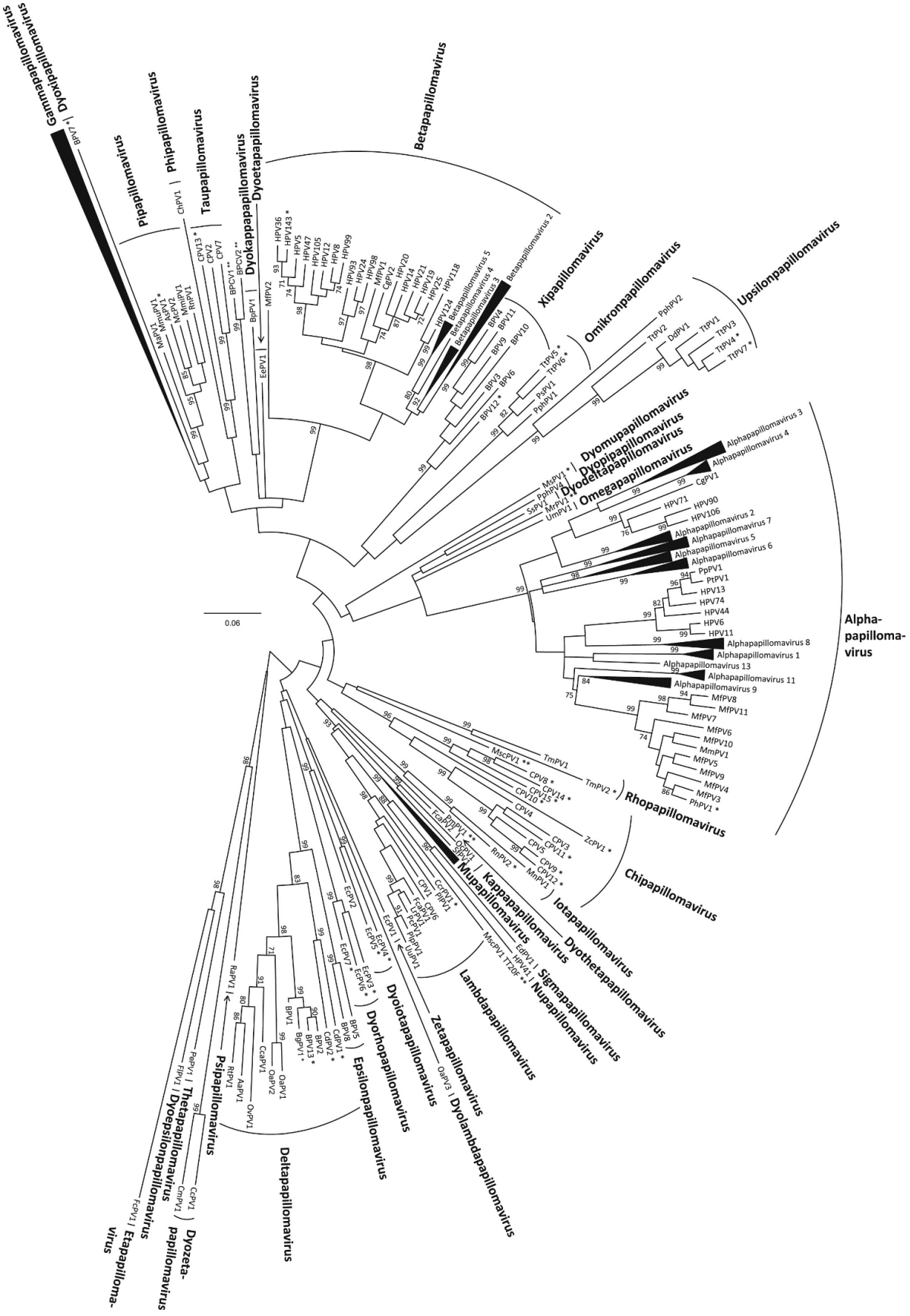

1.7 Ovine papillomaviruses and associated diseases

The first evidence of the association between fibropapillomas (characterized by a strong connective and epithelial tissue proliferation) and the presence of papillomavirus in sheep was established by Gibbs et al. in 1975 (E.P.J. Gibbs, C.J. Smale, 1975). The two first complete ovine papillomavirus genomes (OaPV1 and OaPV2) were isolated from fibropapillomas of merinos sheep in Australia in the early 1990s (Karlis et al., Unpublished) (Uzal et al., 2000) and belong to the Deltapapillomaviruses. This genus includes artiodactyl papillomaviruses that have fibroblasts as primary target and cause fibropapillomas. They are characterized by the lack of the pRB-binding domain within the E7 ORF associated with the presence of the E5 oncoprotein (Narechania et al., 2004). Ovine fibropapillomaviruses are always detected in benign neoplasms and they were never associated with precancerous lesions or non-melanoma skin cancers (NMSCs) such as squamous cell carcinoma (SCC).

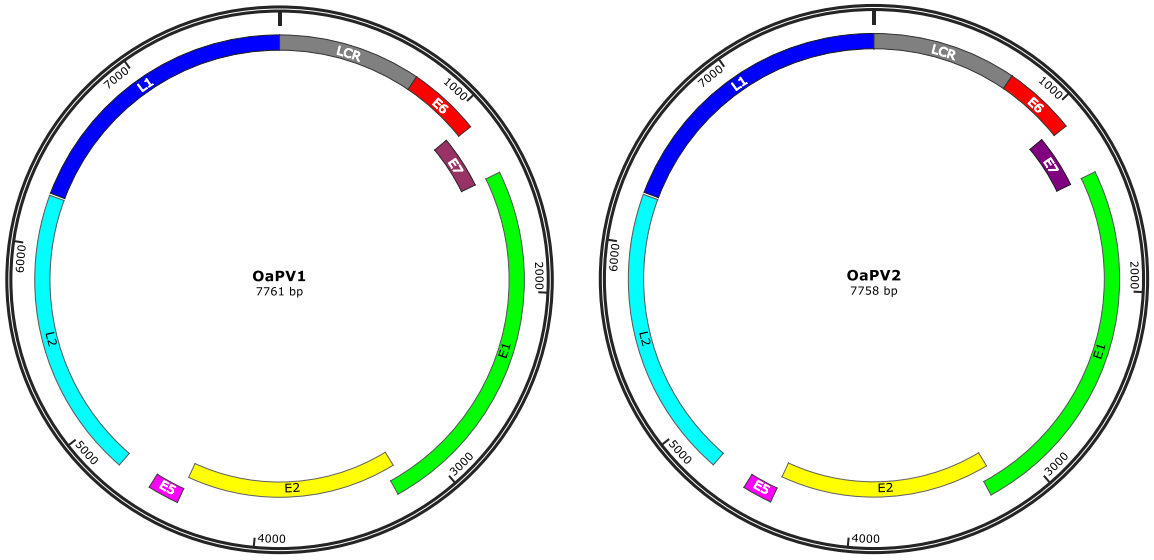

Figure 6 *OaPV1 and OaPV2 genome maps.*

The association between papillomavirus infection and SCC development was supposed since early 1980s when PV DNA was observed in precancerous lesions of sheep skin (Hawkins et al., 1981; Hayward et al., 1993; Norval et al., 1985; Trenfield et al., 1990; Vanselow et al., 1982; Vanselow and Spradbrow, 1983). SCC has high incidence in flocks in some parts of the world and it poses a direct threat to sheep, especially to those highly selected for milk production, such as Sarda breed sheep, by compromising the udders of ewes (Alberti et al., 2010). SCC develops in UV-exposed body parts, and it is heightened by procedures such as mulesing and tail docking that overexpose the perineal area to direct sunlight. A papillomaviral joint cause has been proposed in the past, e.g. Vanselow et al. (1982) reported the apparent transformation of ovine facial papillomas into carcinomas and the presence of virions that resembled papillomaviruses.

In 2009 our scientific team identified and sequenced the genome of the third type of ovine papillomavirus (OaPV3) from cases of well differentiated SCC (Alberti et al., 2010) (Figure 7).

Figure 7 *Severe cases of squamous cell carcinoma in sheep.*

OaPV3 is classified within the new genus Dyokappa together with a papillomavirus type recently recovered from a nasolabial cutaneous neoplasia in a free-ranging alpine chamois (*Rupicapra rupicapra*) (Mengual-Chuliá et al., 2014). OaPV3 and RrPV1 share a 77% L1 nucleotide identity, they cannot be included into any of the four large PV crown groups and are very distantly related to any other known PV. Unlike OaPV1 and OaPV2, OaPV3 lacks the E5 gene and maintains the conserved retinoblastoma tumour suppressor binding sequence motif in E7 (LXCXE). For these reasons, the OaPV3 genome does not meet the criteria for fibroblasts infection and fibropapilloma development typical of Arctiodactyl papillomaviruses, while its gene repertoire is reminiscent of the epitheliotropic human papillomavirus of the *Beta* genus (Alberti et al., 2010) suggesting a role in SCC development.

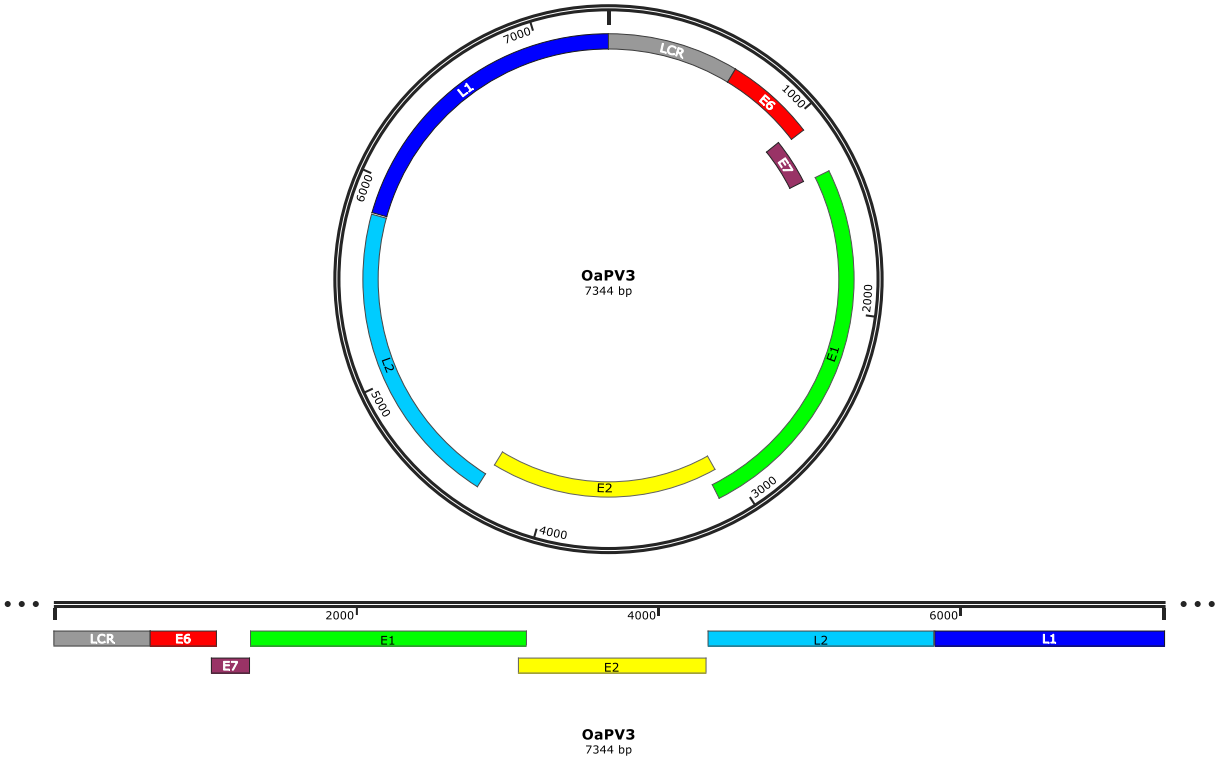

Figure 8 *OaPV3 genome map.*

2. AIMS OF THE RESEARCH

Human is the only well studied host regarding papillomaviral infections; therefore the main goal of this study is to improve knowledge about non-human papillomavirus diversity and biology with a focus within the ovine species.

The research intends to :

- Identify and characterize unknown ovine papillomavirus types from both healthy and lesioned skin and mucosa using sequence-independent amplification methods (rolling circle amplification-RCA).

- Evaluate tissue and cellular tropism of papillomaviral infections in sheep.

- Analyse the *in vitro* transforming abilities of E6 and E7 oncogenes of ovine PVs in a comparative study between the newly discovered Delta papillomavirus OaPV4 and the Dyokappa papillomavirus OaPV3.

- Study the role of cutaneous papillomaviruses in the genesis of non-melanoma skin cancer (NMSC), and suggest OaPVs as useful model systems for PV-associated diseases.

3. MATERIALS

3.1 Bacterial culture media

LB
Tryptone 10g
Yeast extract 5g
NaCl 10g
dH_2O up to 1L

LB AGAR PLATES
Tryptone 10g
Yeast extract 5g
NaCl 10g
dH_2O up to 1L

LB AGAR SELECTION PLATES: pLXSN/pCMV HA-N
Tryptone 10g
Yeast extract 5g
NaCl 10g
dH_2O up to 1L
Add ampicillin 100 µg/ml

LB AGAR SELECTION PLATES: pGEX4T1
Tryptone 10g
Yeast extract 5g
NaCl 10g
dH_2O up to 1L
Add ampicillin 100 µg/ml
Add cloramphenicol 35 µg/ml

3.2 Mammalian cell culture media

DMEM COMPLETE
DMEM 1X
10% FBS
1% penicillin/streptomycin
2Mm L-glutamine

FAD MEDIUM	FAD MEDIUM 400ml
1 part DMEM 1X	100 ml DMEM 1X
3 parts HAM'S F12	300 ml HAM'S F12
2,5% FBS	10 ml FBS
1% penicillin/streptomycin	4 ml penicillin/streptomycin
24 µg/ml adenine	4 ml adenine working solution
0,4 µg/ml hydrocortisone	400 µl hydrocortisone working solution
10ng/ml epidermal growth factor (EGF)	400 µl epidermal growth factor (EGF) working solution
5 µg/ml insulin	250 µl insulin solution human (Sigma Aldrich)
8,4ng/ml cholera toxin	400 µl cholera toxin working solution

PLK (primary lamb keratinocyte) MEDIUM	PLK MEDIUM 500ml
3 parts DMEM 1X	337,5 ml DMEM 1X
1 part HAM'S F12	112,5ml HAM'S F12
10% FBS	50 ml FBS
1% penicillin/streptomycin	5 ml penicillin/streptomycin
2Mm L-glutamine	5 ml L-glutamine 200 mM
1mM sodium pyruvate	5 ml sodium pyruvate 100 mM
20 µg/ml adenine	4ml adenine working solution
0,5 µg/ml hydrocortisone	500 µl hydrocortisone working solution
2ng/ml epidermal growth factor (EGF)	100 µl epidermal growth factor (EGF) working solution
5 µg/ml insulin	250 µl insulin solution human (Sigma Aldrich)
12,6ng/ml cholera toxin	760 µl cholera toxin working solution
5 µg/ml transferrin	1,25 ml transferrin working solution
1,5ng/ml 3,3',5-triiodo-2-thyronine T3	37,5 µl 3,3',5-triiodo-2-thyronine T3 working solution

3.2.1 Supplements

DMEM 1X

With high glucose, L-glutamine

HAM'S F12 1X nutrient mix

With L-glutamine

Penicillin (10000U/ml)/Streptomycin (10,000 µg/ml)

Recombinant insulin solution human (Sigma-Aldrich)

Adenine ≥99% (Sigma-Aldrich)

For working solution, dissolve 484mg of powder in 200ml HCl 0.05N, filter, aliquot and store at -20°C

Cholera Toxin from Vibrio cholerae

Dissolve 1mg of powder in 1180 µl ddH_2O, store stock solution at +4°C.

For working solution, dilute 100 µl of stock solution in 10 ml of serum-free DMEM, filter, aliquot and store at +4°C.

hEGF (Sigma-Aldrich)

Dissolve 2mg of powder in 2ml of acetic acid 10mM, aliquot and store stock solution at -80°C.
For working solution, dilute 100 µl of stock solution in 10 ml of serum-free DMEM, filter, aliquot and store at -20°C.

Hydrocortisone (Sigma-Aldrich)

Prepare a stock solution of 5mg/ml in 100% EtOH.

For 400 µg/ml working solution, dilute stock solution in serum-free DMEM, filter, aliquot and store at -20°C.

apo-Transferrin human (Sigma-Aldrich)

For working solution dissolve 2 mg of powder in 1 ml of ddH_2O, filter and store at +4°C for 5-10 days

3,3',5-triiodo-L-thyronine (Sigma-Aldrich)

For stock solution, dissolve 1mg of powder in 1 ml of 1N NaOH.

For working solution, add 49 of serum-free DMEM, filter, aliquot and store at -20°C.

Mitomycin C (Sigma-Aldrich)

For working solution, dissolve 2 mg of powder in 4 ml of serum-free DMEM, filter, aliquot and store at -20°C.

3.3 Agarose gel electrophoresis buffers and solutions

Agarose gel %

Dissolve agarose (w/v) in TAE1X.

Add 1 µl/10 ml of Gel Red or Gel Green 10000X (Biotium)

TAE 50X

242 g of Tris base

57.1 mL of acetic acid glacial

100 mL of 0.5 M EDTA (pH 8.0)

dH_2O up to 1L

Loading dye 10X

3.9 mL glycerol

500 µL 10% (w/v) SDS

200 µL 0.5 M EDTA

0.025 g bromophenol blue

0.025 g xylene cyanol

dH_2O up to 10ml

3.4 SDS-PAGE gel electrophoresis and western blot buffers and solutions

Stacking gel 2ml

1,4 ml dH_2O

0,33 ml 30% Acrylamide mix

0,250 ml 1,0 M Tris (pH 6.8)

0,02 ml 10% SDS

0,02 ml 10% APS

0,002 ml TEMED

Separating gel 10% 6 ml

2,4 ml dH_2O

2 ml 30% Acrylamide mix

1,6 ml 1,5 M Tris (pH 8.8)

0,06 ml 10% SDS

0,06 ml 10% APS

0,003 ml TEMED

SimplyBlue™ SafeStain (Invitrogen Life Technologies)

Comassie blue staining solution
1,25g Comassie brilliant blue R250
35ml Acetic acid glacial
250ml 100% EtOH
dH_2O up to 500 ml

Western blot buffer 10X
30,3 g Tris base
144g Glycine
dH_2O up to 1L

Running buffer 1X
100ml western blot buffer 10X
10ml 10% SDS (v/v)
890 ml dH_2O

Transfer buffer 1X
100ml Western blot buffer 10X
200 ml Methanol
700 ml dH_2O

PBS-T
PBS1X
0,05% Tween-20 (v/v)

Blocking solution
5-10 % (w/v) skim milk in PBS-tween 0,05% (PBS-T)

3.4.1 Protein analysis buffers

SDS gel-loading buffer 4X (Laemmli buffer)
8% SDS (w/v)
40% Glycerol 99% (v/v)
10% β-Mercaptoethanol (v/v)
240 mM Tris-HCl pH 6.8
0,04% Bromophenol blue (w/v)

dH_2O up to volume

NETN lysis buffer

20 mM Tris-HCl pH 8.0

100mM NaCl

1 mM EDTA pH 8.0

0,5% NP-40

Pierce EDTA-Free Protease Inhibitor Tablet (Thermo Scientific)

IP lysis buffer

20 mM Tris-HCl pH 8.0

200mM NaCl

1 mM EDTA pH 8.0

0,5% NP-40

Pierce EDTA-Free Protease Inhibitor Tablet (Thermo Scientific)

3.5 Antibodies

Horseradish Peroxidase-Conjugated Antibodies (Promega). Dilution 1/2000
Secondary antibodies (Southern Biotech). Dilution 1/50000
Anti-E6 antibody (unpublished)
anti-digoxigenin-AP Fab fragments (Sigma-Aldrich)
mAb Anti-Pan Cytocheratin FITC conjugate (clone PCK 26) (Sigma Aldrich)
Purified Mouse Anti-Human Retinoblastoma Protein Clone G3-245 (RUO) (BD Pharmingen)
Rb (4H1) Mouse mAb (Cell Signaling Technology)
p53 Antibody (Cell Signaling Technology)
p53 mAntibody (DO-1) (Santa Cruz biotechnology)
Phospho-Rb (Ser795) Antibody (Cell Signaling Technology)
Phospho-p53 (Ser15) (16G8) Mouse mAb (Cell Signaling Technology)
cyclin A Antibody (H-432) (Santa Cruz biotechnology)
Anti-cdc2 (p34) Antibody (Santa Cruz biotechnology)
Cdc2 (POH1) Mouse mAb (Cell Signaling Technology)
GST Antibody (Cell Signaling Technology)
HA epitope Tag Antibody (Thermo Scientific)

3.6 Plasmids

pUC19

pUC19 vector was used for RCA fragment cloning in *E. coli*. and the following vectors were generated:

pUC19+OaPV4_3kb

pUC19+OaPV4_4,7kb

pLXSN (Chlontech)

pLXSN retroviral vector was used for retroviral delivery and expression of E6+E7in primary keratinocytes. It contains the retroviral packaging sequence (Ψ+) and so, when transfected into a cell line expressing the retroviral structural proteins (gag, pol, and env), leads to packaging of viral particles. The 5' viral LTR in this vector contains a viral promoter that controls expression of the gene of interest. The following vectors were generated:

pLXSN+OaPV3-E6E7

pLXSN+OaPV4-E6E7

pLXSN+HPV38-E6E7

Gently provided by Infection and Cancer Biology (ICB) laboratory at IARC

pGEX4T1

pGEX4T1 bacterial vector was used for expression of GST fusion proteins. The following vectors were generated:

pGEX4T1+OaPV3-E6

pGEX4T1+OaPV3-E7

pGEX4T1+OaPV4-E6

pGEX4T1+OaPV4-E7

pCMV HA-N (Chlontech)

pCMV HA-N mammalian vector was used for expression of HA-tagged protein. The following vectors were generated and used in immunoprecipitation assays

pCMV HA-N+OaPV3-E6

pCMV HA-N+OaPV3-E7

pCMV HA-N+OaPV4-E6

pCMV HA-N+OaPV4-E7

3.7 Primers

3.7.1 Walking primers for OaPV4 genome sequencing

M13 forward sequencing primer

5’ GTAAAACGACGGCCAGT 3’

M13 reverse sequencing primer

5’ AACAGCTATGACCATG 3’

OaPV4_control3000R1

5’ TGTGCAGAGTAGTACAAACC 3’

OaPV4_3000SEQF1

5’ GAGCATTCCTGCAACAGTAG 3’
OaPV4_3000SEQR1
5’ TACTGTCACAGTTAGCAAGC 3’
OaPV4_control5000R1
5’ CAATGTCCATGCATCACGAC 3’
OaPV4_5000SEQF1
5’ ATCTCTTAGACCCGACTCAG 3’
OaPV4_5000SEQR1
5’ GTCAGAGGCTACAGTGATAG 3’
OaPV4_5000SEQF2
5’ CTGGGATAAGTATGGCTGTC 3’
OaPV4_5000SEQR2
5’ TGTATGGCCACTGATAGCTC 3’
OaPV4_5000SEQF3
5’ AGCTCTGCAGACACATTG 3’
OaPV4_5000SEQF4
5’ TGCATTTGAGGAAGTTGACC 3’

3.7.2 Primers for generation of OaPV4-E6 DIG-probe.

OaPV4E6probeF
5’ CGCTGCACCTCAAAAGGTAT 3’

OaPV4E6probeR
5’ CTGTTGCAGGAATGCTCTGT 3’

3.7.3 Primers for cloning into pLXSN

OaPV3_E6E7_EcoRIF
5’ GAGAATTCATGGAGGGAAGCCCTCGTAC 3’

OaPV3_E6E7_BamHIstopR
5’ AAGGATCCCTATGCAGCACACGGCGGAC 3’

OaPV4_E6E7_EcoRIF
5’ GGGAATTCATGCTGAGCAGTAAATTCCTGG 3’

OaPV4_E6E7_BamHIstopR
5’ AAGGATCCTCATGGTCGGTTTGCACAGG3’

3.7.4 Primers for cloning into pGEX4T1

OaPV3_E6_start_BamHI.F
5’ TTATGGATCCGAGGGAAGCCCTCGTACAAT 3’
OaPV3.E6_end_EcoRI.R
5’ TATGAATTCTCAGGGAGTGTGGGCTGCTGA 3’

OaPV3E7_start_BamHI.F
5’ ATATGGATCCCGTGGTCAGCAGCCCACACT 3’
OaPV3_E7_end_EcoRI.R
5’ AGTCGAATTCCTATGCAGCACACGGCGGAC 3’
OaPV4E6_start BamHI.F
GAGGATCCATGCTGAGCAGTAAATTCC
OaPV4E6_end_EcoRI.R
CCGAATTCTTATGGGTATTTGGTCCGTGC
OaPV4E7_start BamHI.F
GAGGATCCATGGTGCACGGACCAAA
OaPV4E7_end_EcoRI.R
CCGAATTCTCATGGTCGGTTTGCACAGG

3.7.5 Primers for cloning into pCMV HA-N

OaPV4E6_EcoRI_pCMV
5’ GGGAATTCACATGCTGAGCAGTAAATTCCTGG 3’
OaPV4E6_XhoI_stop
5’ TTCTCGAGTTATGGGTATTTGGTCCGTGC 3’
OaPV4E7_EcoRI_pCMV
5’ GGGAATTCACATGGTGCACGGACCAAATAC3’
OaPV4E7_XhoI_stop
5’ TTCTCGAGTCATGGTCGGTTTGCACAGG 3’
OaPV3E6_EcoRI_pCMV
5’ GAGAATTCACATGGAGGGAAGCCCTCGTAC 3’
OaPV3E6_XhoI_stop
5’ TTCTCGAGTCAGGGAGTGTGGGCTGCTG 3’
OaPV3E7_EcoRI_pCMV
5’ AAGAATTCACATGCGTGGTCAGCAGCCCAC 3’
OaPV3E7_XhoI_stop
5’ TTCTCGAGCTATGCAGCACACGGCGGAC 3’

4. METHODS

4.1 Samples

Tissue samples were excised from cutaneous proliferations located in the scrotum of a Sarda breed ram and were tested for the presence of papillomavirus DNA. A subset of tissue samples were fixed in 10% neutral buffered formalin and used for histological and in situ hybridization (ISH) analyses. A second set of tissues was stored at -80°C until nucleic acid extraction. All samples originated from patients hospitalized at the teaching hospital of the Veterinary Medicine Department (University of Sassari).

4.2 DNA extraction from tissue samples

Total DNA was extracted and purified from 25mg of tissue samples using the DNeasy blood and tissue kit (Qiagen), following manufacturer's instructions for *"Purification of Total DNA from Animal Tissues (Spin-Column Protocol)"*.

4.3 Rolling circle amplification (RCA)

Rolling circle amplification (RCA) was performed using the TempliPhi 100 Amplification kit (GE Healthcare), following the modified protocol for amplification of papillomavirus complete genome (Alberti et al., 2010; Rector et al., 2004). 5µl of total DNA extraction were mixed with 10µl of TempliPhi sample buffer, heated for 3' at 95°C and then transferred on ice. A mix cointained 10µl of TempliPhi reaction buffer, 0.4µl of TempliPhi enzyme mix and 0.4µl of 10mM dNTPs was prepared and added to the cooled sample. The final reaction was incubated for at least 16 hours at 30°C. Phi 29 polymerase was inactivated at 65 °C for 10 min. RCA products were digested with restriction enzymes (4.6.1).

4.4 Polymerase chain reaction (PCR)

Amplification of E6 and E7 genes was performed with the Pfx50™ DNA Polymerase (Invitrogen) using pUC19+OaPV4_3kb as DNA template.

Component	**Volume**	**Final concentration**
10X Pfx50™ PCR Mix	5 µl	1X
10 mM dNTP Mix	1,5 µl	300 µM
10 µM Primer Forward	1,5 µl	0,3 µM
10 µM Primer Reverse	1,5 µl	0,3 µM
DNA Template (600pg/ µl)	1 µl	600 pg
Pfx50™ DNA Polymerase (5U/ µl)	1 µl	5 U
sterile deionized H_2O	37,5 µl	

PCR profile

Initial denaturation	94°C 2’	
Denaturation	94°C 15’’	35 cycles
Annealing	57-60°C 30’’	
Extension	68°C 30’’	
Final extension	68°C 10’	

PCR fragments were subjected to agarose gel electrophoresis control (4.5) before purification (4.7) and digestion (4.6.2).

4.5 Agarose gel electrophoresis

Agarose gels were prepared in a microwave dissolving the agarose powder in 1X TAE buffer according to desired percentage. After boiling, GelRed® (Biotium) or GelGreen® (Biotium) was added to final 1X concentration and mixed. GelRed® (Biotium) was used for analytical visualization while GelGreen® (Biotium) was used for excision and purification of DNA fragments. The melted agarose was poured into a gel casting tray containing a comb. When solidified, the gel was placed in the running chamber filled with 1X TAE buffer. DNA samples suplemented with loading buffer were loaded into wells together with 100bp or 1kb plus DNA ladder (Invitrogen). Agarose gel electrophoresis was performed at 80V, and DNA was visualized with the GelDoc EZ® system (Biorad).

4.6 Restriction enzyme digestion of DNA

All digestions were performed with NEB's Restriction enzymes (New England Biolabs).

4.6.1 Restriction enzyme analysis of RCA product

Component	Volume
RCA product	5 µl
NEB enzyme	10 U
Cut Smart Buffer 10X	3 µl
ddH_2O	up to 30 µl

Digested RCA products were resolved in agarose gel supplemented with 1X GelGreen® (Biotium), and visualized and excised from the gel under visible blue-light in order to prevent mutations. After excision, RCA gel fragments were purified as described below (4.7).

4.6.2 Preparative digestion of PCR fragments and empty plasmids

Component	Volume
PCR product/empty plasmid	1-3 µg
NEB enzyme 1	10-20 U
NEB enzyme 2	10-20 U
Cut Smart Buffer 10X	4 µl
ddH_2O	up to 40 µl

Preparative digestions were resolved in agarose gel supplemented with 1X GelGreen® (Biotium), visualized and excised from the gel under visible blue-light in order to prevent mutations. After excision, DNA gel fragments were purified as described below (4.7).

4.6.3 Analytical digestion of plasmid DNA minipreparations

Component	Volume
DNA plasmid	500 ng
NEB enzyme 1	4-6 U
NEB enzyme 2	4-6 U
Cut Smart Buffer 10X	2 µl
ddH_2O	up to 20 µl

Analytical digestions were resolved in agarose gel supplemented with 1X GelRed® (Biotium) and visualized under UV light.

4.7 DNA purification

PCR products and agarose gel DNA fragments were purified with DNA Clean & Concentrator™-25 (Zymo Research) and Zymoclean™ Gel DNA Recovery Kit (Zymo Research) respectively, following manufacturer's instruction.

Small-scale and large-scale preparations of plasmid DNA were performed with Zyppy™ Plasmid Miniprep Kit (Zymo Research) and PureLink® HiPure Plasmid Maxiprep Kit (Invitrogen) respectively, following manufacturer's instruction.

4.8 Dephosphorilation and ligation of DNA fragments

After digestion and purification, PCR and RCA products were ligated into empty vectors with Rapid DNA Dephos & Ligation KIT (Roche).

Dephosphorilation of empty digested plasmids

Component	Volume	Final concentration
Vector DNA	x µl	up to 1 µg
rAPid Alkaline Phosphatase buffer 10X	2 µl	1X
rAPid Alkaline Phosphatase	1 µl	1 U
ddH_2O	up to 20 µl	

Reactions were incubated at 37°C for 30 min and the rAPid Alkaline Phosphatase inactivated at 75°C for 2 min. The dephosphorilation mixture was used in the following ligation reaction with a ratio of 1:3 (vector/insert).

Component	Volume	Final concentration
Vector DNA	X µl	50 ng
Insert DNA	X µl	150 ng
DNA diluition buffer	2 µl	10 X
ddH_2O	up to 10 µl	
Mix thoroughly and add:		
T4 DNA Ligation Buffer 2X	10 µl	1 X
T4 DNA ligase	1 µl	5 U

Reactions were incubated at 16°C O/N. The ligation mixture was used for bacterial transformation of TOP10 chemically competent *E.coli* (4.14.1).

4.9 Plasmid design

All plasmids were created with Snapgene® software (GSL Biotech LLC)

4.9.1 Retroviral vectors for E6+E7 expression in primary keratinocytes

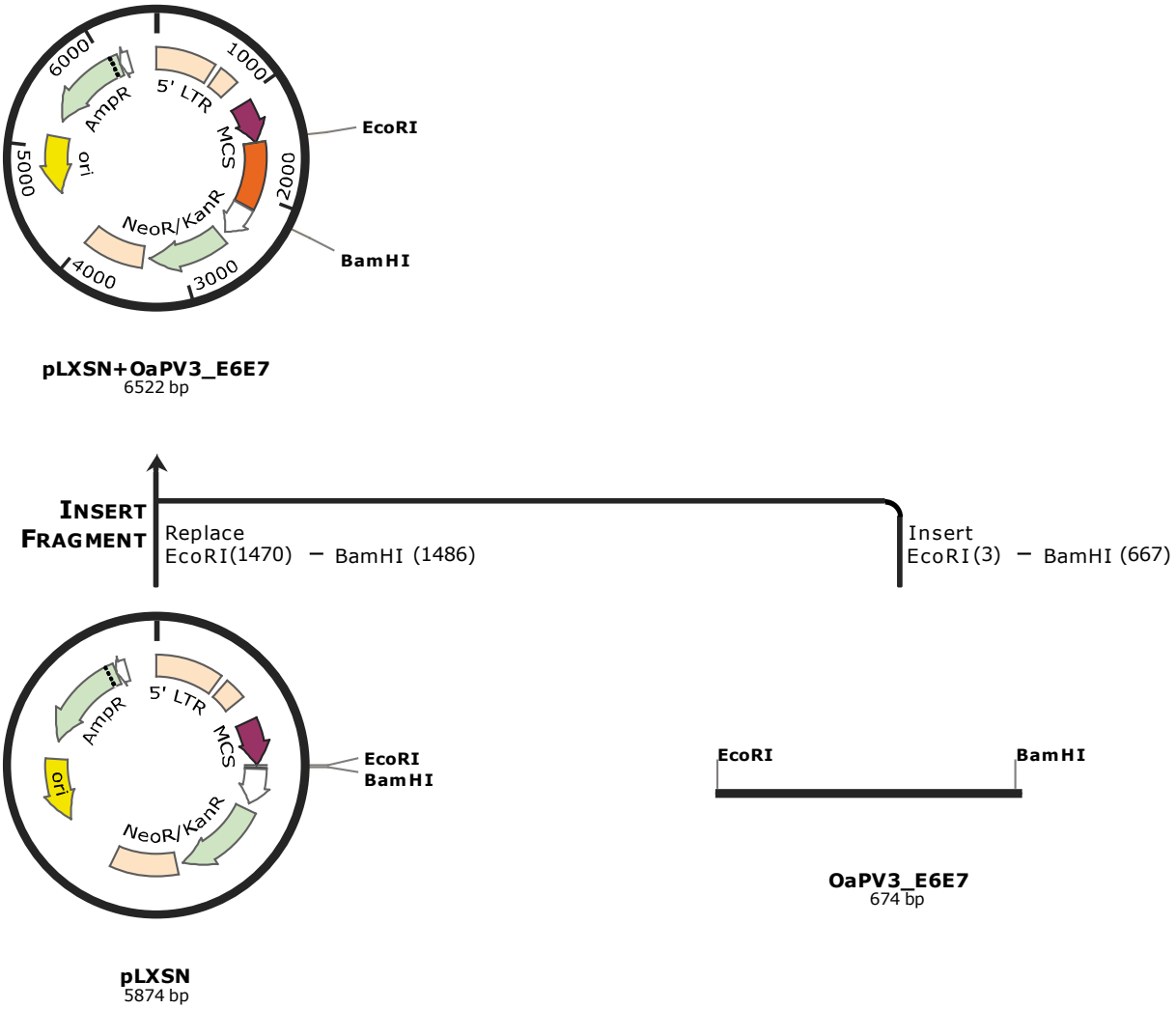

Figure 9 *pLXSN+OaPV3-E6E7*

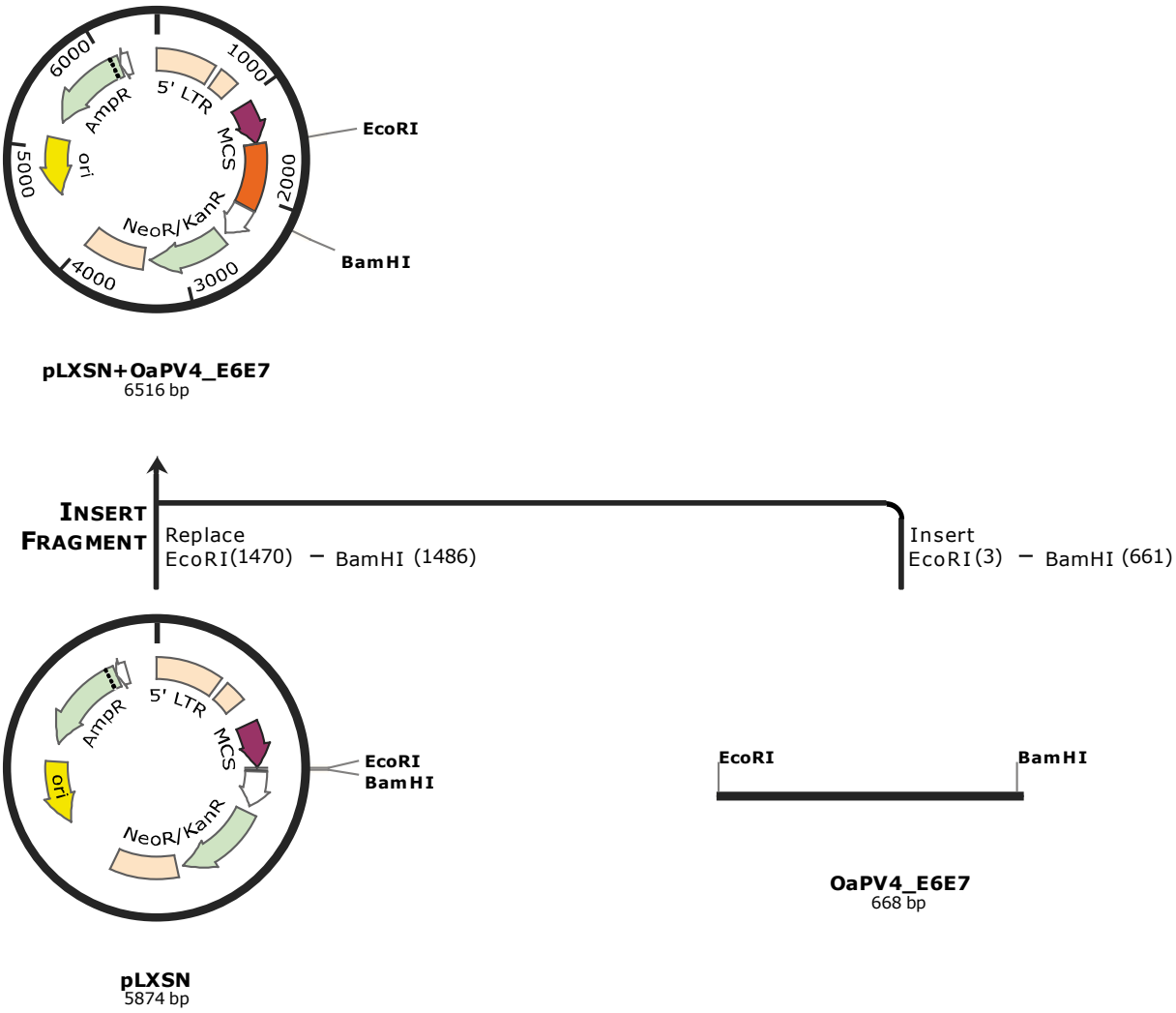

Figure 10 *pLXSN+OaPV4-E6E7*

4.9.2 Vectors for E6 and E7 GST fusion protein expression in E. coli

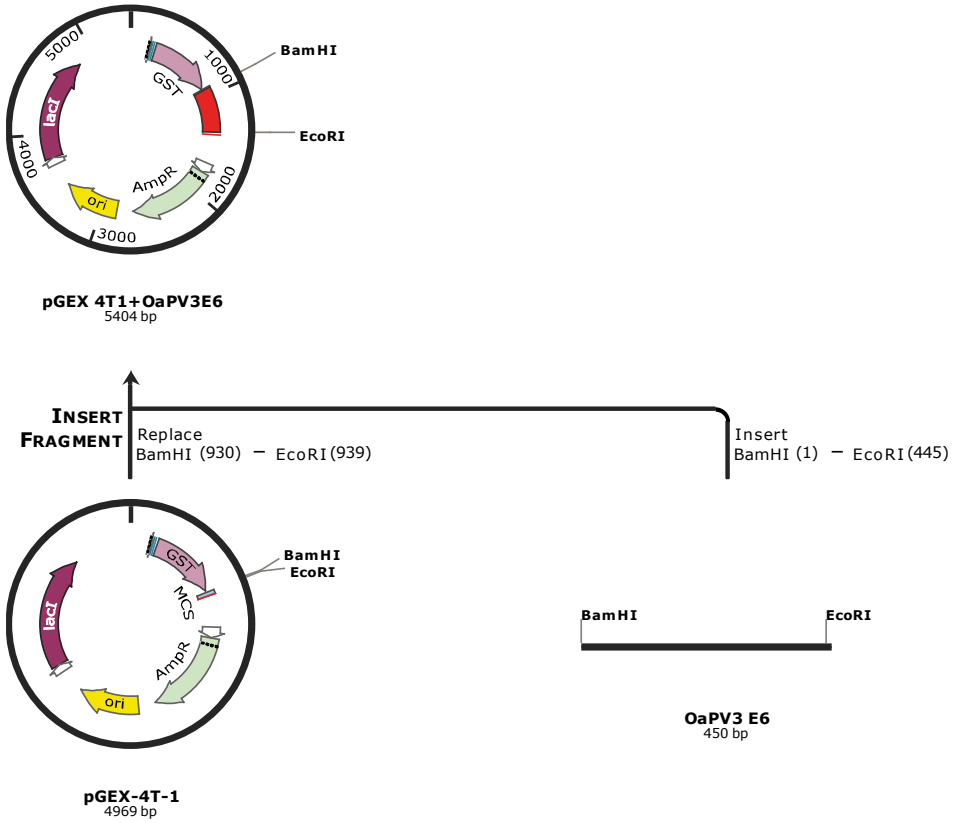

Figure 11 *pGEX4T1+OaPV3-E6.*

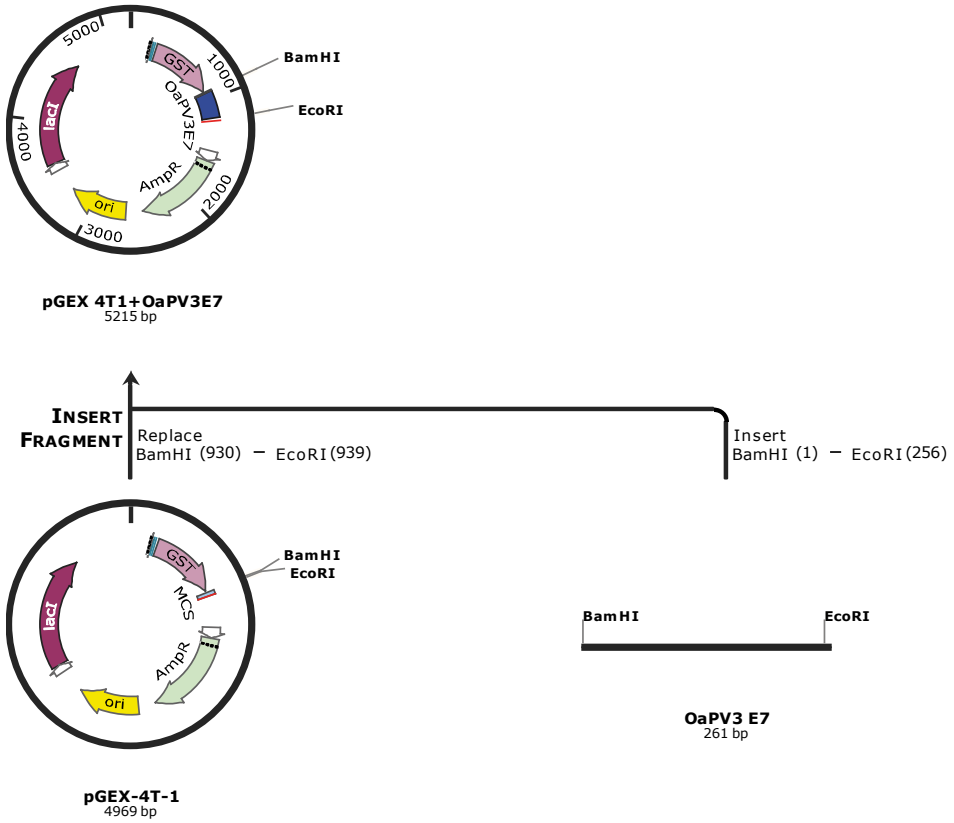

Figure 12 *pGEX4T1+OaPV3-E7.*

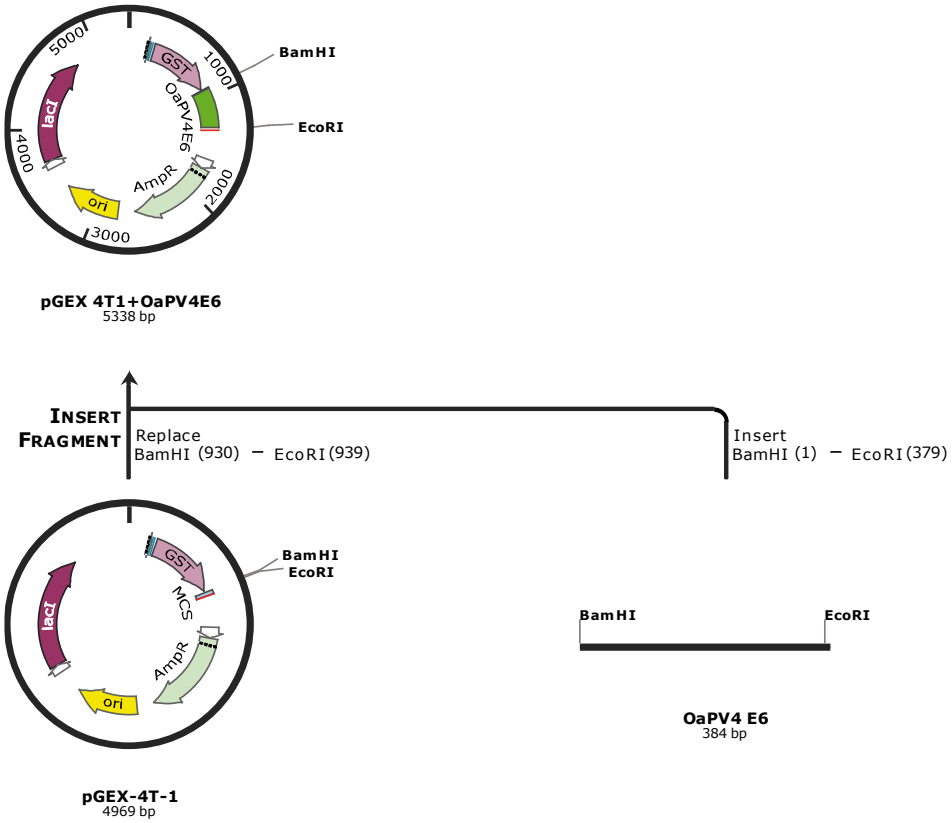

Figure 13 *pGEX4T1+OaPV4-E6.*

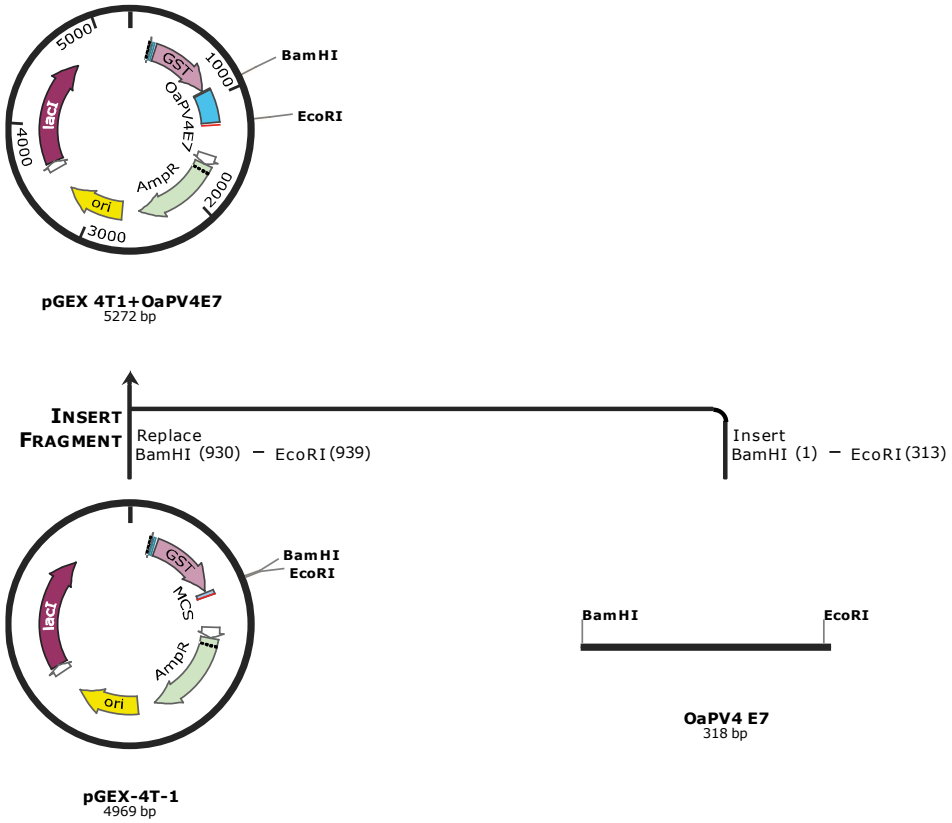

Figure 14 *pGEX4T1+OaPV4-E7.*

4.9.3 *Vectors for E6 and E7 HA-tagged protein expression in mammalian cells*

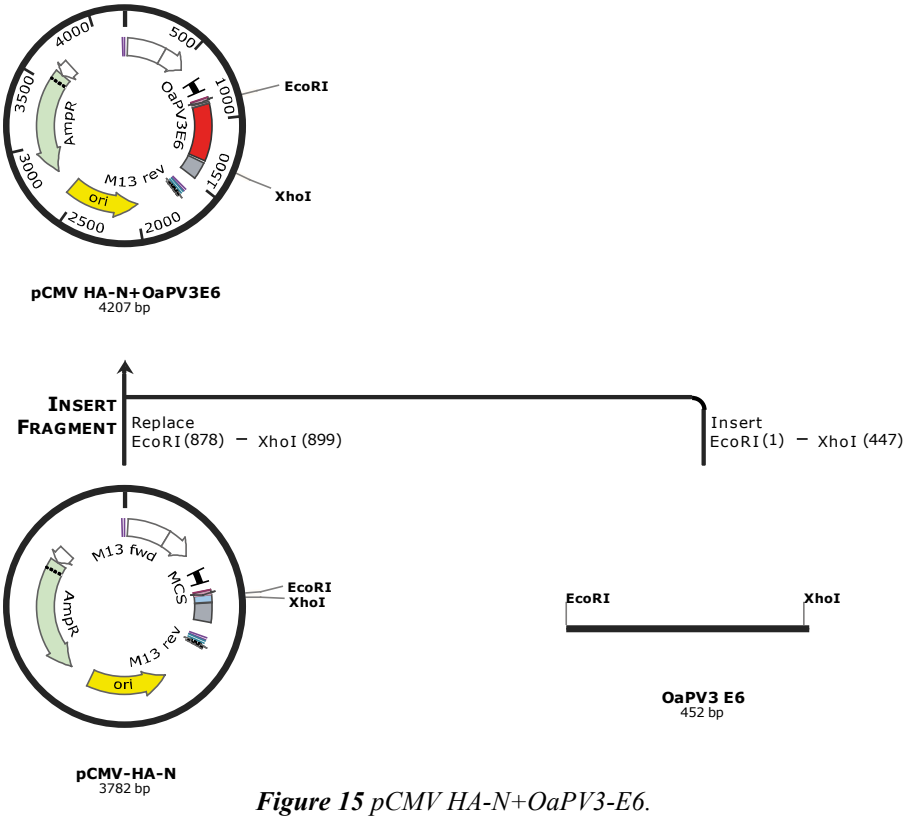

Figure 15 *pCMV HA-N+OaPV3-E6.*

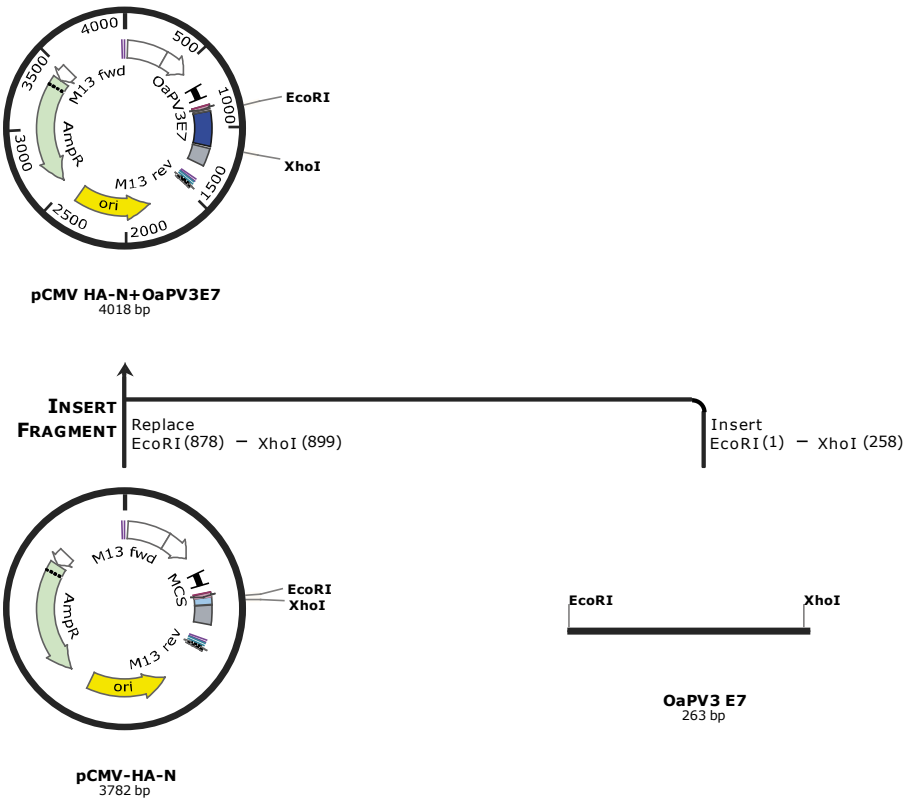

Figure 16 *pCMV HA-N+OaPV3-E7*

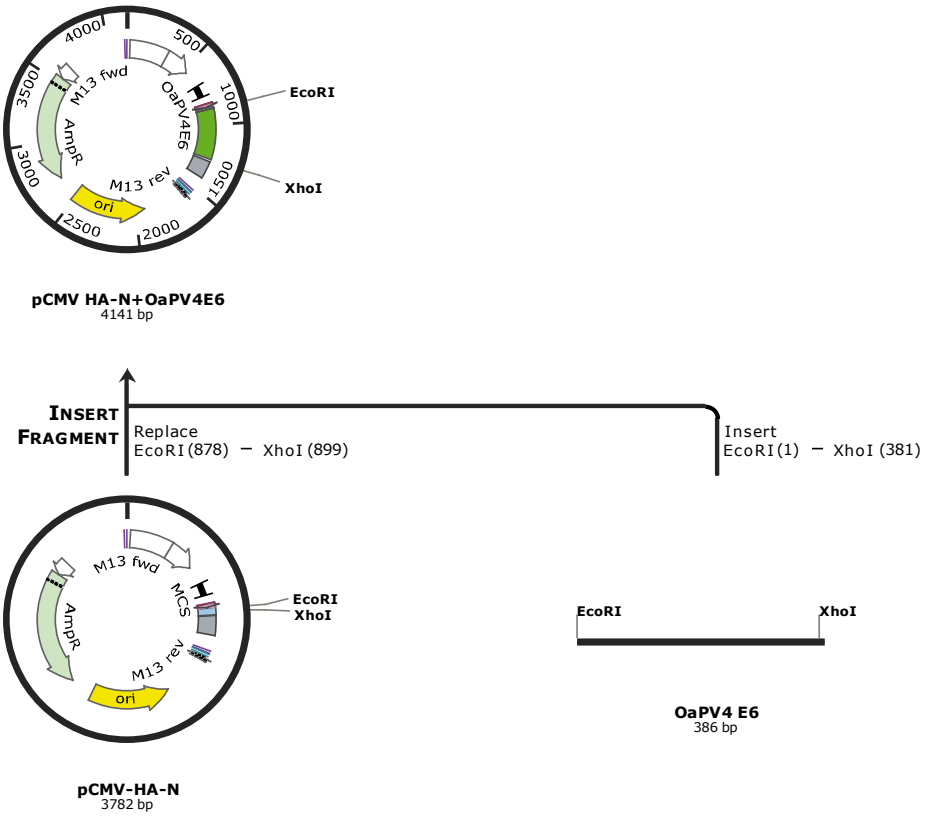

Figure 17 *pCMV HA-N+OaPV4-E6*

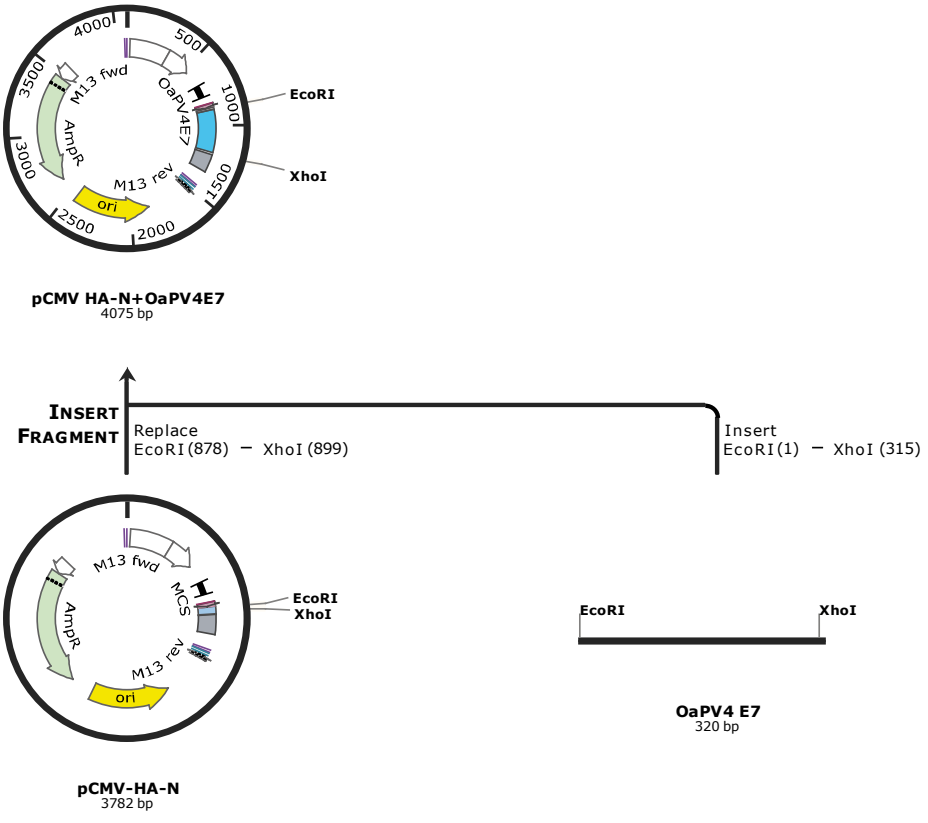

Figure 18 *pCMV HA-N+OaPV4-E7*

4.10 Phylogenetic analyses and divergence time estimation

To perform multiple nucleotide sequence alignments, the sequences of OaPV4 and 98 other PVs (listed in Table 1) were imported in DAMBE version 4.2.7 (Xia and Xie, 2001) and aligned at the amino acid level with ClustalW, after which the nucleotide sequences were aligned according to the aligned amino acid sequences. According to Gottschling et al. (Gottschling et al., 2011), this was done separately for the different ORFs, and the E1, E2, and L1 ORFs were pasted together in one compiled alignment. The highly variable E4 gene region nested within the E2 gene was excluded from molecular analyses.

The evolutionary history of OaPV4 and the 98 PVs considered in this study was inferred by using the Maximum Likelihood method based on the General time reversible model (Le and Gascuel, 2008), identified as the best-suited evolutionary model for our data. Initial tree(s) for the heuristic search were obtained by applying the Neighbor-Joining method to a matrix of pairwise distances estimated using the Maximum Composite Likelihood (MCL) approach. A discrete Gamma distribution was used to model evolutionary rate differences among sites [5 categories (+G, parameter = 1.2459)]. The rate variation model allowed for some sites to be evolutionarily invariable ([+I], 0.0000% sites). The analysis involved 99 nucleotide sequences. All positions containing gaps and missing data were eliminated. There were 3126 positions in the final dataset. Evolutionary analyses were conducted in MEGA6 (Tamura et al., 2013).
Statistical support for internal branches of the trees was evaluated by bootstrapping with 1000 iterations (Felsenstein, 1985). Maximum parsimony (MP) trees and consensus values were generated using the same software. Trees were edited with NJplot (Perrière and Gouy, 1996) and Treeview v. 1.5.2 (Page, 1996).

Trees were also generated based on concatenated amino acid alignments. MEGA6 was also used to scale to time phylogenetic trees, and branch lengths were calibrated according to divergence times calculated for HPV45, HPV18, and HPV97 (Chen et al., 2009), and based on a fixed (known) mean substitution rate of HPV genes, $1.95E^{-08}$ (95% confidence interval, $1.32\ E^{-08}$ to $2.47\ E^{-08}$) substitutions per site per year.

4.11 OaPV4 genome sequencing and characterization

The complete genome of the Ovis aries Papillomavirus type 4 (OaPV4) was determined by primer-walking sequencing of the cloned RCA fragments starting from M13 universal primers set into pUC19 (3.7.1). A private company (BMR-Genomics, Padova) performed sequencing.

The ORF Finder tool on the NCBI server of the National Institutes of Health (http://www.ncbi.nlm.nih.gov/gorf.html) was used for prediction of open reading frames (ORFs). Molecular weight of the putative proteins was calculated by using the ExPASy (Expert Protein Analysis System) Compute pI/ MW tool (http://www.expasy.org/tools/pi_tool.html). Pairwise sequence alignments and sequence similarities were calculated using the ClustalW and the identity matrix options in Bioedit, respectively. Putative nucleotide and amino acid features were identified using FIMO (http://meme-suite.org/tools/fimo) and ScanProsite (http://prosite.expasy.org/scanprosite/) online tools respectively.

4.12 RNA extraction from cultured cells

RNA was extracted from keratinocyte cell pellets using the NucleoSpin® RNA kit (Macherey Nagel) or the RNeasy Mini Kit (Qiagen), following vendor recommendations. RNA was treated with DNase I on column or by using the DNA-free™ DNase Treatment and Removal Reagents kit (Ambion). RNA was retrotranscribed using the RevertAid First Strand cDNA Synthesis Kit (Thermo Scientific) or the GoScript™ ReverseTranscription System (Promega), following manufacturer's instruction.

4.13 RT-PCR

cDNA of E6E7 expressing keratinocytes was used for RT-PCR to check E6+E7 gene transcription. RT-PCR was performed with HotStarTaq DNA Polymerase (Qiagen) according to following conditions.

Component	**Volume**	**Final concentration**
10X PCR buffer	2,5 µl	1X
10 mM dNTP Mix	0,5 µl	200 µM
10 µM Primer Forward	0,75 µl	0,3 µM
10 µM Primer Reverse	0,75 µl	0,3 µM
cDNA	1 µl	
HotStarTaq DNA Polymerase (5U/ µl)	0,125 µl	0,625 U
dd H_2O	19,375 µl	

PCR profile

Initial activation step	94°C 15’	
Denaturation	94°C 30’’	35 cycles
Annealing	60°C 30’’	
Extension	72°C 30’’	
Final extension	72°C 10’	

4.14 Culture and transformation of Bacteria

Both TOP10 chemically competent and BL21 *E.coli* were cultured in liquid or agar Luria Bertani (LB) broth at 37°C, with 220 rpm shaking for liquid cultures. The appropriate antibiotic was added for bacteria selection according to antibiotic resistance carried by the vector.

4.14.1 TOP10 Heat shock transformation

50 µl vial of One Shot® TOP10 Chemically Competent *E. coli* (Invitrogen) were allowed to thaw on ice and transformed using heat shock method. 5-10 µl of ligation mixture was added and mixed by tapping gently. Cells were incubated for 30 min on ice, shocked for 40 sec in a 42°C water bath and placed on ice for 1-2 min. 250 µl of SOC medium were added and cells were incubated at 37°C for exactly 1 hour at 220 rpm in a shaking incubator. 50-150 µl of transformation were spread on LB agar selective plates supplemented with the appropriate antibiotic and incubated at 37°C overnight.

4.14.2 BL21 transformation using TransformAid Bacterial Transformation Kit

Non-competent BL21 Codon plus *E.coli* were transformed with pGEX4T1 derived plasmids (4.9.2) by using the TransformAid Bacterial Transformation Kit (Fermentas) and following vendor recommendations.

4.15 Isolation of primary lamb keratinocytes

Primary ovine keratinocytes were isolated from foreskin of two lambs following protocols already described (Aasen and Izpisúa Belmonte, 2010; Dal Pozzo et al., 2005). Foreskin tissues were collected at the slaughterhouse and deeply rinsed with PBS supplemented with penicillin/streptomycin before isolation. Tissues were cleaned trimming away any fat and loose fascia. Thin sheets of foreskin tissue were cut into small pieces and incubated in a trypsin 0,25%/EDTA 1X solution at 37°C for at least 30 min. Trypsinized cells were filtered with a 70 µm pore size filter and centrifuged at 1200 rpm for 10 min. The cell pellets were resuspended with PLK medium.

4.16 Culture of mammalian cells

For this research several cell lines were used; growth medium components and supplements are listed above (3.2). All cells were grown at 37°C in an incubator with 5% CO2 and 95% humidity.

NIH/3T3 fibroblasts and Phoenix cells for amphotropic retrovirus production were cultured in complete DMEM medium.

Monolayer cultures of human primary keratinocytes (HPKs) were grown in T25 flasks together with mitotically inactivated NIH/3T3 using FAD medium. Feeder layer of NIH/3T3 was prepared by treatment with 200µl of Mitomycin C working solution for 2 hours at 37°C. Treated NIH/3T3 were collected, counted and added to keratinocytes cultures ($2,5x10^5$ cells/$25cm^2$ flask). Feeder layer was detached with PBS 2mM EDTA and changed 1-2 times/week.

NIKS (naturally immortalized human keratinocytes) cell line was grown as HPKs in T75 flasks together with $7,5X10^5$ of NIH/3T3 per flask as feeder. All human cell lines were kindly provided by the Infection and Cancer Biology (ICB) laboratory at IARC.

Primary ovine fibroblasts were provided by Laboratorio di Ostretricia e Riproduzione animale (University of Sassari) and cultured in complete DMEM medium.

Primary lamb keratinocytes (PLKs) were isolated as described above and grown in PLK medium supplemented with 10% FBS and without a feeder layer.

Stably transduced HPKs and PLKs were selected with, respectively, 0,1mg/ml and 0,2mg/ml of G418 disulfate salt selective antibiotic (Sigma Aldrich).

4.17 Retroviral gene delivery and expression

Human and ovine primary keratinocytes were infected with high titer of retroviral supernatants generated by transient transfection of Phoenix cells according to the following protocol already described (Caldeira et al., 2003).

Day 1: Transfection of phoenix cells with CalPhos Mammalian transfection kit (Clontech).

Phoenix cells are seeded in 10 cm dishes the day before in order to have 50-70% cell confluence prior to use.

Transfection solutions with pLXSN retroviral vectors (4.9.1) are prepared in 15 ml tubes as follows:

- Mix 10µg of DNA plasmid + ddH_2O up to 440µl.
- Add 62 µl of CaCl2 2M.
- Mix gently.
- Add 500 µl of HBS2X.dropwise.

- Remove old medium from the phoenix cell culture, and add 5ml of fresh complete DMEM and 5 µl of 25mM Cloraquine (25 µM as final concentration).
- Add plasmid suspension to cells dropwise and homogenously.
- 6/8 hours after transfection remove medium and wash twice with PBS (optional)
- Add 5ml of fresh complete DMEM.

Day 2: Change medium to Phoenix cells 24 hours post transfection

Day3: Infection

- Primary keratinocytes are seeded in 25cm^2 flasks two days before infection
- 48 hours post-transfection, collect medium of the phoenix dishes (the supernatant contains retroviral particles) and filter it through 0.2 µm filter twice.
- Add 5 µg/µl of PolyBren into each 5ml retroviral suspension.
- Remove old medium from keratinocytes.
- Add retrovirus suspension to keratinocytes.
- 3hours after infection, remove retroviral suspension.
- Replace with fresh medium (FAD or PLK medium).

Day4: Beginning of selection

- 24 hours post infection, start selection of transduced cells.
- Split infected cells 1/1 or 1/2 according to cell confluence.
- Add fresh medium supplemented with 0,1mg/ml (HPK) or 0,2 mg/ml (PLK) of G418 selective antibiotic.
- Continue selection until death of selection control cells (not-infected keratinocytes).

4.18 Colony formation assay (clonogenic assay)

After transduction with empty pLXSN vector (control) or E6E7 genes and selection in G418 supplemented medium, 1x10^3 PLKs were seeded, in triplicate, in 25cm^2 flasks. Cells were allowed to grow and proliferate for 15 days. PLK medium was replaced twice a week. Cells were then fixed with a cold solution of methanol:acetic acid (3:1) and stained with 0,5% (w/v) crystal violet in 25% methanol. Colonies containing more than 50 cells were counted and the fold change rate in colony numbers was calculating setting the control culture as 1. The experiment was performed in two different biological repeats.

4.19 Total protein extraction from cultured cells

For total protein extraction, pelleted cells were resuspended in IP buffer supplemented with protease inhibitors and incubated on ice for 30 min. After centrifugation at 10000rpm for 10 min at 4°C, supernatants were transferred in a new tube. Protein quantification of supernatants was carried out using Pierce BCA protein assay kit (Thermo Scientific). Equal amounts of protein extracts were loaded onto SDS-PAGE and subjected to Western immunoblotting.

4.20 SDS-Polyacrilamide Gel Electrophoresis (SDS-PAGE)

Proteins were resolved in 10% SDS polyacrilamide separating gels. Before loading onto gel, proteins were dissolved in 4X Laemmli buffer and boiled at 95°C for 5-10 min to allow denaturation. Electrophoresis was performed in a Mini-PROTEAN® Tetra Cell system (Bio-Rad). After running, proteins were subjected to Western blot or directly visualized by staining with Commassie blue or SimplyBlue™ SafeStain.

4.21 Western immunoblotting

After SDS-PAGE, proteins were transferred to a nitrocellulose membrane with Mini Trans-Blot® 3 cell (BioRad). Gels and membranes were equilibrated in transfer buffer and placed between three pieces of filter paper (3MM Whatmann paper). Blotting was perfomed at 250 mA for one hour at 4°C and membranes were blocked with 5-10% skim milk in PBS-T for at least 1 hour. Membranes were incubated with the primary antibody diluted in 3% skim milk in PBS-T under gentle agitation at 4°C overnight. After incubation, membranes were washed 3 times for 5-10 min with PBS-T and then incubated with the secondary antibody HRP-conjugated (dilution from 1:2000 to 1:50000 in 3% skim milk in PBS-T) under gentle agitation at room temperature (RT) for 1 hour. After whashes, membranes were developed with Clarity ECL Substrate (50% solution A + 50% solution B) (BioRad) or Luminata Forte Western HRP substrate (Millipore). Chemiluminescence was acquired with The ChemiDoc XRS+ System (Bio-Rad). Densitometric values and normalization to housekeeping gene were calculated with ImageLab 5.2.1 software.

4.22 GST fusion protein expression

BL21 *E.coli* were transformed with the appropriate pGEX4T1 derived plasmid (4.9.2). Single transformed colonies were grown overnight in 10 ml of LB medium supplemented with 100 μg/ml of ampicillin and 34 μg/ml of chloramphenicol.

The overnight bacterial cultures were diluted 1:20 in fresh LB and grown until they reached an OD_{600} of 0,4. At this point, the expression of fusion proteins was induced by adding isopropylthio-β-galactoside (UltraPure IPTG-Invitrogen) to a final concentration of 0,1 mM. *E.coli* cultures were grown for further 3 hours at 37°C and 50 ml aliquots were pelleted by centrifugation at 4000 rpm for 10 min. Pellets were stored at -80°C until purification. Correct expression of recombinant proteins was verified by SDS-PAGE before purification.

4.23 GST fusion protein purification

For bacterial lysis and protein purification, a bacterial pellet corresponding to 50 ml of culture was resuspended in 1 ml of NETN buffer supplemented with protease inhibitors. Resuspended bacteria were lysed by sonication on ice (4 cycles of 20 sec with 5 sec ON and 5 sec OFF, 50%-70% power) avoiding foam and overheating. The insoluble bacterial debris were removed by centrifugation at 10000 rpm for 10 min at 4°C. Supernatants were filtered through a sterile 0,45 µm filter to obtain a clear bacterial extract. Fusion proteins were then purified through incubation of lysed bacterial extracts with 75µl of Glutathione Sepharose 4B (GE Healthcare). Glutathione beads were previously washed three times with cold NETN buffer containing 0,5% (w/v) skim milk. After each washing, beads were collected by centrifugation at 800 rpm for 2 min. Mixtures of bacterial extract and beads were incubated for 1 to 3 hours rocking at 4°C. After incubation, beads were recovered by centrifugation, washed 5 times with cold NETN buffer and stored at -20°C. 10 µl of bead-immobilised recombinant proteins were loaded onto SDS-PAGE to verify purification. A BSA curve was prepared and included in the running to estimate purified protein quantification.

4.24 GST pulldown assay

GST pulldown was performed using NIKS cells or primary ovine firbroblasts or PLKs Whole cell lysates were prepared from cell pellets using the total protein extraction method (4.19) and precleared through incubation with empty Glutathione Sepharose 4B beads (30 min rocking at 4°C) to avoid aspecific bindings. Equal amounts (1 to 2 µg) of bead-immobilised GST/recombinant proteins were mixed with equal amounts of pre-cleared cell lysate (~ 600 mg of protein extract for each pulldown) in a volume of at least 400 µl, and incubated at 4°C for 1-3 hours with gentle rotation. Beads were collected by centrifugation at 800 rpm for 2 min and washed 10 times with cold NETN buffer. After washes, samples were directly resuspended in 10 µl of 4X Laemmli buffer and subjected to western immunoblotting.

4.25 Co-Immunoprecipitation assay

Primary ovine firbroblasts and PLKs were used in Co-Immunoprecitation assays. The day before transfection, ~ $6x10^5$ cells were seeded in 6 cm dishes in triplicate for each pulldown. Cells were transfected with 6 µg of plasmid DNA (4.9.3) using the TurboFect Transfection Reagent (Thermo Scientific) and following manufacturer's instructions. Mock cells and cells transfected with only the empty vector (pCMV HA-N) were included as controls.

Cells were harvested 48 hours after transfection and total protein lysates were obtained as already described (4.19). Equal amounts of protein extracts were used for each assay. Co-Immunoprecicpitation was performed with the Pierce HA Tag IP/Co-IP Kit (Thermo Scientific) following manufacturer's instructions, with the only exception that incubation of lysates with the anti-HA agarose was extended from 1 hour to 3 hours. Elution was obtained following protocol N°2 and immunoprecipitates were directly subjected to western immunoblotting.

4.26 Histopathology

Tissue sections were deparaffinised through three passages in xylene followed by hydration in alcohol at decreasing concentrations (100%, 90%, 80%, and 70%) and water. Sections were first stained in haematoxylin for 3-5 minutes, washed in running tap water for 5 min or less and stained with 1% Eosin Y for 1-2 minutes. After washing in distilled water, sections were dehydrated using increasing concentrations of alcohol and cleared in xylene. At the end, slides were mounted with Eukitt Mounting Medium (BiOptica) and observed under microscope.

4.27 Immunohistochemistry (IHC)

Histological sections (3 µm thick) from formalin-fixed, paraffin-embedded tissue samples were mounted on positively charged Superfrost slides (Fisher Scientific). Slides were immersed for 20 min in a 98°C preheated solution (WCAP, citrate pH 6, BiOptica) and mounted in a sequenza chamber (Shandon). Then, tissues were blocked for endogenous peroxidase with a 15 minute incubation in Dako REAL Peroxidase-Blocking Solution (S2023, Dako, Glostrup, DK), and for nonspecific binding with 2.5% normal horse serum (ImmPRESS reagent kit,Vector Labs) for 30 minutes at room temperature. Sections were incubated overnight at 4°C with ovine anti-E6 antibodies raised against the OaPV3 E6 (unpublished), and alternatively with a mouse monoclonal anti-Ki67 antibody (Clone MIB-1**,** Dako**)** at 1:100 dilution. Sections were incubated for 20 min at room temperature with anti-mouse/rabbit secondary antibodies (MP-7500, ImmPRESS reagent kit, Vector Laboratories). 3,3'-Diaminobenzidine (DAB) (ImmPACT DAB, Vector Laboratories) was used as chromogen.

All washing steps were performed three times with TBS-0.1% Tween 20 (BiOptica). Tissues were counterstained with haematoxylin, dehydrated and mounted with Eukitt Mounting Medium (BiOptica). An ovine OaPv3-positive skin lesion (Alberti et al., 2010), and an intestine tissue section were used as positive controls for OaPV3 and Ki67, respectively. To rule out aspecific binding of secondary antibodies, primary antibodies were replaced with serum collected from uninfected sheep.

4.28 Immunofluorescence (IF)

3,5 x10^5 PLKs were seeded in SPL Cell Culture borosilicate chamber slides (Euroclone) and let grow until 70-80% of confluence was reached. Afterwards, cells were washed twice with 1X PBS and fixed in a 1:1 EtOH:acetone solution at -20°C for 20 min. EtOH has been allowed to evaporate at RT. Fixed cells were incubated with 1% BSA in PBS for 20-30 min in a humid chamber. mAb Anti-Pan Cytocheratin FITC conjugate (clone PCK 26) (Sigma Aldrich) was diluted 1:50 in 1% BSA/PBS and incubated with cells at RT for 2h. Two or more washes with 1X PBS were performed before incubation with DAPI (1µg/mL in milliQ) for 1 min. Cells were washed other two times before slide assembly in a ProLong and analysis with confocal laser scanning microscopy.

4.29 In situ hybridization (ISH)

Digoxigenin labeled and unlabeled probes targeting OaPV4-E6 gene were developed with the PCR DIG Probe Synthesis Kit (Roche) using primers OaPVE6_probeF and OaPV4E6_probeR and following vendor recommendation. Unlabeled probe was generated by using the same protocol, without digoxigenin incorporation in the PCR mix. PCR protocol was profiled according to vendor recommendation for probe synthesis. Tissue sections mounted onto slides were treated with 200 µl of hybridization solution (obtained by adding 5 µl of 40 ng/ml denatured molecular probe to 100 µl molecular grade Fluka hybridization solution II, 86 µl formamide,9 µl mQ water), placed at 95 °C for 8 min, and then transferred in humidity chambers and incubated overnight. The following day, the unhybridized probes were removed with stringency whashes. The digoxigenin-labeled hybrids were detected by incubation with anti-digoxigenin-AP Fab fragments (Sigma-Aldrich) at RT. Slides were rinsed twice and incubated for 50 min at 37 °C in the dark with 5-bromo-4-chloro-3-indolyl phosphate (BCIP) and 4-nitro blue tetrazolium chloride (NBT). Slides were mounted with Top-Water mount (W. Pabisch SpA), and photographed with a light microscope.

5. RESULTS

5.1 OaPV4 genome isolation and cellular tropism

Rolling circle amplification (RCA) conducted on total DNA extracted from a scrotal lesion of a Sarda breed ram *(Ovis aries),* generated two fragments of approximately 4700 and 3000 bp in size, therefore consistent with the presence of a papillomaviral circular genome (Figure 21). Macroscopically, the ram scrotum showed multifocal well demarcated, exophytic papillomatous horny lesions ranging from 0.5 to 1 cm in diameter attached to the hair skin (Figure 19A). At histological examination, all lesions were characterized by the proliferation of epithelial cells forming arborizing papillary finger-like projections supported by dermal proliferation of fibroblasts arranged in interlacing streams and bundles (Figure 19B). The epidermis was hypercheratotic with acanthosis and scattered koilocytes were observed mainly in the stratum spinosum. Mitotic figures ranged from 1 to 3 per HPF (High Power Field). The dermis was characterized by a proliferation of haphazardly arranged fibroblasts with indistinct cell borders, with intermingled chronic inflammatory cells (mainly lymphocytes). Scattered fibroblasts showed vesicular nuclei and prominent nucleoli. The lesion was diagnosed as a fibropapilloma.

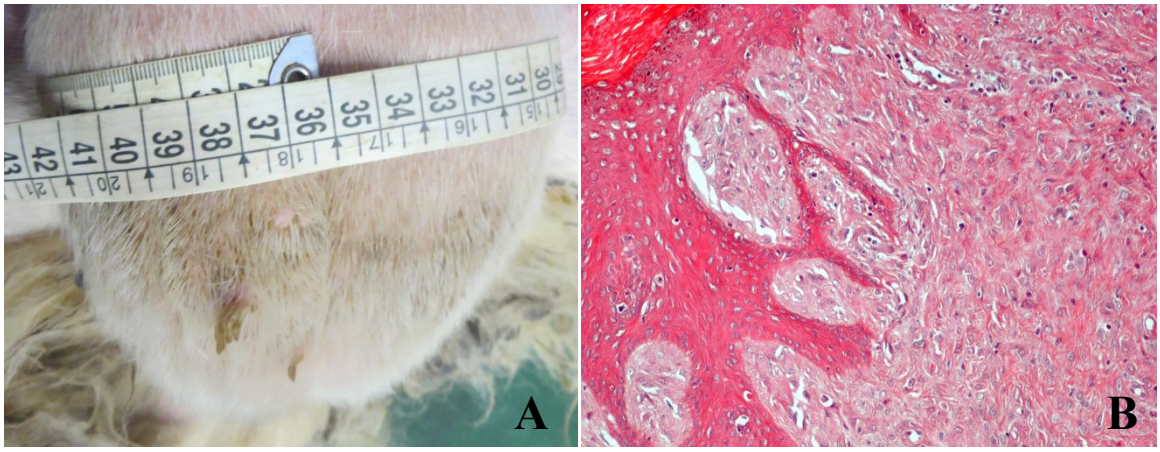

Figure 19*: Macroscopic(A) and microscopic (B) features of ovine fibropapillomas found on the scrotum of a ram.*

Immunohistochemistry revealed a strong and diffuse cytoplasmic immunoreactivity of both squamous epithelial cells and fibroblasts to anti-E6 antibodies, suggesting a widespread presence of viral proteins at epidermis and derma levels (Figure 20A). High proliferative activity mainly observed in the epithelial cells of the supra-basal and basal epidermal layers, as well as in the fibroblasts of superficial dermis was demonstrated by probing the same fields with Ki67 antibodies (Figure 20B). In situ hybridisation conducted with a digoxigenin-labelled nucleic acid probe based on the OaPV4 E6 gene confirmed immunohistochemistry results and demonstrated the presence of viral DNA in both the epithelium and connective tissues (Figure 20C-D).

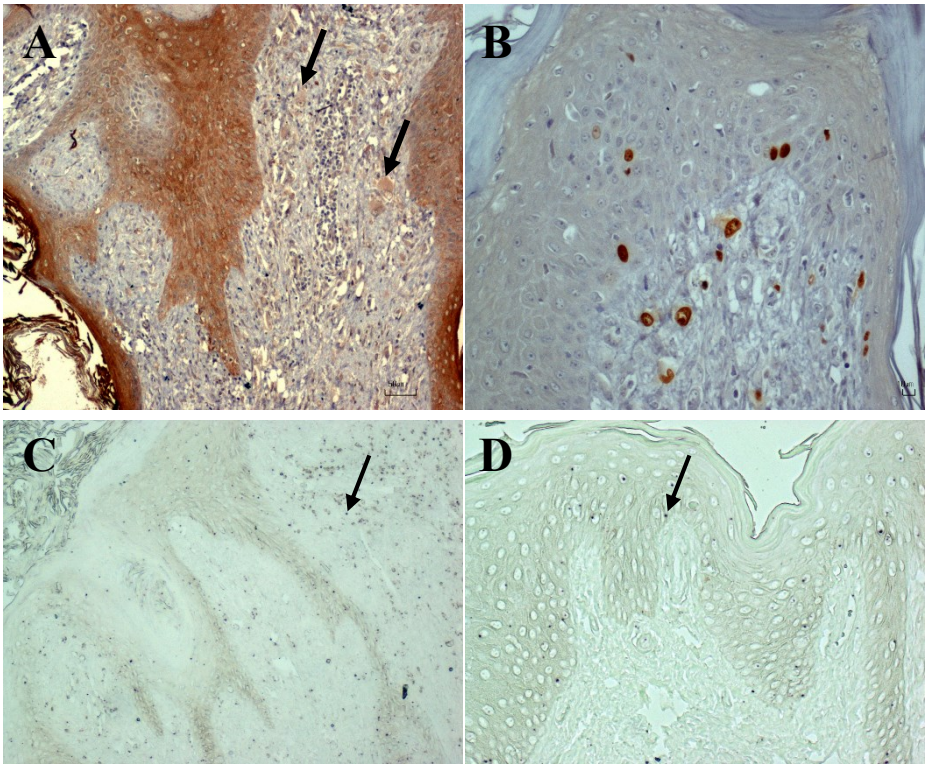

Figure 20 *IHC (A): arrows indicate immunoreactivity of fibroblasts to anti-E6-antibodies. IHC (B): nuclear reactivity of epithelial cells and fibroblasts to Ki-67 antibodies showing increased proliferative activity. ISH (C-D): arrows indicate positive reaction of epithelial and connective cells to anti-E6 gene probe.*

5.2 OaPV4 genome characterization and evolutionary history of ovine papillomaviruses

RCA combined to SacI digestion generated two fragments of approximately 4700 and 3000 bp in size, therefore consistent with the presence of a papillomaviral circular genome (Figure 21). Both the 4700 bp and 3000 bp fragments were successfully cloned into pUC19 (Figure 22).

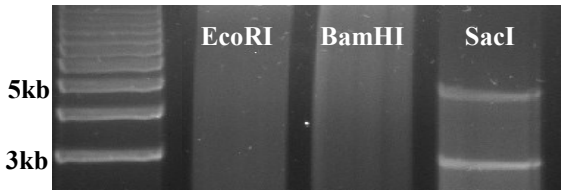

Figure 21 *0,8% agarose gel: RCA product digestions with indicated restriction enzymes*

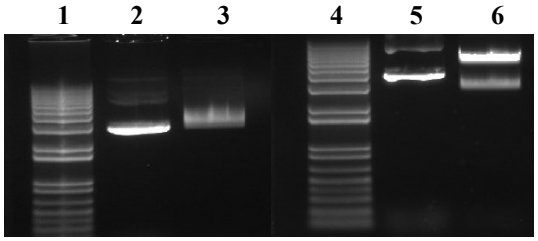

Figure 22 *Agarose gel. Analytical digestion of pUC19 plasmids.* ***1****: 1kb plus DNA ladder* ***2****: not digested pUC19+OaPV4_3kb* ***3****: digested pUC19+OaPV4_3kb* ***4****: 1kb plus DNA ladder* ***5****: not digested pUC19+OaPV4_4,7kb* ***6****: digested pUC19+OaPV4_4,7kb*

RCA fragments were sequenced through primer walking strategy (3.7.1) and resulted in the detection of a novel, unclassified PV genome, designated OaPV4 with size adding up to 7758 bp. The complete nucleotide sequence of Ovis aries PV type 4 (OaPV4, GenBank accession number KX954121) has a GC content of 45,8% and includes the canonical non-coding region (LCR) and.the classical major PV ORFs: E1, E2, E6, E7, E5, L2, L1 (Figure 23).

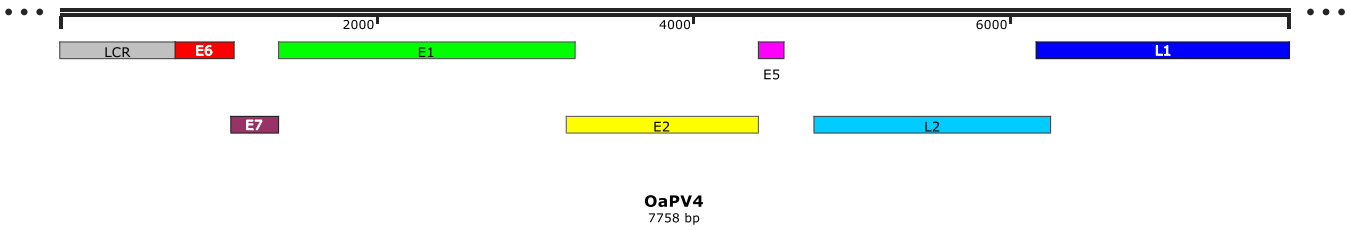

Figure 23 *OaPV4 genome map. Predicted open reading frames (ORFs) are represented. Nucleotide position number one is defined as the first nucleotide following the stop codon of the L1 ORF.*

Moreover, the open reading frame E4 was identified as a result of a spliced message unifying the first few codons of E1 (nt 1380–1098) with a downstream ORF in the +1 frame of the E2 ORF (nt 3802–4413). A small additional NCR located between the early and late regions is also present (nn 4574-4764). Nucleotide and amino acid alignments defined OaPV4 similarity with the other ovine papillomaviruses and RrPV1. Overall, OaPV4 shared the highest nucleotide (nt) and amino acid (aa) identities with OaPV1, and in general with the two ovine deltapapillomaviruses, while similarities with the Dyokappa genus were dramatically lower (Table 2).

Table 2 *Nucleotide (and amino acid) ORF identities between OaPV4 and other ovine papillomaviruses.Results are expressed as percentages. RrpPV1 was included in the analysis.*

	Delta genus		**Dyokappa genus**	
OaPV4	**OaPV1**	**OaPV2**	**OaPV3**	**RrPV1**
E6 (14,05 kDa)	90,5 (91,8)	83,6 (84,5)	38,4 (19,3)	37,8 (18,6)
E7 (11,34 kDa)	94,1 (94)	90,5 (88,1)	37,9 (23,7)	38,9 (27,4)
E1 (70,14 kDa)	94,6 (96,9)	90,8 (95,8)	51,5 (38,2)	51,2 (39,1)
E2 (45,17 kDa)	94,6 (95,7)	87,2 (89)	46,6 (27,3)	45,8 (25,4)
E5 (6,46 kDa)	86 (94,4)	75,7 (87)	-	-
L2 (52,79 kDa)	92,3 (94,5)	85,7 (88,9)	45,1 (24)	44,3 (24,2)
L1 (59,12 kDa)	82,5 (87,9)	75,4 (81,9)	48,3 (41,6)	49,5 (39,6)

According to the predicted amino acid and nucleotide features summarised in Table 3, the main differences found between ovine Delta and Dyokappa PVs were:

a) Absence of canonical E1 binding sites in Dyokappa viruses.

b) Absence of a pRB binding domain and of Zinc-binding motifs in the ovine Deltapapillomavirus E7.

c) Unusual presence of a pRB binding domain in the E6 of ovine Deltapapillomaviruses.

OaPV4 long control region (LCR, 732 bp) was predicted to contain a polyadenylation site located at nt 57 upstream of a CA dinucleotide and a TG cluster. Three TATA box were identified at the nucleotide positions: 56 (TATAAAT), 126 (TATAAA) and 680 (TATAAAA). Ten E2 binding sites (E2BS) motifs were found in the LCR region, six of which with a stringent consensus sequence [ACCG-N(4)-CGGT, nt positions: 210, 243, 283, 321, 427 and 478]. Two additional E2BS were found within E6 (nt 810) and L1 (nt 7137). The E1 binding site [A(A/T)GATTGTTGTTAACAAT] in the LCR has a T at position two as it has been found in OaPV1 and OaPV2.

The predicted E1 protein contains a helicase domain (aa 428-578) with the conserved ATP-binding site [G-X(4)-GK(T/S)] at aa position 454-461.

The late region was predicted to encode two viral capsid proteins L1 and L2. OaPV4-L1 contains a bipartite nuclear localization signal at C-terminus (aa position 511-527), which likely play a role in the nuclear translocation of L1 and L2 during the viral life cycle.

An E5 ORF was identified between the E2 and L2 ORFs. E5 protein contains a glutamine at position 26, an aspartic acid at position 42 and two cysteines at positions 46 and 48. All these four amino acids are known to be essential for the biolocical activity of BPV1 in cultured fibroblasts (DiMaio and Petti, 2013).

Phylogenetic trees were obtained from a concatenated E1/E2/L1 nucleotide sequence alignment of OaPV4 and 98 PV-types representative of the different PV genera and species (Figure 24). Resulting maximum likelihood phylogenetic trees clustered the PVs in their respective genera, according to the most recent PV classification (Bernard et al., 2010). Also, main genera associations observed by Gottschling et al. (2011) were maintained. In particular, the *Artiodactyla*–infecting Delta and Epsilon viruses grouped together with the PVs infecting *Equidae*, namely Zeta, Dyoiota, Dyorho and Dyochi.

In trees (Figure 24) ovine PVs appear as a diverse, ancient, polyphyletic group. OaPV3 clustered together with the alpine chamois RrPV1 in an independent ancient clade basal to Equine and Delta PVs (Figure 4). OaPV3 and RrPV1 started diverging roughly 3.73 ± 1.7 MY (Figure 25). On the other hand, OaPV4 is most closely related to OaPV1, from which split off roughly 0.61 ± 0.24 (Figure 25). OaPV2 diverged from OaPV1/OaPV4 approximately 1.5 ± 0.65 MY.

Table 3 *Genomic nucleotide and amino acid features of Ovine PVs. RrPV1 was included in the analysis.*

Predicted features	DELTAPAPILLOMAVIRUS			DYOKAPPAPAPILLOMAVIRUS	
	OaPV1 U83594	**OaPV2 U83595|**	**OaPV4 KX954121**	**OaPV3 FJ796965**	**RrPV1 K876045**
Predicted nt-feature*					
Genome size (bp)	7761	7758	7758	7344	7256
GC content (%)	45.7	46.4	45.8	46.8	48.6
E2 binding site[1] (ACC-N_{5-7}-GGT)	83, 88, **210**, **244**, **284**, **322**, 456, 694, 813, 891, 4003, 7137	85, 90, **211**, **246**, **287**, **324**, **483**, 816, 4666, 5186, 6738	83, 88, **210**, **243**, **283**, **321**, **427**, 455, **478**, 692, 810, 7137	107, 152, 190, 234, 314, **367**	122, **152**, **282**, 414, 1794, 2178
E1 binding site A(A/T)GATTGTTGTTAACAAT	614 ATGATTGTTGTTAACAAT	619 ATGATTGTTGTTAACAAT	612 ATGATTGTTGTTAACAAT	-	-
Polyadenylation sites ATAAA	34[2], 38[2], 57[3], 127, 155, 683, 799, 2821, 4537, 4756, 5033, 6830, 7367	381, 129, 157, 687, 2554, 2595, 4531, 4753, 4875, 6827, 7052	34[2], 38[2], 57[3], 127, 155, 681, 2545, 2821,4756, 5034, 5136, 6830, 7055, 7465	230, 605, 1012, 3164, 4418[2], 4422[2], 5786, 6893, 7337	79, 1234, 1954, 4349, 5075, 7249
Sp1 binding sites GGCGGG	1577, 2793, 6595, 7045	1580, 2802	1577, 2793	-	192 (LCR)
NF1 binding sites CGGAA	363, 6335	367	362	1489, 2797, 3735, 4025	1410, 3103, 3153, 5483, 6856
AP1 binding sites TGANTCA	1122, 1469	1125, 1472, 5617	1119, 1469	4885	-
TATA signals in LCR [TATAAA or TATA(A/T)A(A/T)]	56, 126, 682	128, 686	56, 126, 680	604	78
Predicted aa-feature#					
Retinoblastoma tumour suppressor binding domain in E7 (LXCXE)	-	-	-	LYCDE (22-26)	LFCEE (22-26)
Retinoblastoma tumour suppressor binding domain in E6 (LXCXE)	LACLE (45-49)	LACLE (45-49)	LACLE (45-49)	-	-

ATP-dependent helicase motive in E1 [G-X(4)-GK(T/S)]	GPPNSGKS (454)	GPPNSGKS (456)	GPPNSGKS (454)	GPSDTGKS (439)	GPSDTGKS (437)
Cyclin interaction motive in E1 (RXL)	57, 77, 113,267, 474	57, 77, 113, 476	57, 77, 113, 474	63, 102, 152	62, 101, 215
Zinc-binding motifs in E6 [CXXC-X(28-30)-CXXC]	11-47, 44-80, 77-113	11-47, 44-80, 77-113	11-47, 44-80, 77-113	26-62, 99-135, 59-102 [CXXC-X(36)-CXXC]	26-62, 99-135, 59-102 [CXXC-X(36)-CXXC]
Zinc-binding motifs in E7 [CXXC-X(28-30)-CXXC]	-	-	-	44-80	44-80
Bipartite nuclear localization signal in L1	478-494 (RRASRSTSSKVPSKRRR)	478-494 (RRVPKSTSDKAPSKRRR)	511-527 (RRTPKSTSSKVPSKRRR)	484-500 (RKAANNSGLNSSKRRRK)	479-495 (RKAASSPAPNTNKRRRR)

*For nucleotide features, positions are numbered starting from the first nucleotide following the stop codon of the L1 ORFs.

#For amino acid features, positions are numbered starting from the first amino acid of the relative protein.

[1] in bold: E2 binding sites with the consensus sequence ACCG-N(4)-CGGT.

[2]is a double polyadenilation signal.

[3]is followed by a CA dinucleotide and a G/T cluster.

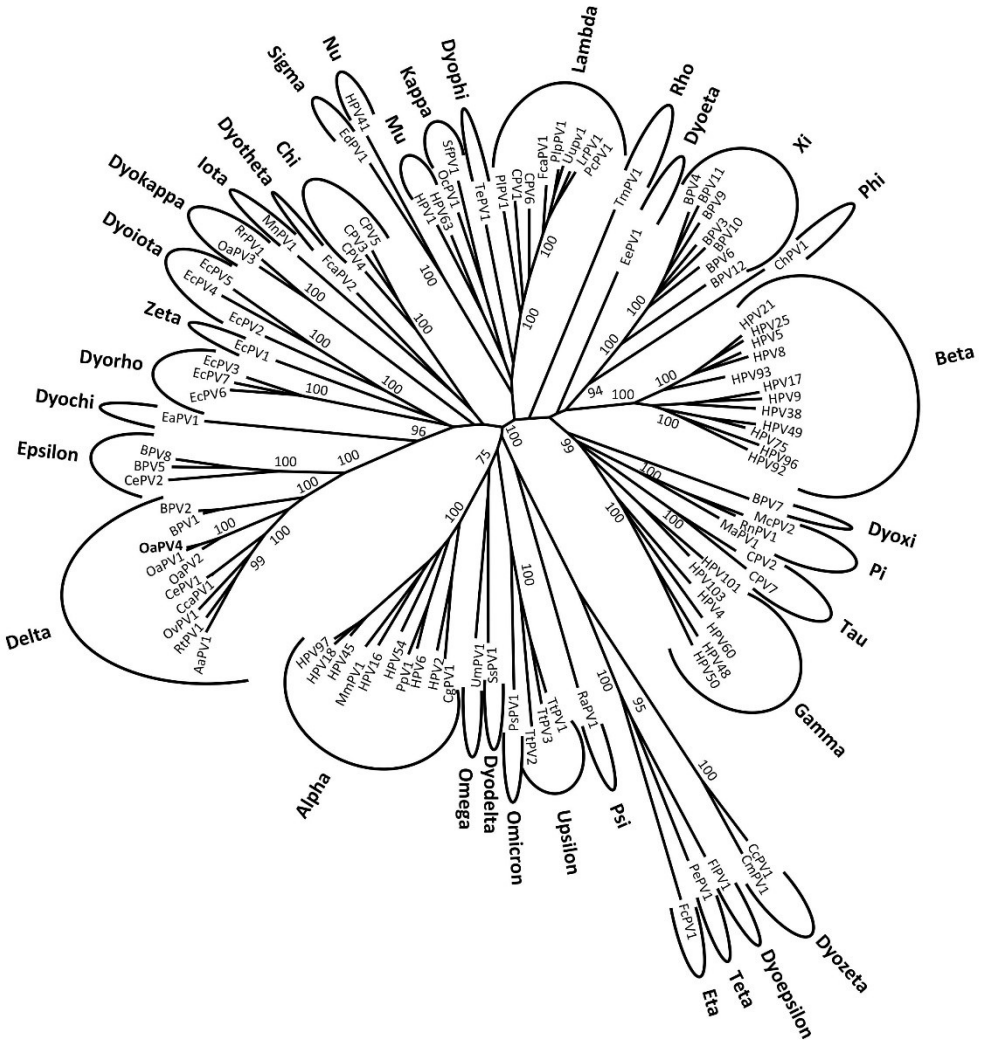

Figure 24 *Well-resolved maximum likelihood tree including OaPV4 and 98 PV-types representative of the different papillomavirus genera and species. ML tree of the 99 PVs was inferred by using a combined E1–E2–L1 nucleotide sequence analysis based on the corresponding amino acid alignments. Branch lengths are drawn to scale. Numbers on branches are ML bootstrap support values. Only values above 90 are shown.*

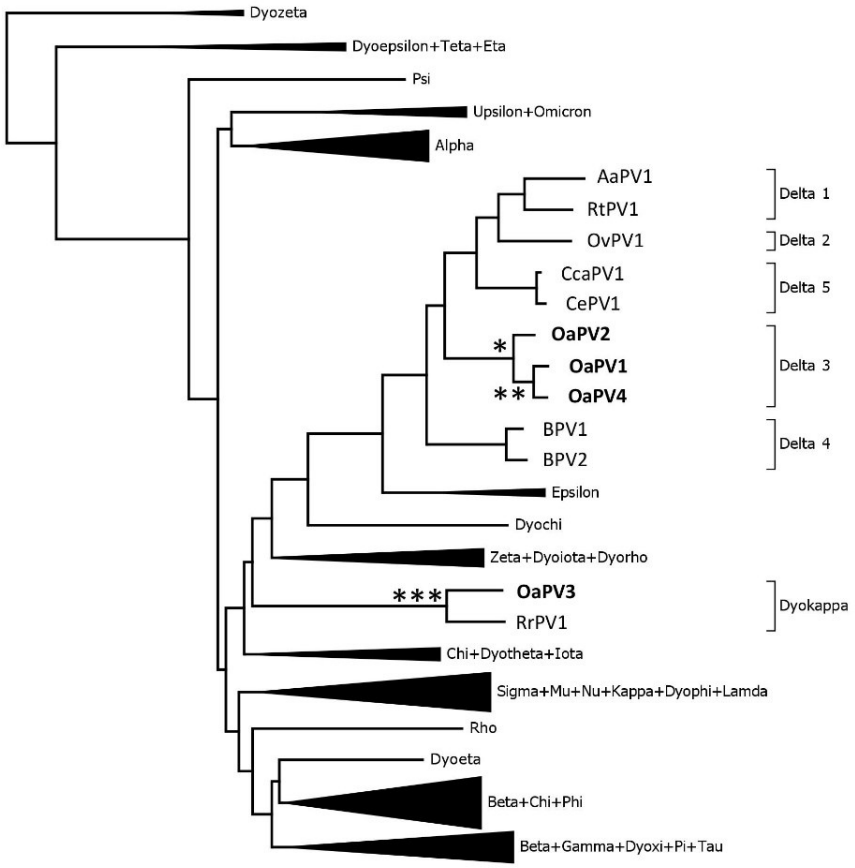

Figure 25 *Maximum likelihood tree showing the Ovine papillomavirus diversity and evolutionary history. Ovine PVs group in two major polyphyletic lineages: the Dyokappa close – to-root lineage, basal to the Delta + Epsilon artiodactyl PVs, and the Delta 3 group (included in the Delta+ Epsilon artiodactyl PVs). Asterisks indicate divergence time of the closer node: * = 1.5 ± 0.65 MY; ** = 0.61 ± 0.24 MY; *** = 3.73 ± 1.7 MY.*

5.3 Comparative analysis of ovine PVs E6 and E7 *in vitro* transforming properties

OaPV3-E6E7 and OaPV4-E6E7 genes were amplified from pUC19+OaPV4_3kb plasmid and successfully cloned into pLXSN retroviral vector (Figure 26).

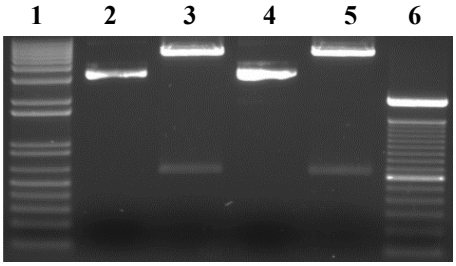

Figure 26 *Agarose gel: analytical digestion of pLXSN plasmids.* ***1****: 1kb plus DNA ladder* ***2****: not digested pLXSN+OaPV3-E6E7* ***3****: digested pLXSN+OaPV3-E6E7* ***4****: not-digested pLXSN+OaPV4-E6E7* ***5****: digested pLXSN+OaPV4-E6E7* ***6****: 100bp DNA ladder*

After transfection of Phoenix cells with retroviral constructs, three different donors of human primary keratinocytes (pooled HPK, HPK210, HPK220) were infected with recombinant retroviral phoenix supernatants and selected with G418 selective antibiotic. Transduction with HPV38_E6E7 was performed as positive control. Total RNA was extracted from transduced HPK and subjected to reverse transcription. PCR was performed with-specific primers using cDNAs as templates (Figure 28).

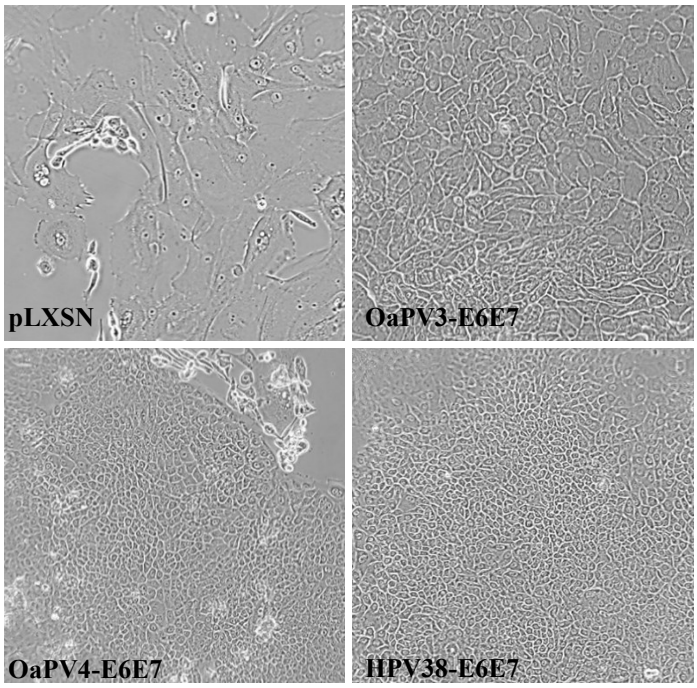

Figure 27 *Cell morphology of HPKs transduced with the indicated recombinant retroviruses and selected with G418. Magnification 10X.*

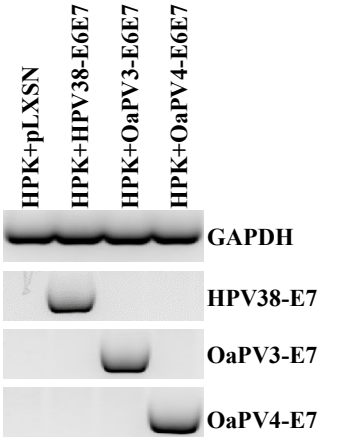

Figure 28 *RT-PCR confirming protein expression in transduced HPKs with the indicated retroviral vectors.*

HPKs were photographed after selection (Figure 27) to monitoring cell morphology. Mock cells (transduced HPKs with empty pLXSN) early acquired a flat and enlarged morphology characteristic of arrested senescent cells. They immediately stopped dividing and entered in a quiescent phase. On the contrary, co-espression of E6 and E7 proteins of both OaPV3 and OaPV4 heightened the proliferation of cells, which acquired a more regular shape with defined borders compared to control.

The analysis of the growth profile of transduced HPKs showed a prolonged lifespan of cells that express OaPV proteins compared to mock cells. The graph (Figure 29) represents the number of population doublings (PD) at the specified times after infection with the different recombinant retroviruses. OaPV3-E6E7 and OaPV4-E6E7 curves overlapped. For the determination of PD level, cells were seeded in 25cm^2 flasks and trypsinized when they reached approximately 80-90% confluence. PD level was calculated taking into consideration the number of passages and the split ratio.

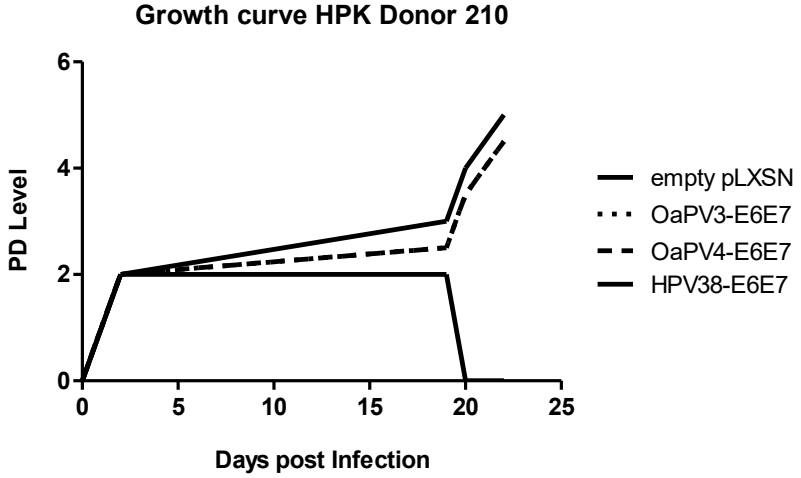

Figure 29 *Growth curve of transduced HPKs. Overexpression of OaPV proteins increases HPK lifespan. PD level indicates the number of times cells have double since their retroviral transduction*

Expression levels of proteins implicated in pRB and p53 pathways were checked through western immunoblotting of total proteins extracted from transduced HPKs (Figure 30). Immunoblotting revealed no significative changes of p53 levels in OaPV3-E6E7 and OaPV4-E6E7 expressing cells compared to control cells in all three donors.

E6 and E7 co-expression led to pRB destabilization. OaPV4-E6E7 seemed to promote pRB degradation, while, on the contrary, OaPV3-E6E7 seemed to cause pRB expression increase. Considering these results, phospho-RB protein levels were also checked and

immublotting showed the accumulation of the inactive phosphorilated form of pRB in OaPV3-E6E7 expressing HPKs. This data were repeatable in at least two donor cell lines. Furthemore, it was established the ability of oncogenes of both ovine viruses to upregulate Cyclin A and cdc2 (CDK1), which are implicated in the pRB/E2F pathway and necessary for S-phase entry. Protein levels of cyclinA and cdc2 (CDK1) are available only for transduced HPK donor 210.

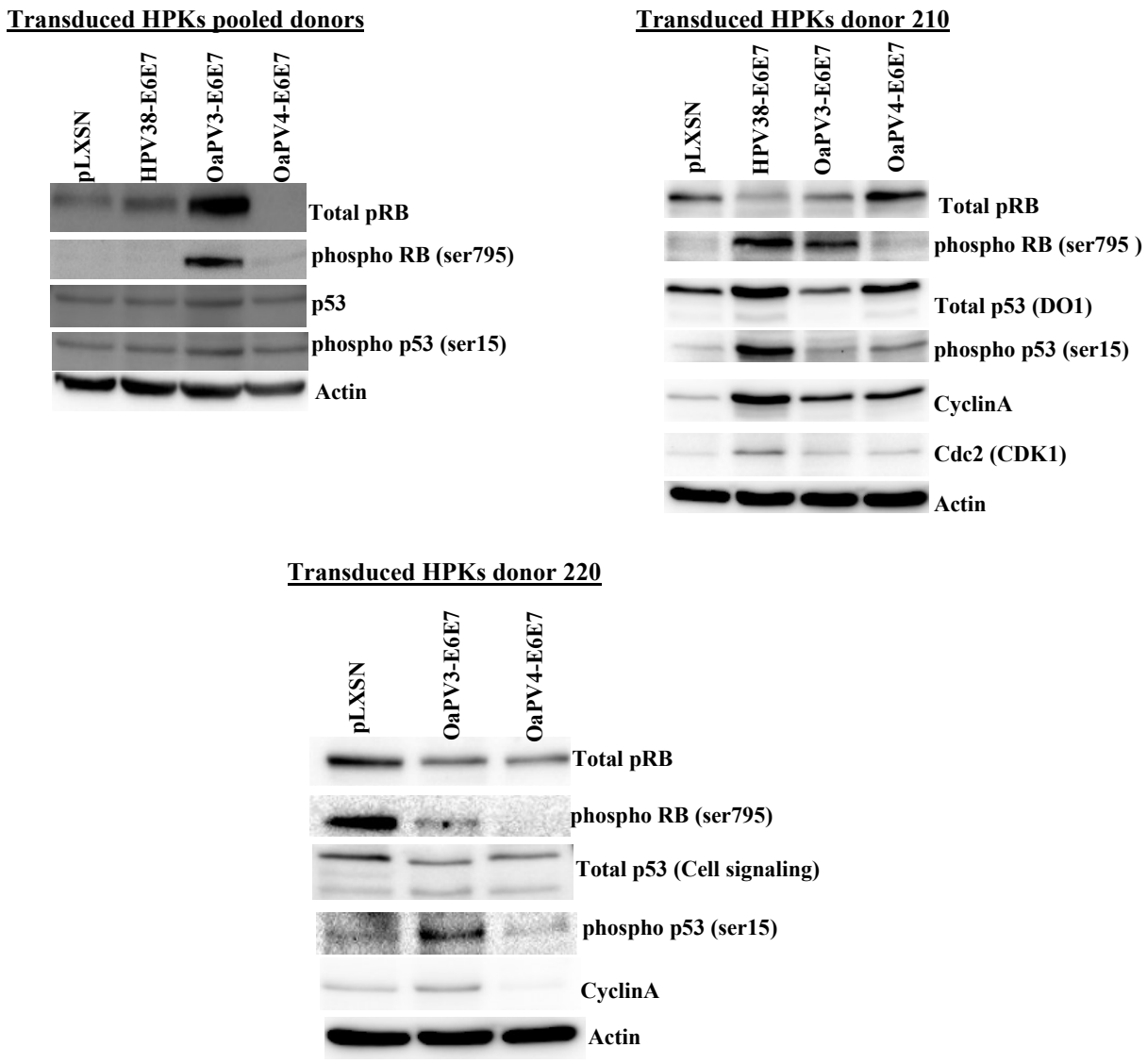

Figure 30 *Western immunoblotting: expression levels of different target proteins in transduced HPKs from three distinct donors.*

Densitometric values of pRB, phospho RB, cdc2 (CDK1) and cyclinA were calculated and normalized to β-actin using ImageLab 5.2.1 software and then represented graphically as fold change relative to control cells. The expression level of the target protein in the control culture (HPK+pLXSN) was set as 1 (Figure 31-Figure 32-Figure 33)

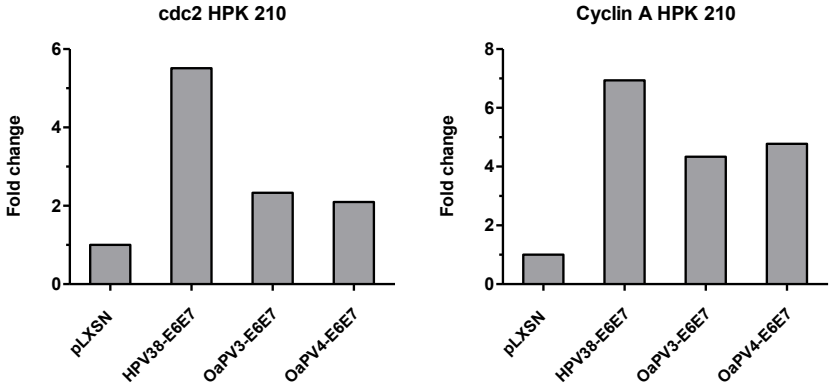

Figure 31 *Relative fold change of cdc2 and cyclinA in HPKs transduced with the indicated recombinant retroviruses. Target protein level was normalized to β-actin levels.*

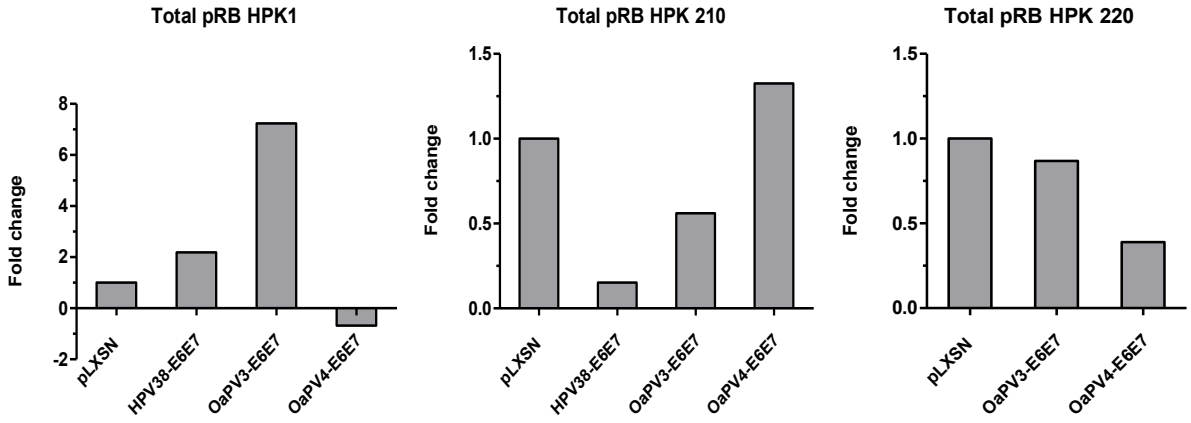

Figure 32 *Relative fold change of total RB in HPKs transduced with the indicated recombinant retroviruses. Target protein level was normalized to β-actin levels*

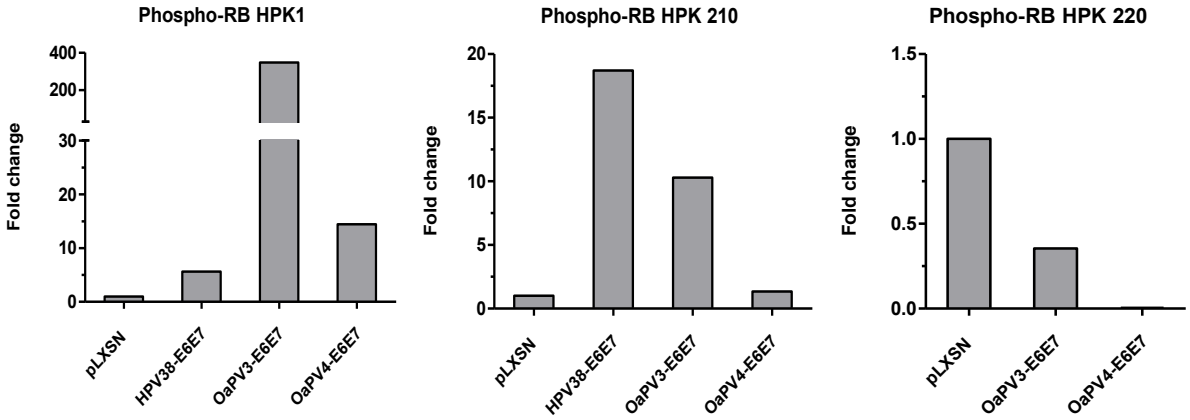

Figure 33 *Relative fold change of phospho- pRB in HPK transduced with the indicated recombinant retroviruses. Target protein level was normalized to β-actin levels.*

Retroviral transductions were repeated using two different donors of ovine primary keratinocytes (PLKs). Isolated PLKs were characterized through immunofluorescence with monoclonal antibody against Pan Cytocheratin before experiments (Figure 34).

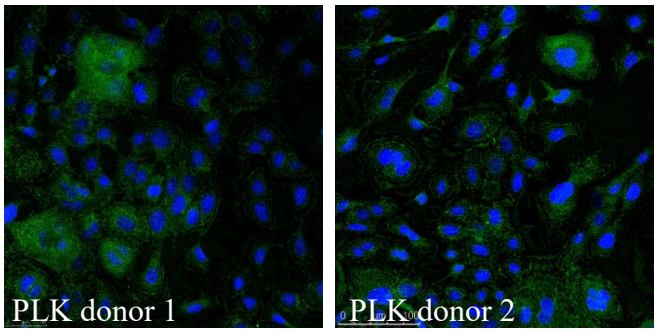

Figure 34 *IF: green fluorescence indicates positive reaction of isolated PLKs to mAb Anti-Pan Cytocheratin. In blue, nuclei counterstained with DAPI.*

After retroviral infection with OaPV3-E6E7 and OaPV4-E6E7 genes or empty pLXSN and selection, PLKs were photographed (Figure 35). A well-demarcated difference in cell morphology was appreciable between mock cells and cells that express OaPV oncogenes. In particular, OaPV3-E6E7 expressing PLKs were smaller, acquired regular borders and looked more like stem cells than epithelial cells. On the contrary, OaPV4-E6E7 expression did not lead to modification of cell shape that appeared similar to cells after their isolation from tissue. Late OaPV4-E6E7 passages showed heterogeneous cultures with a majority of large flat cells with low nucleus/cytoplasm ratio. These differences are better observable in photographs with higher magnification (Figure 36).

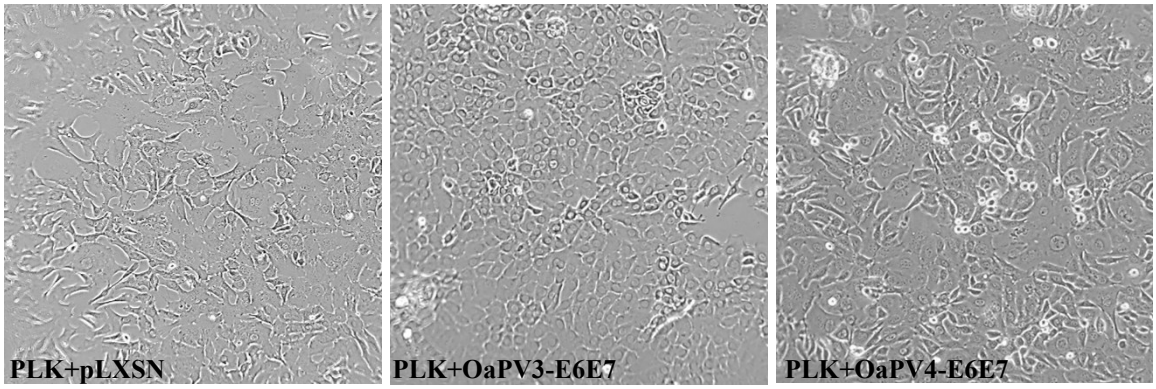

Figure 35 *Cell morphology of HPKs transduced with the indicated recombinant retroviruses. Magnification 10X.*

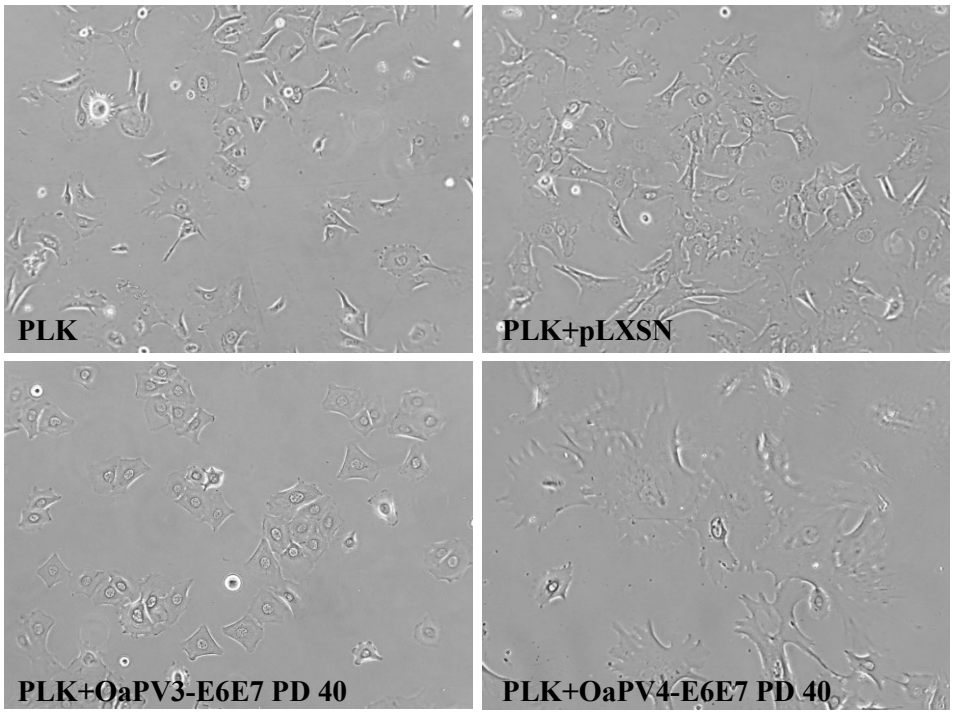

Figure 36*Cell morphology of mock and transduced PLKs. Magnification 20X.*

According to current data, the cell growth profile demonstrates that E6E7 expression of both OaPV3 and OaPV4 has determined a significative increase of primary ovine keratinocyte lifespan (Table 4). In fact, PLKs transduced with the empty retroviral vector stopped proliferating early after infection: PLK1+pLXSN died at PD 7.5 and PLK2+pLXSN died at PD6.

Table 4 *Population doubling levels in primary ovine keratinocytes from two donors transduced with the indicated recombinant retroviruses. Data referred to ongoing experiments and are updated to current results.*

	N° of population doublings in PLKs from donor:	
Retrovirus	1	2
Empty pLXSN	Dead at PD 7.5	Dead at PD 6
pLXSN+OaPV3-E6E7	PD 46	PD 45
pLXSN+OaPV4-E6E7	PD 43	PD 34.5

Graphs (Figure 37) of the two donor cell lines represent the number of population doublings (PDs) at the specified times after infection with the different recombinant retroviruses. PD levels were calculated as described above.

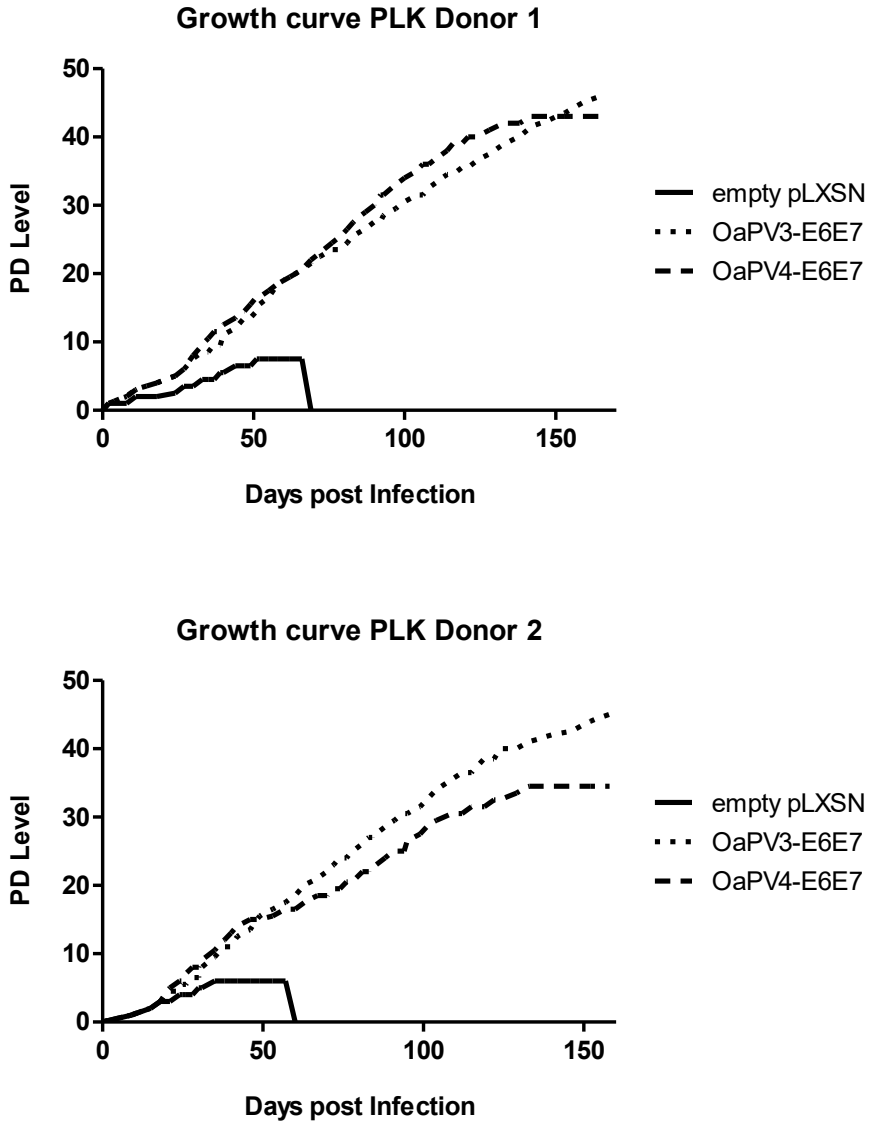

Figure 37 *Growth curve of transduced PLKs from donor 1 (top) and 2 (bottom). PD level indicates the number of times cells have double since their retroviral transduction.*

An additional evaluation of the growth potential conferred by the various E6E7 genes was to look at the population doubling time (PD time) which correspond to the number of days it took each culture to reach 80-90% confluence (at which point cultures were split). E6E7 expressing PLK cell lines always exhibited a statistically significant shorter PD time compared to mock cells (pLXSN). Moreover, OaPV3-E6E7 PLKs manifested the shortest time length and the higher proliferative activity in both donor cell lines even if the difference between OaPV3 and OaPV4 PD times is not significative for PLK of donor 1 (Figure 38).

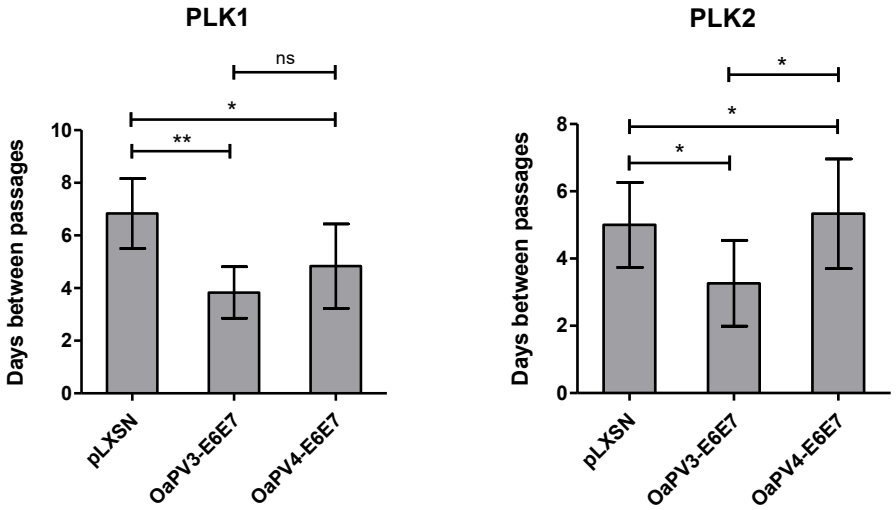

Figure 38 *Time length (days) between post-selection passages of transduced PLKs from donor 1 and 2. Results are the mean of 6 values for each experiment. Error bars show standard deviation. p value ≤0,05*

OaPV3-E6E7 and OaPV4-E6E7 were also tested for the ability to alter the p53 and pRB pathways in ovine keratinocytes. Western immunoblotting of total proteins extracted from transduced PLKs showed no significant changes in p53 expression levels confirming data obtained from human keratinocyte model (Figure 39).

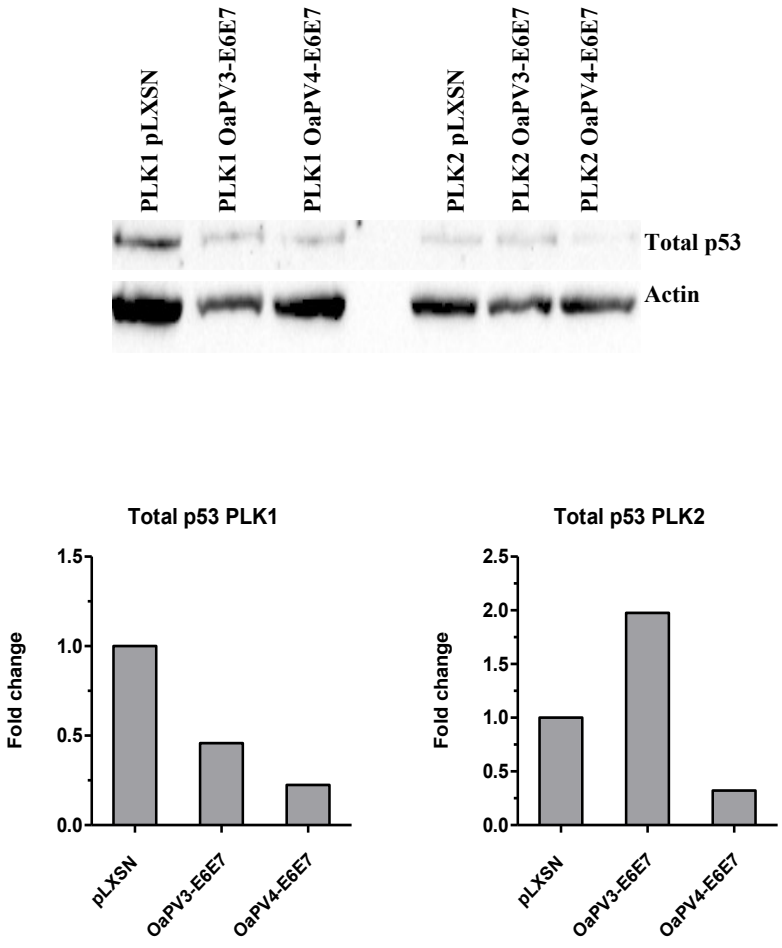

Figure 39 *Western immunoblotting: total p53 expression in transduced PLK1 and PLK2. At the bottom, protein levels are represented graphically as relative fold change after normalization to β-actin. The expression level of the target protein in the control cultures was set as 1.*

Immnoblotting provided evidences for alterations of total pRB protein expression in E6E7 expressing PLKs, even if the use of human primary antibodies to detect ovine proteins gave rise to technical issues. The phosphorylated inactive form of pRB accumulated in oncogenes expressing PLKs compared to control (Figure 40).

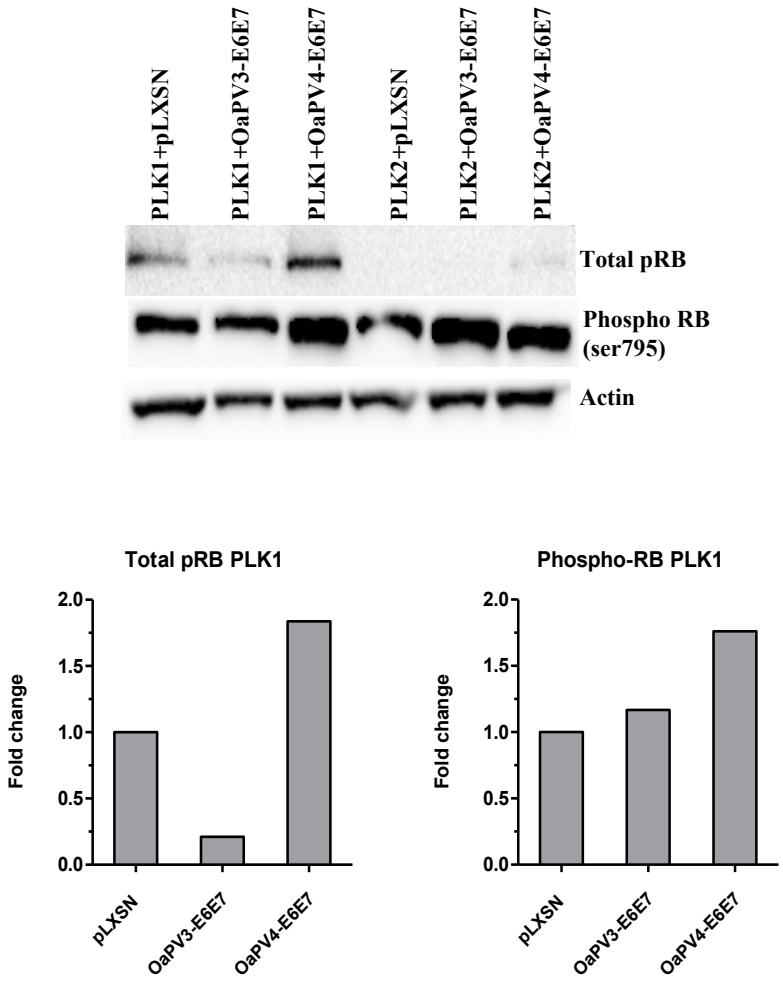

Figure 40 *Western immunoblotting: total pRB and phospho RB expression in transduced PLK1 and PLK2. At the bottom, protein levels are represented graphically as relative fold change after normalization to β-actin. The expression level of the target protein in the control cultures was set as 1.*

Furthemore, cdc2 (CDK) protein expression was sifnificantly upregulated in E6E7 expressing PLKs from both donors (Figure 41).

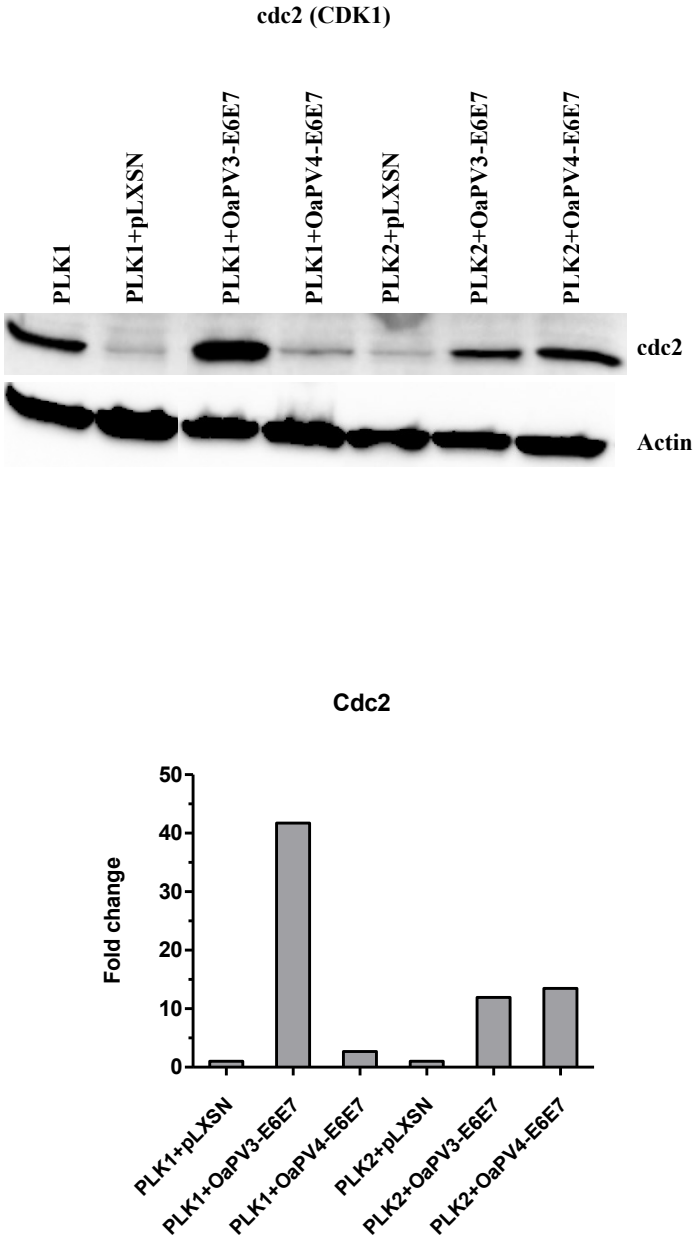

Figure 41 *Western immunoblotting: cdc2 expression in transduced PLK1 and PLK2. At the bottom, protein levels are represented graphically as relative fold change after normalization to β-actin. The expression level of the target protein in the control cultures was set as 1*

5.3.1 Colony formation assay

OaPV3-E6E7 and OaPV4-E6E7 were also tested for enhanced proliferation capacity in a clonogenicity assay, which evaluates the ability of a single cell to proliferate and form a colony. Colony formation assays revealed a 3,2 and 2,5-relative fold increase in the number of colonies in, respectively, OaPV3-E6E7 and OaPV4-E6E7 expressing cultures compared to control (Figure 43). Furthermore, a statistically significant difference was also found between OaPV3-E6E7 and OaPV4-E6E7 expressing PLKs, revealing a stronger clonogenic efficiency of OaPV3 compared to OaPV4 (Figure 42).

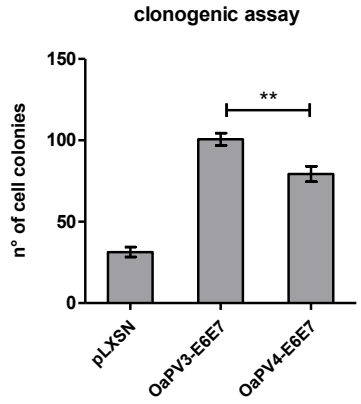

Figure 42 *Clonogenic assay: number of generated colonies. Error bars show standard deviation. Values are means from two indipendent experiments. p value ≤0,01*

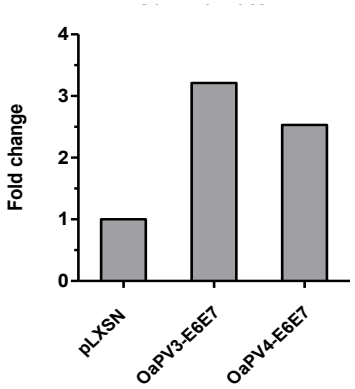

Figure 43 *Fold increase in the number of colonies. The control culture was set as 1.*

OaPV3-E6E7 expressing keratinocytes generated narrower colonies but composed of copious, small, packed, proliferative cells. On the other hand, OaPV4-E6E7 expressing colonies were macroscopically and microscopically more similar to control colonies and constituted by sparse, flat and large keratinocytes (Figure 44-Figure 45).

Colony formation assays in soft agar were perfomed in order to verify the ability of transduced keratinocytes to grow in an anchorage independent manner. None of the cell lines generated any colony (data not shown).

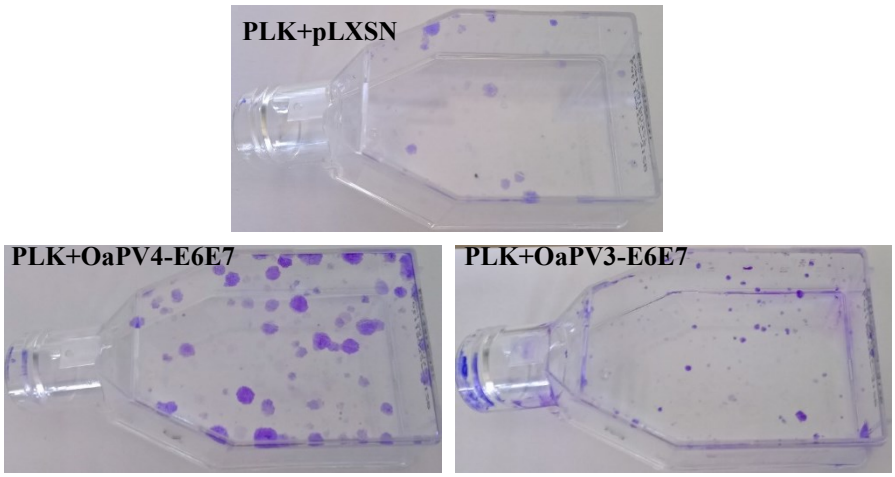

Figure 44 *Colony formation assay: macroscopic aspect of colonies stained with crystal violet.*

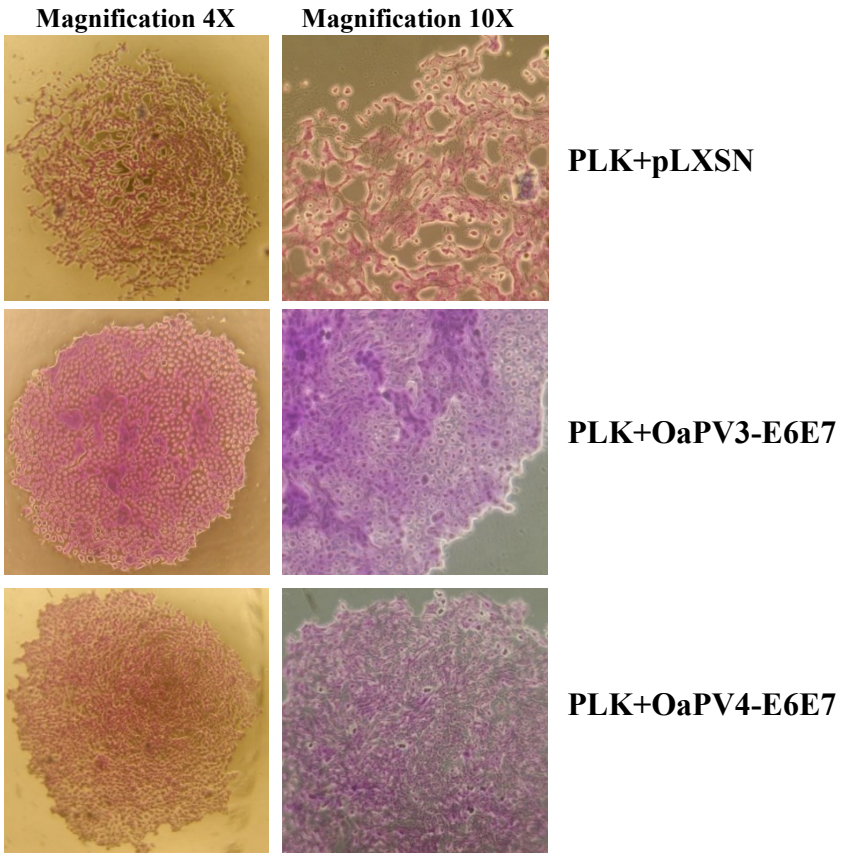

Figure 45 *Colony formation assay: microscopic aspect of colonies at different magnfications.*

5.3.2 GST pulldown assay

E6 and E7 of both OaPV3 and Oapv4 were amplified from pUC19+OaPV4_3kb plasmid and successfully cloned into pGEX4T1 bacterial expression vector in order to generate GST fusion proteins (Figure 46).

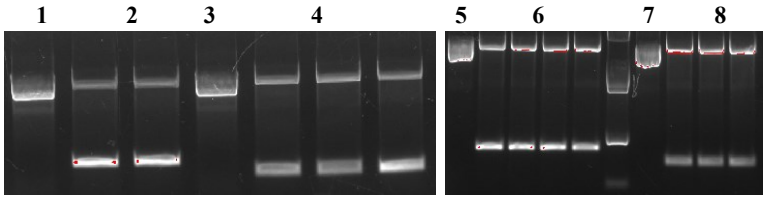

Figure 46 *Agarose gel: analytical digestion of pGEX4T1 plasmids.* ***1****: not digested* ***2****: digested pGEX4T1+OaPV4-E6* ***3****: not digested plasmid* ***4****: digested pGEX4T1+OaPV4-E7* ***5****: not digested plasmid* ***6****: digested pGEX4T1+OaPV3-E6* ***7****: not digested plasmid* ***8****: digested pGEX4T1+OaPV3-E7*

BL21 Codon plus *E.coli* were transformed with the plasmids mentioned above and induced with IPTG. The correct expression of all GST fusion proteins was checked on SDS-PAGE before purification (Figure 47-Figure 48).

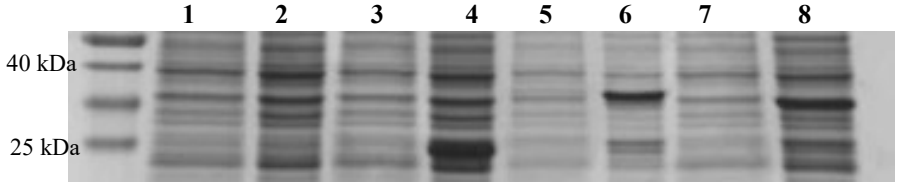

Figure 47 *SDS-PAGE: OaPV4-E6 and E7 expression.* ***1****: empty BL21 not induced* ***2****: empty BL21 induced* ***3****: GST not induced* ***4****: GST induced* ***5****: OaPV4-E6 not induced* ***6****: OaPV4-E6 induced 7: OaPV4-E7 not induced* ***8****: OaPV4-E7 induced.*

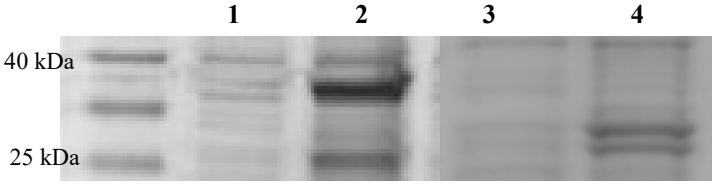

Figure 48 *SDS-PAGE: OaPV3-E6 and E7 expression.*
1*: OaPV3-E6 not induced* ***2****: OaPV3-E6 induced* ***3****: OaPV3-E7 not induced* ***4****: OaPV3-E7 induced.*

Fusion proteins run faster on SDS-PAGE than expected, and protein bands had lower molecular weights compared to those predicted by *in silico* analysis. GST fusion proteins were purified using glutathione beads and purification was checked through SDS-PAGE. In order to estimate the amount of purified proteins, a BSA curve was included in the running (Figure 49).

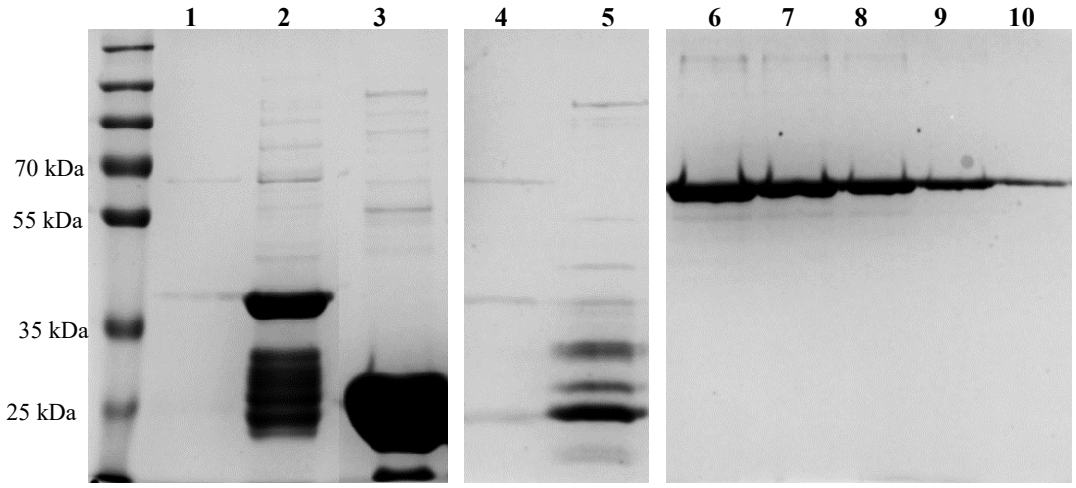

Figure 49 *SDS-PAGE: GST fusion protein purifications.*
1*: OaPV4-E6* ***2****:OaPV4 E7* ***3****: GST alone* ***4****: OaPV3-E6* ***5****:OaPV3 E7* ***6****: BSA 2 µg* ***7:*** *BSA 1,5 µg* ***8****: BSA 1 µg* ***9*** *BSA: 0,5 µg* ***10****: BSA 0,1 µg*

Purification of both E6 fusion proteins did not result in a clear band of the expected size (lines 1 and 4 of Figure 49). This can be explained by the formation of protein aggreagates. In fact, E6 proteins from various papillomaviruses become insoluble when expressed in bacteria and concentrated (Vande Pol and Klingelhutz, 2013; Zanier et al., 2007).

GST pulldown assay was initially performed using whole cell lysate of human naturally immortalized keratinocytes (NIKS). It confirmed the ability of OaPV3-E7 and OaPV4-E6 to associate *in vitro* with human pRB, since the two oncoproteins contain a canonical pRB-binding motif. Interestingly, also OaPV4-E7 showed the capacity to bind human pRB. None of the oncoproteins associated with neither human p53 nor E6AP (Figure 50).

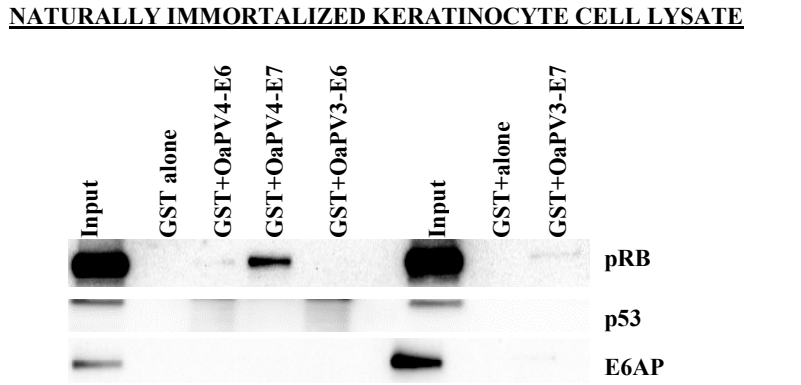

Figure 50 *GST pulldown showing interaction of OaPV3-E7, OaPV4-E6 and OaPV4-E7 with pRB. Assay was performed using a total protein extract of human immortalized keratinocytes.*

GST pulldown assay was repeated using total protein extracts of primary ovine cells (fibroblasts and keratinocytes). Experiments confirmed the absence of the association with p53 and the strong affinity of OaPV3-E7 for pRB, despite technical problems caused by the use of human primary antibodies (Figure 51).

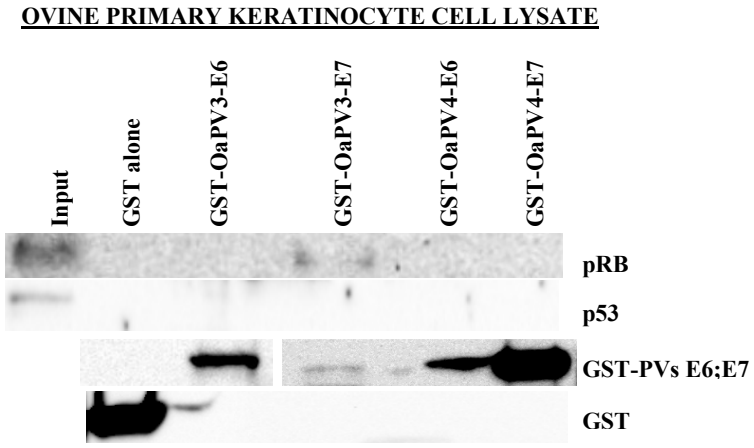

Figure 51. *GST pulldown showing interaction of OaPV3-E7 with pRB. Assay was performed using total protein extracts of ovine cells. Blots are cut as they are shown at different exposure times; bands were properly aligned basing on the migration with respect to molecular marker loaded onto the gel.*

5.3.3 Co-Immunoprecipitation

E6 and E7 of both OaPV3 and Oapv4 were amplified from pUC19+OaPV4_3kb plasmid and successfully cloned into pCMV HA-N mammalian expression vector in order to generate HA-tagged proteins (Figure 52).

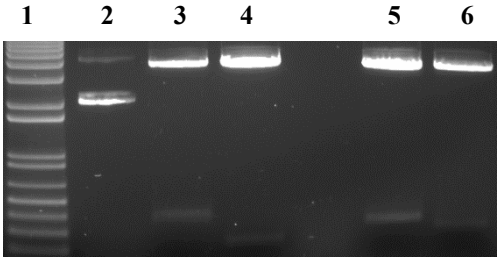

Figure 52 *Agarose gel: analytical digestion of pCMV HA-N plasmids.* ***1****: 1kb plus DNA ladder* ***2****: not digested plasmid* ***3****: digested pCMV HA-N+OaPV3_E6* ***4****: digested pCMV HA-N+OaPV3_E7* ***5****: digested pCMV HA-N+OaPV4_E6* ***6****: digested pCMV HA-N+OaPV4_E7*

Ovine primary fibroblast and keratinocytes were transfected with the plasmids mentioned above and collected 48 hours after. Whole cell lysates were extracted from cell pellets and used to perform co-immunoprecipitation assays. Immunoprecipitates were subjected to SDS-PAGE and subsequent western blot.

Immunoblotting verified the ability of OaPV3E7 to bind pRB *in vitro* with high efficiency (Figure 53).

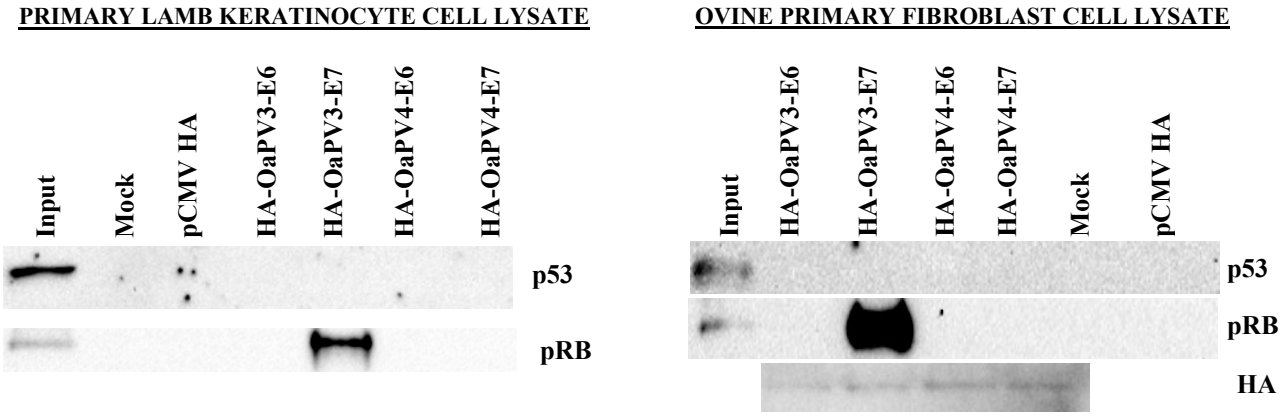

Figure 53 *Co-Immunoprecipitation assays showing interaction of OaPV3-E7 with pRB. No association was found with p53.*

6. DISCUSSION

6.1 Identification, characterization and evolutionary history of ovine papillomaviruses

At present, global animal PV genotype diversity does not reach up the one found in human (Rector and Van Ranst, 2013). Therefore, each single animal species is expected to host an overlooked number of PV types comparable to the human one. 71 PV species (belonging to 46 PV genera) have been rescued from 75 vertebrate host species, including 5 birds, 3 reptiles and 1 fish so far. Considering these numbers, it becomes clear that a great proportion of animal papillomavirus diversity is still to be uncovered. To date, 3 types of PV have been described in sheep. Information about ovine *Deltapapillomavirus* OaPV1 and OaPV2 (unpublished) is limited to data available in the relative GenBank entries (U83594 and U83595 respectively), such as their geographic origin, genome sequence, and isolation source from fibropapillomas, and this hampers making any general assumption about ovine PV biology. The third ovine PV, OaPV3 (Alberti et al., 2010) is the prototype of *Dyokappapapillomaviruses,* a genus distantly related to *Deltapapillomaviruses* also comprising the alpine chamois RrPV1. Both OaPV3 and RrPV1 have been rescued from squamous cell carcinomas located in sun-exposed areas of the face.

This research reports the identification of a novel ovine papillomavirus, designated OaPV4 (GenBank accession number KX954121), from a fibropapilloma located in the scrotum of an adult Sarda breed ram. Following the criteria established for the classification of PVs (Bernard et al., 2010; De Villiers et al., 2004), and considering that OaPV4 L1 nucleotide sequence is at least 10% dissimilar from that of any other PV type, OaPV4 was included in a novel PV type within *Deltapapillomavirus* 3. OaPV1, OaPV2, and OaPV4 (*Delta* 3 species PVs) are closely related viruses so far rescued from European and Australian sheep, and all of them are associated to fibropapillomatosis. They lack a pRB binding domain and zinc-binding motifs in the E7 gene. Notably, a putative pRB binding domain in E6 can be observed in both OaPV4 and the other ovine PVs of the Delta genus. Additionally to canonical genes, they possess an E5 gene. Interestingly, the presence of an E5 gene and the lack of a pRB binding domain in E7 have been related to the development of fibropapillomas (Narechania et al., 2004). In situ hybridisation and immunohistochemistry results obtained in this study indicate that ovine deltapapillomaviruses are able to infect both epithelial cells and fibroblasts, and cause proliferation of both the epidermis and the underlying connective tissue in lesions.

On the contrary, the novel OaPV4 and the ovine Dyokappa PVs are very distantly related with only 48,3% L1 nucleotide identity among OaPV4 and OaPV3. Furthermore, Dyokappa PVs infect exclusively epithelial cells, maintain a pRB binding domain in E7 and lack an E5 gene (Alberti et al., 2010).

Phylogenetic analysis of OaPV4 and 98 other PVs (Figure 24, Table 1) is consistent with previous observations and confirms the presence of four major strongly supported PV crown groups, as previously described (Gottschling et al., 2011). Since several new animal PV types not considered by Gottschling and coworkers were included in our phylogenetic analysis, the crown groups were updated based on significant associations observed among: *Alpha*, *Omega*, *Dyodelta*, *Psi, Omicron, Upsilon* (Alpha + Omicron crown); *Beta, Dyoeta, Dyoxy, Gamma, Tau, Pi, Phi, Rho, Xi* (Beta + Xi crown); *Delta, Epsilon, Zeta, Dyoiota, Dyorho, Dyochi*, (Delta + Zeta crown); *Dyophi, Kappa, Mu, Lambda* (Lambda + Mu crown). OaPV4 confirms that ovine PVs, which are polyphyletic and distributed in two lineages (Figure 24-Figure 25), are characterised by a broad genetic diversity. OaPV4 appears to be most closely related to OaPV1 (Fig. 5), from which it diverged around 0.61 ± 0.24 Myr ago, while OaPV1/OaPV4 split off from OaPV2 about 1.5 ± 0.65 Myr ago. During the same period the Urial sheep *O. vignei* diverged from the mouflon *O. orientalis*, paving the way for the radiation of modern wild and domestic sheep species (Rezaei et al., 2010). OaPV3 (*Dyokappapapillomavirus*) is a more ancient virus that split off from its most close relative RrPV1 about 3.73 ± 1.7 Myr, nearly when the monophyletic genus *Ovis* was diverging from the other *Caprinae,* roughly 2–3 million Myr ago. (Bunch et al., 2006; Ropiquet and Hassanin, 2005).

Further investigation utilizing more sequence data from a larger number of *Caprine* viruses and extensive epidemiological studies including different species are required to fill in the existing gaps in the PV phylogenetic tree, and to better understand the coevolution of papillomaviruses with their hosts. Further research could also elucidate the presence and distribution of OaPV4 in other domestic sheep breeds and wild sheep species in Eurasia and North Africa.

6.2 Comparative analysis of ovine PVs E6 and E7 *in vitro* transforming properties

Studying the biological properties of the viral oncoproteins E6 and E7 might be helpful in the process towards the understanding of the association between papillomavirus and skin cancer onset. Determining whether these viruses have *in vitro* transforming activity would at least support or refute their potential role in the development of malignancies *in vivo* (Massimi

et al., 2008). Few studies have been conducted on cutaneous animal papillomaviruses transforming abilities to date. Most of them are centred on BPV but there is little evidence that BPVs influence the development of cutaneous NMSCs in cattle, while PVs have been associated with skin cancer in other domestic species (Altamura et al., 2016; Munday, 2014; Munday and Kiupel, 2010). Moreover, the majority of these studies were performed using fibroblasts as *in vitro* models.

For this research project, cell culture immortalization and transformation assays were used to assess the biological properties of OaPV3-E6E7 and OaPV4-E6E7 in a comparative study between the two viruses. OaPV3 has been identified in cutaneous SCCs and its gene repertoire resembles the cutaneous beta-HPV (Alberti et al., 2010), some of which are involved in skin tumours. On the other hand, OaPV4 has been recovered from a benign fibropapilloma like others deltapapillomaviruses and its genome features are not predictive for a role in NMSC development.

It has been established that several cutaneous papillomaviruses, mostly beta-HPVs, can determine the immortalization, or at least the lifespan increase, of monolayer cultures of primary keratinocytes (Caldeira et al., 2003; Cornet et al., 2012; Massimi et al., 2008). Basing on previous studies (Caldeira et al., 2003; Cornet et al., 2012), the putative transforming abilities of OaPV3-E6E7 and OaPV4-E6E7 were tested in primary keratinocytes stably transduced with ovine PV E6/E7 oncogenes. Our data show that the overexpression of E6/E7 of both ovine viruses is sufficient to increase the life span of primary human keratinocytes. When experiments were conducted by using ovine keratinocytes, both OaPV3 and OaPV4 oncogenes determined an even more substantial life span increase and transduced cells have grown for over 40 population doublings after infection. Keratinocytes must be cultured for more population doublings in order to verify for sure the oncogene immortalization effect. Nevertheless, a difference in proliferative activity was noticed during late passages between OaPV3-E6E7 and OaPV4-E6E7 expressing PLKs. While OaPV3-E6E7 cell lines conserved a high proliferative activity, OaPV4-E6E7 keratinocytes started to be more quiescent. Furthermore, OaPV3-E6E7 keratinocytes exhibit shorter time length between passages than OaPV4-E6E7. Consequently, current partial data about cell growth profiles endorse the hypothesis that OaPV3 might promote keratinocyte immortalization while OaPV4 promotes only a lifespan increase.

FBS deprivation (from 10% to 5%) does not interfere with growth ability of ovine E6E7 expressing PLKs, while mock cell do not proliferate and show features of senescence when

cultured in low-serum medium. This result further supports the thesis of the possible role of ovine E6 and E7 in cell transformation.

As evident from cell shape, OaPV3-E6E7 overexpression allows keratinocytes to acquire a stem cell-like morphology, distant from typical epithelial morphology of cells after their isolation. This is known to be a property common among cancer cells. Moreover, colony formation assays reveal that OaPV3-E6E7 expressing PLKs have the highest clonogenic activity both compared to control and OaPV4-E6E7 cultures. Differences are found not only in the number of mature colonies but also in their morphology. While OaPV4-E6E7 colonies are comparable to control colonies and are formed by large flat cells, OaPV3-E6E7 colonies mostly resemble *foci* of transformed cells and are constituted by small packed keratinocytes. Nevertheless, OaPV3-E6E7 expression do not induce anchorage-independent growth. Results of colony formation assay corroborate the hypothesis that OaPV3 but not OaPV4 might have oncogenic capacities.

Papillomavirus E6 and E7 oncogenes play a key role in the induction of benign and malignant lesions by associating with several cellular factors and altering their function. p53 and pRB and their related pocket proteins are commonly impaired during mucosal alpha HR-HPV infection. The most studied property of HR-HPV E7 oncoproteins is the ability to functionally complement the tumour suppressor pRB promoting its degradation. pRB destabilization is a key factor in S-phase progression and cell proliferation, thus contributing to cancer development. There are also a number of specific studies regarding cutaneous HPV E7 proteins and pRB association. For instance, HPV38 E7 has been shown to bind pRB with a similar efficiency as HPV16 E7 and promote pRB destabilization (Caldeira et al., 2003). OaPV3-E6E7 and OaPV4-E6E7 determine pRB destabilization when in transduced primary keratinocytes with mechanisms that have not been clarified yet. However, the accumulation of the inactive phosphorylated form of pRB has been attested in both human and ovine transduced cell lines. Furthermore, pulldown assays always reveal stronger ability of OaPV3-E7 to efficiently associate with pRB leading to its destabilization. Interestingly, OaPV4-E6 and OaPV4-E7 can bind human pRB when pulldown assay is conducted using human cells. Nonetheless, pRb binding efficiency does not necessarily correlate with the ability to degrade the tumour suppressor and to induce cellular transformation (Caldeira et al., 2003; Ciccolini et al., 1994).

One of the best-characterized properties of HR-HPV E6 is its ability to induce degradation of the tumour suppressor protein p53 via the ubiquitin pathway. This assumption

is not always true for E6 proteins of cutaneous types, which in some cases do not interfere with p53 signalling or use different mechanisms. For instance, the HPV 38 E6 and E7 increase ΔNp73 expression, which inhibits the capacity of p53 to induce transcription of genes involved in growth suppression and apoptosis (Accardi et al., 2006). Our *in vitro* studies are not consistent with a significant alteration of p53 expression upon ovine E6E7 oncogene expression. Furthermore, neither E6 nor E7 of both OaPV3 and OaPV4 associate with p53 in any of the cells adopted for pulldown assays. These findings suggest that these viruses may not have developed mechanisms to impair the p53 pathway.

Mitogenic stimuli such as oncogene expression deregulate the expression of cyclins and the related cyclin-dependent kinases (CDKs) leading to the their activation that is necessary for cell cycle progression (Tommasino, 2016). Consistently with this assumption, we found that the pro-proliferative proteins Cyclin A and Cdc2 are upregulated upon OaPV3 and Oapv4-E6E7 expression in both human and ovine primary keratinocytes.

Concluding, all these findings are hallmarks of cell immortalization and transformation, particularly in OaPV3-E6E7 expressing keratinocytes, and support our hypothesis of a role of OaPV3 during squamous cell carcinomas development in sheep. Further analyses are clearly required to understand if ovine PV E6 and E7 can associate with cellular factors other than pRB and p53 to overcome cell cycle control signalling pathways and promote cellular transformation.

7. CONCLUSION

Human is the only widely PV host studied so far; therefore, further investigations about papillomavirus variability within other species are necessary. Thanks to the spreading of sequence independent genome amplification methods, the number of novel characterized PV types is increasing, improving our knowledge about PVs taxonomy, evolutionary history, and pathogenicity, which will not progress without a more systematic sampling of PV diversity (Gottschling et al., 2011).

This research allowed to identify and characterize the fourth ovine papillomavirus type (OaPV4, GenBank accession number KX954121) belonging to the Delta 3 species. As other artiodactyl Delta papillomaviruses, OaPV4 has both epithelial and dermal cell tropism and is associated with fibropapilloma onset. The identification of OaPV4 allows making several general assumptions on ovine PVs and confirms their broad diversity suggesting, similarly to what observed in humans, that *Caprinae* could also host a great number of PV types.

Association between cutaneous papillomavirus infection and skin carcinogenesis has not been well characterized to date, and very few studied have been conducted on biological properties of these specific types compared to mucosal alpha HR-HPVs (typically HPV16). For this reason, our data obtained from an *in vitro* ovine papillomavirus model represent a step towards the understanding of oncogenic properties of cutaneous papillomavirus types and towards the finding of the best suitable animal model for the study of HPV-induced diseases.

SCC has high incidence in flocks and it poses a direct threat to sheep especially to those highly selected for milk production, such as Sarda breed sheep, by compromising the udders of ewes. OaPV3 has been found in association with skin carcinomas and our *in vitro* results are compatible with a possible oncogenic role of this virus *in vivo* together with already known risk factors (e.g., UV exposition, chemicals). Considering this, further studies are welcomed to better clarify how OaPV3 oncogenes impair cell cycle control pathways and how this virus interacts with UV exposition leading to skin carcinogenesis.

Concluding, the ovine *in vitro* model renforces the thesis of a direct link between cutaneous papillomaviruses, cellular tramsformation and NMSC progression.

ABBREVIATIONS

BPV Bovine Papillomavirus (Bos taurus Papillomavirus)

BSA Bovine Serum Albumin

cdc2 cell division cycle 2

CDK Cyclin Dependent Kinase

COPV Canine Oral Papillomavirus

CRPV Cottontail Rabbit Papillomavirus

E1BS E1 Binding Site

E2BS E2 Binding Site

GST Glutathione S-Transferase

HPK Human Primary Keratinocyte

HPV Human Papillomavirus

HR-HPV High Risk-Human Papillomavirus

IARC International Agency for Research on Cancer

ICTV International Committee on Taxonomy of Viruses

IF Immunofluorescence

IHC Immunohistochemistry

ISH In Situ Hybridization

LCR (URR, NCR) Long Control Region (Non Coding region)

LR-HPV Low Risk-Human Papillomavirus

NMSC Non Melanoma Skin Cancer

OaPV Ovis aries Papillomavirus

ORF Open Reading Frame

Ori Origin of replication

PBS-T Phosphate Buffered Saline Tween-20

PD Population Doubling

PLK Primary Lamb Keratinocyte

PV Papillomavirus

RCA Rolling Circle Amplification

ROPV Rabbit Oral Papillomavirus

RT Room Temperature

SCC Squamous Cell Carcinoma

UV UltraViolet

REFERENCES

Aasen, T., Izpisúa Belmonte, J.C., 2010. Isolation and cultivation of human keratinocytes from skin or plucked hair for the generation of induced pluripotent stem cells. Nat Protoc 5, 371–382. doi:10.1038/nprot.2009.241

Accardi, R., Dong, W., Smet, A., Cui, R., Hautefeuille, A., Gabet, A.-S., Sylla, B.S., Gissmann, L., Hainaut, P., Tommasino, M., 2006. Skin human papillomavirus type 38 alters p53 functions by accumulation of DNp73. EMBO Rep. 7, 334–340. doi:10.1038/sj.embor.7400615

Accardi, R., Gheit, T., 2014. Cutaneous HPV and skin cancer. Presse Med. 43, e435–e443. doi:10.1016/j.lpm.2014.08.008

Alberti, A., Pirino, S., Pintore, F., Addis, M.F., Chessa, B., Cacciotto, C., Cubeddu, T., Anfossi, A., Benenati, G., Coradduzza, E., Lecis, R., Antuofermo, E., Carcangiu, L., Pittau, M., 2010. Ovis aries Papillomavirus 3: A prototype of a novel genus in the family Papillomaviridae associated with ovine squamous cell carcinoma. Virology 407, 352–359. doi:10.1016/j.virol.2010.08.034

Altamura, G., Corteggio, A., Pacini, L., Conte, A., Pierantoni, G.M., Tommasino, M., Accardi, R., Borzacchiello, G., 2016. Transforming properties of Felis catus papillomavirus type 2 E6 and E7 putative oncogenes in vitro and their transcriptional activity in feline squamous cell carcinoma in vivo. Virology 496, 1–8. doi:10.1016/j.virol.2016.05.017

Anacker, D.C., Moody, C.A., 2016. Modulation of the DNA Damage Response During the Life Cycle of Human Papillomaviruses. Virus Res. doi:10.1016/j.virusres.2016.11.006

Antonsson, A., McMillan, N.A.J., 2006. Papillomavirus in healthy skin of Australian animals. J. Gen. Virol. 87, 3195–3200. doi:10.1099/vir.0.82195-0

Ashrafi, G.H., Brown, D.R., Fife, K.H., Campo, M.S., 2006. Down-regulation of MHC class I is a property common to papillomavirus E5 proteins, Virus Research. doi:10.1016/j.virusres.2006.02.005

Ashrafi, G.H., Tsirimonaki, E., Marchetti, B., O'Brien, P.M., Sibbet, G.J., Andrew, L., Campo, M.S., 2002. Down-regulation of MHC class I by bovine papillomavirus E5 oncoproteins. Oncogene 21, 248–59. doi:10.1038/sj.onc.1205008

Bergvall, M., Melendy, T., Archambault, J., 2013. The E1 proteins. Virology 445, 35–56. doi:10.1016/j.virol.2013.07.020

Bernard, H.U., Burk, R.D., Chen, Z., van Doorslaer, K., Hausen, H. zur, de Villiers, E.M., 2010. Classification of papillomaviruses (PVs) based on 189 PV types and proposal of taxonomic amendments. Virology 401, 70–79. doi:10.1016/j.virol.2010.02.002

Borzacchiello, G., Russo, V., Gentile, F., Roperto, F., Venuti, A., Nitsch, L., Campo, M., Roperto, S., 2006. Bovine papillomavirus E5 oncoprotein binds to the activated form of the platelet-derived growth factor b receptor in naturally occurring bovine urinary bladder tumours. Oncogene 25, 1251–1260. doi:10.1038/sj.onc.1209152

Bottalico, D., Chen, Z., Dunne, A., Ostoloza, J., McKinney, S., Sun, C., Schlecht, N.F., Fatahzadeh, M., Herrero, R., Schiffman, M., Burk, R.D., 2011. The oral cavity contains abundant known and novel human papillomaviruses from the Betapapillomavirus and Gammapapillomavirus genera. J. Infect. Dis. 204, 787–92. doi:10.1093/infdis/jir383

Bouvard, V., Baan, R., Straif, K., Grosse, Y., Secretan, B., El Ghissassi, F., Benbrahim-Tallaa, L., Guha, N., Freeman, C., Galichet, L., Cogliano, V., 2009. A review of human carcinogens--Part B: biological agents. Lancet Oncol. 10, 321–322. doi:10.1016/S1470-2045(09)70096-8

Brimer, N., Lyons, C., Wallberg, A.E., Vande Pol, S.B., 2012. Cutaneous papillomavirus E6

oncoproteins associate with MAML1 to repress transactivation and NOTCH signaling. Oncogene 31, 4639–46. doi:10.1038/onc.2011.589

Buck, C.B., Cheng, N., Thompson, C.D., Lowy, D.R., Steven, A.C., Schiller, J.T., Trus, B.L., 2008. Arrangement of L2 within the Papillomavirus Capsid. J. Virol. 82, 5190–5197. doi:10.1128/JVI.02726-07

Buck, C.B., Day, P.M., Trus, B.L., 2013. The papillomavirus major capsid protein L1. Virology 445, 169–174. doi:10.1016/j.virol.2013.05.038

Bunch, T.D., Wu, C., Zhang, Y.P., Wang, S., 2006. Phylogenetic analysis of snow sheep (Ovis nivicola) and closely related taxa. J. Hered. 97, 21–30. doi:10.1093/jhered/esi127

Caldeira, S., Zehbe, I., Accardi, R., Malanchi, I., Dong, W., Giarrè, M., de Villiers, E.-M., Filotico, R., Boukamp, P., Tommasino, M., 2003. The E6 and E7 proteins of the cutaneous human papillomavirus type 38 display transforming properties. J. Virol. 77, 2195–206. doi:10.1128/JVI.77.3.2195-2206.2003

Campo, M.S., 2002. Animal models of papillomavirus pathogenesis, in: Virus Research. pp. 249–261. doi:10.1016/S0168-1702(02)00193-4

Cerqueira, C., Schiller, J.T., 2016. ARTICLE IN PRESS G Model Papillomavirus assembly: An overview and perspectives. Virus Res. Virus Res. doi:10.1016/j.virusres.2016.11.010

Chambers, G., Ellsmore, V.A., O'Brien, P.M., Reid, S.W.J., Love, S., Campo, M.S., Nasir, L., 2003. Association of bovine papillomavirus with the equine sarcoid. J. Gen. Virol. doi:10.1099/vir.0.18947-0

Chellappan, S., Kraus, V.B., Kroger, B., Munger, K., Howley, P.M., Phelps, W.C., Nevins, J.R., 1992. Adenovirus E1A, simian virus 40 tumor antigen, and human papillomavirus E7 protein share the capacity to disrupt the interaction between transcription factor E2F and the retinoblastoma gene product. Proc. Natl. Acad. Sci. U. S. A. 89, 4549–53. doi:10.1073/pnas.89.10.4549

Chen, E.Y., Howley, P.M., Levinson, A.D., Seeburg, P.H., 1982. The primary structure and genetic organization of the bovine papillomavirus type 1 genome. Nature 299, 529–34.

Chen, Z., DeSalle, R., Schiffman, M., Herrero, R., Burk, R.D., 2009. Evolutionary dynamics of variant genomes of human papillomavirus types 18, 45, and 97. J. Virol. 83, 1443–55. doi:10.1128/JVI.02068-08

Ciccolini, F., Di Pasquale, G., Carlotti, F., Crawford, L., Tommasino, M., 1994. Functional studies of E7 proteins from different HPV types. Oncogene 9, 2633–8.

Cole, S.T., Danos, O., 1987. Nucleotide sequence and comparative analysis of the human papillomavirus type 18 genome: Phylogeny of papillomaviruses and repeated structure of the E6 and E7 gene products. J. Mol. Biol. 193, 599–608. doi:10.1016/0022-2836(87)90343-3

Cornet, I., Bouvard, V., Campo, M.S., Thomas, M., Banks, L., Gissmann, L., Lamartine, J., Sylla, B.S., Accardi, R., Tommasino, M., 2012. Comparative analysis of transforming properties of E6 and E7 from different beta human papillomavirus types. J. Virol. 86, 2366–70. doi:10.1128/JVI.06579-11

Dal Pozzo, F., Andrei, G., Holý, A., Van Den Oord, J., Scagliarini, A., De Clercq, E., Snoeck, R., 2005. Activities of acyclic nucleoside phosphonates against orf virus in human and ovine cell monolayers and organotypic ovine raft cultures. Antimicrob. Agents Chemother. 49, 4843–4852. doi:10.1128/AAC.49.12.4843-4852.2005

de Villiers, E.-M., 2013. Cross-roads in the classification of papillomaviruses. Virology 445, 2–10. doi:10.1016/j.virol.2013.04.023

De Villiers, E.M., Fauquet, C., Broker, T.R., Bernard, H.U., Zur Hausen, H., 2004. Classification of papillomaviruses. Virology. doi:10.1016/j.virol.2004.03.033

DiMaio, D., Petti, L.M., 2013. The E5 proteins. Virology 445, 99–114. doi:10.1016/j.virol.2013.05.006

Doorbar, J., 2016. Model systems of human papillomavirus-associated disease. J. Pathol. doi:10.1002/path.4656

Doorbar, J., 2013. The E4 protein; structure, function and patterns of expression. Virology 445, 80–98. doi:10.1016/j.virol.2013.07.008

Doorbar, J., 2005. The papillomavirus life cycle. J. Clin. Virol. doi:10.1016/j.jcv.2004.12.006

Doorbar, J., Quint, W., Banks, L., Bravo, I.G., Stoler, M., Broker, T.R., Stanley, M.A., 2012. The biology and life-cycle of human papillomaviruses. Vaccine. doi:10.1016/j.vaccine.2012.06.083

Dreer, M., van de Poel, S., Stubenrauch, F., 2016. Control of viral replication and transcription by the papillomavirus E8^E2 protein. Virus Res. doi:10.1016/j.virusres.2016.11.005

E.P.J. Gibbs, C.J. Smale, M.J.P.L., 1975. Identification of a papillomavirus and transmission of infection to sheep. J. Comp. Pathol. 85, 327–334. doi:10.1016/0021-9975(75)90075-4

Egawa, K., 2003. Do human papillomaviruses target epidermal stem cells? Dermatology 207, 251–4. doi:73085

Fauquet, C.M., Mayo, M.A., 2001. The 7th ICTV report. Arch. Virol. 146, 189–94.

Felsenstein, J., 1985. Confidence limits on phylogenies: an approach using the bootstrap. Evolution (N. Y). 39, 783–791. doi:10.2307/2408678

Figge, J., Webster, T., Smith, T.F., Paucha, E., 1988. Prediction of similar transforming regions in simian virus 40 large T, adenovirus E1A, and myc oncoproteins. J. Virol. 62, 1814–8.

Ghittoni, R., Accardi, R., Hasan, U., Gheit, T., Sylla, B., Tommasino, M., 2010. The biological properties of E6 and E7 oncoproteins from human papillomaviruses. Virus Genes 40, 1–13. doi:10.1007/s11262-009-0412-8

Giroglou, T., Florin, L., Fer, F.S., Streeck, R.E., Sapp, M., 2001. Human Papillomavirus Infection Requires Cell Surface Heparan Sulfate. J. Virol. 75, 1565–1570. doi:10.1128/JVI.75.3.1565–1570.2001

Gottschling, M., Göker, M., Stamatakis, A., Bininda-Emonds, O.R.P., Nindl, I., Bravo, I.G., 2011. Quantifying the phylodynamic forces driving papillomavirus evolution. Mol. Biol. Evol. 28, 2101–2113. doi:10.1093/molbev/msr030

Graham, S. V, Faizo, A.A.A., 2016. Control of human papillomavirus gene expression by alternative splicing. Virus Res. doi:10.1016/j.virusres.2016.11.016

Hawkins, C.D., Swan, R.A., Chapman, H.M., 1981. The epidemiology of squamous cell carcinoma of the perineal region of sheep. Aust. Vet. J. 57, 455–7.

Hayward, M.L., Baird, P.J., Meischke, H.R., 1993. Filiform viral squamous papillomas on sheep. Vet. Rec. 132, 86–8.

Howley, P.M., Pfister, H.J., 2015. Beta genus papillomaviruses and skin cancer. Virology. doi:10.1016/j.virol.2015.02.004

Jackson, S., Harwood, C., Thomas, M., Banks, L., Storey, A., 2000. Role of Bak in UV-induced apoptosis in skin cancer and abrogation by HPV E6 proteins. Genes Dev. 14, 3065–3073. doi:10.1101/gad.182100

Johne, R., Müller, H., Rector, A., van Ranst, M., Stevens, H., 2009. Rolling-circle amplification of viral DNA genomes using phi29 polymerase. Trends Microbiol. 17, 205–211. doi:10.1016/j.tim.2009.02.004

Johnson, K.M., Kines, R.C., Roberts, J.N., Lowy, D.R., Schiller, J.T., Day, P.M., 2009. Role of Heparan Sulfate in Attachment to and Infection of the Murine Female Genital Tract by Human Papillomavirus. J. Virol. 83, 2067–2074. doi:10.1128/JVI.02190-08

Lancaster, W.D., Theilen, G.H., Olson, C., 1979. Hybridization of bovine papilloma virus type 1 and type 2 dna to dna from virus-induced hamster tumors and naturally occurring equine tumors. Intervirology 11, 227–233. doi:10.1159/000149038

Le, S.Q., Gascuel, O., 2008. An improved general amino acid replacement matrix. Mol. Biol. Evol. 25, 1307–1320. doi:10.1093/molbev/msn067

López-Bueno, A., Mavian, C., Labella, A.M., Castro, D., Borrego, J.J., Alcami, A., Alejo, A., 2016. Concurrence of Iridovirus, Polyomavirus, and a Unique Member of a New Group of Fish Papillomaviruses in Lymphocystis Disease-Affected Gilthead Sea Bream. J. Virol. 90, 8768–8779. doi:10.1128/JVI.01369-16

Maglennon, G.A., Doorbar, J., 2012. The biology of papillomavirus latency. Open Virol. J. 6, 190–7. doi:10.2174/1874357901206010190

Maglennon, G.A., McIntosh, P.B., Doorbar, J., 2014. Immunosuppression facilitates the reactivation of latent papillomavirus infections. J. Virol. 88, 710–6. doi:10.1128/JVI.02589-13

Massimi, P., Thomas, M., Bouvard, V., Ruberto, I., Campo, M.S., Tommasino, M., Banks, L., 2008. Comparative transforming potential of different human papillomaviruses associated with non-melanoma skin cancer. Virology 371, 374–379. doi:10.1016/j.virol.2007.10.015

McBride, A.A., 2013. The Papillomavirus E2 proteins. Virology 445, 57–79. doi:10.1016/j.virol.2013.06.006

McLaughlin-Drubin, M.E., Münger, K., 2009. The human papillomavirus E7 oncoprotein. Virology. doi:10.1016/j.virol.2008.10.006

Mengual-Chuliá, B., Domenis, L., Robetto, S., Bravo, I.G., 2014. A novel papillomavirus isolated from a nasal neoplasia in an Italian free-ranging chamois (Rupicapra r. rupicapra). Vet. Microbiol. 172, 108–119. doi:10.1016/j.vetmic.2014.05.006

Meyers, J.M., Spangle, J.M., Munger, K., 2013. The human papillomavirus type 8 E6 protein interferes with NOTCH activation during keratinocyte differentiation. J. Virol. 87, 4762–7. doi:10.1128/JVI.02527-12

Meyers, J.M., Uberoi, A., Grace, M., Lambert, P.F., Munger, K., 2017. Cutaneous HPV8 and MmuPV1 E6 Proteins Target the NOTCH and TGF-β Tumor Suppressors to Inhibit Differentiation and Sustain Keratinocyte Proliferation. PLOS Pathog. 13, e1006171. doi:10.1371/journal.ppat.1006171

Muench, P., Probst, S., Schuetz, J., Leiprecht, N., Busch, M., Wesselborg, S., Stubenrauch, F., Iftner, T., 2010. Cutaneous papillomavirus E6 proteins must interact with p300 and block p53-mediated apoptosis for cellular immortalization and tumorigenesis. Cancer Res. 70, 6913–6924. doi:10.1158/0008-5472.CAN-10-1307

Munday, J.S., 2014. Bovine and Human Papillomaviruses: A Comparative Review. Vet. Pathol. 51, 1063–1075. doi:10.1177/0300985814537837

Munday, J.S., Kiupel, M., 2010. Papillomavirus-associated cutaneous neoplasia in mammals. Vet. Pathol. 47, 254–264. doi:10.1177/0300985809358604

Munday, J.S., Thomson, N., Dunowska, M., Knight, C.G., Laurie, R.E., Hills, S., 2015. Genomic characterisation of the feline sarcoid-associated papillomavirus and proposed classification as Bos taurus papillomavirus type 14. Vet. Microbiol. 177, 289–295. doi:10.1016/j.vetmic.2015.03.019

Munger, K., Werness, B.A., Dyson ', N., Phelps2, W.C., Harlow ', E., Howley, P.M., 1989. Complex formation of human papillomavirus E7 proteins with the retinoblastoma tumor suppressor gene product. EMBO J. 813, 4099–4105.

Narechania, A., Terai, M., Chen, Z., DeSalle, R., Burk, R.D., 2004. Lack of the canonical pRB-binding domain in the E7 ORF of artiodactyl papillomaviruses is associated with the development of fibropapillomas. J. Gen. Virol. 85, 1243–1250. doi:10.1099/vir.0.19765-0

Nindl, I., Gottschling, M., Stockfleth, E., 2007. Human papillomaviruses and non-melanoma skin cancer: Basic virology and clinical manifestations. Dis. Markers 23, 247–259.

Norval, M., Michie, J.R., Apps, M. V, Head, K.W., Else, R.E., 1985. Rumen papillomas in sheep. Vet. Microbiol. 10, 219–29.

Page, R.D.M., 1996. TreeView: an application to display phylogenetic trees on personal computers. Comput. Appl. Biosci. 12, 357–358. doi:10.1093/bioinformatics/12.4.357

Pennie, W.D., Grindlay, G.J., Cairney, M., Campo, M.S., 1993. Analysis of the Transforming Functions of Bovine Papillomavirus Type 4. Virology 193, 614–620. doi:10.1006/viro.1993.1169

Pennie, W.D., Saveria Campo, M., 1992. Synergism between bovine papillomavirus type 4 and the flavonoid quercetin in cell transformation in vitro. Virology 190, 861–865. doi:10.1016/0042-6822(92)90926-G

Perrière, G., Gouy, M., 1996. WWW-Query: An on-line retrieval system for biological sequence banks. Biochimie 78, 364–369. doi:10.1016/0300-9084(96)84768-7

Phelps, W.C., Münger, K., Yee, C.L., Barnes, J.A., Howley, P.M., 1992. Structure-function analysis of the human papillomavirus type 16 E7 oncoprotein. J. Virol. 66, 2418–27.

Rangarajan, A., Talora, C., Okuyama, R., Nicolas, M., Mammucari, C., Oh, H., Aster, J.C., Krishna, S., Metzger, D., Chambon, P., Miele, L., Aguet, M., Radtke, F., Dotto, G.P., 2001. Notch signaling is a direct determinant of keratinocyte growth arrest and entry into differentiation. EMBO J. 20, 3427–3436. doi:10.1093/emboj/20.13.3427

Rector, A., Tachezy, R., Ranst, M. Van, 2004. A Sequence-Independent Strategy for Detection and Cloning of Circular DNA Virus Genomes by Using Multiply Primed Rolling-Circle Amplification. J. Virol. 78, 4993–4998. doi:10.1128/JVI.78.10.4993

Rector, A., Van Ranst, M., 2013. Animal papillomaviruses. Virology 445, 213–223. doi:10.1016/j.virol.2013.05.007

Rezaei, H.R., Naderi, S., Chintauan-Marquier, I.C., Taberlet, P., Virk, A.T., Naghash, H.R., Rioux, D., Kaboli, M., Pompanon, F., 2010. Evolution and taxonomy of the wild species of the genus Ovis (Mammalia, Artiodactyla, Bovidae). Mol. Phylogenet. Evol. 54, 315–326. doi:10.1016/j.ympev.2009.10.037

Ropiquet, A., Hassanin, A., 2005. Molecular evidence for the polyphyly of the genus Hemitragus (Mammalia, Bovidae). Mol. Phylogenet. Evol. 36, 154–168. doi:10.1016/j.ympev.2005.01.002

Scagliarini, A., Gallina, L., Battilani, M., Turrini, F., Savini, F., Lavazza, A., Chiari, M., Coradduzza, E., Peli, A., Erdélyi, K., Alberti, A., 2013. Cervus elaphus papillomavirus (CePV1): New insights on viral evolution in deer. Vet. Microbiol. 165, 252–259. doi:10.1016/j.vetmic.2013.03.012

Schlegel, R., Wade-Glass, M., Rabson, M., Yang, Y., 1986. The E5 transforming gene of bovine papillomavirus encodes a small, hydrophobic polypeptide. Science (80-.). 233.

Schmitt, A., Rochat, A., Zeltner, R., Borenstein, L., Barrandon, Y., Wettstein, F.O., Iftner, A.T., 1996. The Primary Target Cells of the High-Risk Cottontail Rabbit Papillomavirus Colocalize with Hair Follicle Stem Cells. J. Virol. 70, 1912–1922.

Shope, R.E., Hurst, E.W., 1933. INFECTIOUS PAPILLOMATOSIS OF RABBITS. J. Exp. Med. 58.

Stevens, H., Rector, A., van Ranst, M., 2010. Multiply primed rolling-circle amplification method for the amplification of circular DNA viruses. Cold Spring Harb. Protoc. 5, pdb.prot5415-prot5415. doi:10.1101/pdb.prot5415

Tamura, K., Stecher, G., Peterson, D., Filipski, A., Kumar, S., 2013. MEGA6: Molecular evolutionary genetics analysis version 6.0. Mol. Biol. Evol. 30, 2725–2729. doi:10.1093/molbev/mst197

Tan, M.J., White, E.A., Sowa, M.E., Harper, J.W., Aster, J.C., Howley, P.M., 2012. Cutaneous beta-human papillomavirus E6 proteins bind Mastermind-like coactivators and repress Notch signaling. Proc Natl Acad Sci U S A 109, E1473-80.

doi:10.1073/pnas.1205991109
Tommasino, M., 2016. The biology of beta human papillomaviruses. Virus Res. doi:10.1016/j.virusres.2016.11.013
Tommasino, M., 2014. The human papillomavirus family and its role in carcinogenesis. Semin. Cancer Biol. 26, 13–21. doi:10.1016/j.semcancer.2013.11.002
Trenfield, K., Spradbrow, P.B., Vanselow, B.A., 1990. Detection of papillomavirus DNA in precancerous lesions of the ears of sheep. Vet. Microbiol. 25, 103–116. doi:10.1016/0378-1135(90)90070-C
Underbrink, M.P., Howie, H.L., Bedard, K.M., Koop, J.I., Galloway, D.A., 2008. E6 proteins from multiple human betapapillomavirus types degrade Bak and protect keratinocytes from apoptosis after UVB irradiation. J. Virol. 82, 10408–17. doi:10.1128/JVI.00902-08
Uzal, F.A., Latorraca, A., Ghoddusi, M., Horn, M., Adamson, M., Kelly, W.R., Schenkel, R., 2000. An apparent outbreak of cutaneous papillomatosis in merino sheep in patagonia, Argentina. Vet. Res. Commun. 24, 197–202.
Van Doorslaer, K., 2013. Evolution of the Papillomaviridae. Virology 445, 11–20. doi:10.1016/j.virol.2013.05.012
Van Doorslaer, K., Sidi, A.O.M.O., Zanier, K., Rybin, V., Deryckère, F., Rector, A., Burk, R.D., Lienau, E.K., van Ranst, M., Travé, G., 2009. Identification of unusual E6 and E7 proteins within avian papillomaviruses: cellular localization, biophysical characterization, and phylogenetic analysis. J. Virol. 83, 8759–8770. doi:10.1128/JVI.01777-08
Vande Pol, S., Rector, A., Ranst, M. Van, Doorslaer, K. Van, Pol, S. Vande, Klingelhutz, A., Moody, C., Laimins, L., Roman, A., Munger, K., Scheffner, M., Werness, B., Huibregtse, J., Levine, A., Howley, P., Huibregtse, J., Scheffner, M., Howley, P., Ansari, T., Brimer, N., Pol, S. Vande, Pim, D., Bergant, M., Boon, S., Ganti, K., Kranjec, C., Oh, S., Longworth, M., Laimins, L., White, E., Kramer, R., Tan, M., Hayes, S., Harper, J., Brimer, N., Lyons, C., Wallberg, A., Pol, S. Vande, Rozenblatt-Rosen, O., Deo, R., Padi, M., Adelmant, G., Calderwood, M., Tan, M., White, E., Sowa, M., Harper, J., Aster, J., Nicolas, M., Wolfer, A., Raj, K., Kummer, J., Mill, P., Ramoz, N., Rueda, L., Bouadjar, B., Montoya, L., Orth, G., Wallace, N., Robinson, K., Howie, H., Galloway, D., Wade, R., Brimer, N., Pol, S. Vande, Bohl, J., Das, K., Dasgupta, B., Pol, S. Vande, Zanier, K., Charbonnier, S., Sidi, A., McEwen, A., Ferrario, M., 2015. Papillomavirus E6 Oncoproteins Take Common Structural Approaches to Solve Different Biological Problems. PLOS Pathog. 11, e1005138. doi:10.1371/journal.ppat.1005138
Vande Pol, S.B., Klingelhutz, A.J., 2013. Papillomavirus E6 oncoproteins. Virology 445, 115–137. doi:10.1016/j.virol.2013.04.026
Vanselow, B.A., Spradbrow, P.B., 1983. Squamous cell carcinoma of the vulva, hyperkeratosis and papillomaviruses in a ewe. Aust. Vet. J. 60, 194–5.
Vanselow, B.A., Spradbrow, P.B., Jackson, A.R., 1982. Papillomaviruses, papillomas and squamous cell carcinomas in sheep. Vet. Rec. 110, 561–2.
Wang, J.W., Roden, R.B.S., 2013. L2, the minor capsid protein of papillomavirus. Virology 445, 175–186. doi:10.1016/j.virol.2013.04.017
Xia, X., Xie, Z., 2001. DAMBE: Software package for data analysis in molecular biology and evolution. J. Hered. 92, 371–373. doi:10.1093/jhered/92.4.371
Yu, T., Ferber, M.J., Cheung, T.H., Chung, T.K.H., Wong, Y.F., Smith, D.I., 2005. The role of viral integration in the development of cervical cancer. Cancer Genet. Cytogenet. 158, 27–34. doi:10.1016/j.cancergencyto.2004.08.021
Zanier, K., Nomin??, Y., Charbonnier, S., Ruhlmann, C., Schultz, P., Schweizer, J., Trav??, G., 2007. Formation of well-defined soluble aggregates upon fusion to MBP is a generic property of E6 proteins from various human papillomavirus species. Protein Expr. Purif.

51, 59–70. doi:10.1016/j.pep.2006.07.029
Zanier, K., ould M'hamed ould Sidi, A., Boulade-Ladame, C., Rybin, V., Chappelle, A., Atkinson, A., Kieffer, B., Travé, G., 2012. Solution Structure Analysis of the HPV16 E6 Oncoprotein Reveals a Self-Association Mechanism Required for E6-Mediated Degradation of p53. Structure 20, 604–617. doi:10.1016/j.str.2012.02.001
Zheng, Z.-M., Baker, C.C., 2006. Papillomavirus genome structure, expression, and post-transcriptional regulation. Front. Biosci. 11, 2286–302. doi:1971 [pii]
zur Hausen, H., 2009. Papillomaviruses in the causation of human cancers - a brief historical account. Virology. doi:10.1016/j.virol.2008.11.046
zur Hausen, H., 2002. Papillomaviruses and cancer: from basic studies to clinical application. Nat. Rev. Cancer 2, 342–350. doi:10.1038/nrc798